UNIVERSITÀ DEGLI STUDI DI TRIESTE

UNIVERSITÀ DEGLI STUDI DI UDINE

# UNIVERSITÀ DEGLI STUDI DI TRIESTE
# UNIVERSITÀ DEGLI STUDI DI UDINE

## XXXVIII CICLO DEL DOTTORATO DI RICERCA IN

AMBIENTE E VITA

# *Salinity and organic matter as interacting factors affecting root iron plaques formation in flooded soils*

Settore scientifico-disciplinare: **AGR – 06/B**


DOTTORANDO
**DANIEL MORO**

COORDINATORE
**PROF.SSA LUCIA MUGGIA**

SUPERVISORE DI TESI
**PROF. MARCO CONTIN**

CO-SUPERVISORE DI TESI
**DOTT.SSA ELISA PELLEGRINI**


**ANNO ACCADEMICO 2024/2025**

# *Index*

# *General introduction*

## Climate change and water cycle disruption

The global water cycle describes a continuous redistribution of water through the atmosphere, oceans, cryosphere, terrestrial ecosystems, and subsurface reservoirs, thereby regulating both climate and life-supporting processes on Earth (Oki & Kanae, 2006; Allan et al., 2020). While oceans and ice sheets contain the largest water stores, smaller but highly dynamic compartments include rivers, lakes, soils, aquifers, vegetation, and even the biosphere of animals, all of which interact through fluxes of precipitation, evapotranspiration, runoff, and infiltration (Gimeno et al., 2012). Precipitation over land is particularly dependent on the transport of water vapor from the ocean, with river discharge providing the main return pathway to the sea, thus closing the continental branch of the cycle (van der Ent et al., 2010). Paleoclimate reconstructions show that the hydrological cycle has undergone marked shifts in intensity and distribution during glacial and interglacial transitions and past warming episodes (Buckley et al., 2010; IPCC, 2023). However, actual fluctuations are increasingly dominated by human activities, both indirectly through climatic response to emissions of greenhouse gases and aerosol particles, and directly via the interference with deforestation, irrigation, and groundwater extraction, which alter evapotranspiration and recharge regimes (Li et al., 2019).

One of the clearest manifestations of this disruption is the alteration of precipitation patterns. Anthropogenic climate change is linked to more frequent and intense heavy rainfall events in many regions, as a warmer atmosphere holds more water vapour and fuels convective storms (Allan et al., 2020; Pendergrass et al., 2017). Simultaneously, subtropical and continental areas are projected to experience longer dry periods and higher evapotranspiration rates, amplifying the risk of agricultural drought and hydrological scarcity (Dai, 2013; Cook et al., 2020). Such contrasting trends, with wetter regions generally projected to experience intensified precipitation and drier regions facing more severe water deficits, are consistently reproduced across climate projections, despite regional variability (Held and Soden, 2006; IPCC, 2023).

These changes also influence soil-water interactions. Droughts and heatwaves intensify soil moisture deficits and affect plant productivity, while the lower number of stronger rainfalls often increase surface runoff, soil erosion, and flood risk, with limited infiltration and groundwater recharge (Trenberth et al., 2014; Seneviratne et al., 2021). The combined effect results in a hydrological regime that is both more extreme and less predictable, threatening water security for agriculture, ecosystems, and societies worldwide (Shrivastava and Kumar, 2015).

One critical consequence of the disruption of the water cycle is the impact on soil salinity and salt accumulation on anthropic and natural habitats. It is estimated that salt-affected soils occupy more than 20% of global irrigated land (Qadir et al. 2014), and the climate projections forecast an increase of up to 1.5 million ha of soils experiencing worsening salt accumulation within few decades (FAO, 2021).While this phenomenon involves many regions worldwide, coastal habitats and arid and semi-arid areas are some of the most vulnerable to these changes (Hassani et al., 2021; Adams et al., 2024).

In arid and semi-arid regions, where the scarcity of water is already an ongoing problem, higher temperatures and reduced rainfall enhance evapotranspiration and decrease leaching, exacerbating the concentration of salts in the upper soil profile (Huang et al., 2017). Conversely, coastal areas, following their geographical position, are prone to sea-level rise, saltwater intrusion, and storm surges, which expose soils and aquifers to salt accumulation, further threatening agricultural productivity and ecosystem stability (Palutikof et al., 2008; Bellafiore et al., 2021).

The reasons behind the salinization process in arid and coastal areas are substantially different. In arid and semi-arid habitats, salt accumulation derives from the weathering of the parent material following the release of soluble salts, which, under low rainfall conditions, accumulate in lower soil horizons, being brought to the surface layers by water evaporation processes (Jordán et al., 2004; Qadir et al., 2014). In addition, human unsustainable irrigation practices and bad resource management further worsen the problem. The repeated use of brackish irrigation water, combined with inadequate drainage, causes salts to accumulate in the soil and contributes to rising water tables, mobilising salts toward the surface (Shahid et al., 2018a). The main consequences on soil integrity and on microorganisms and plant communities depend on the salts that are mostly present. Saline soils are defined as those with an electrical conductivity (ECe) of the saturated paste extract

greater than 4 dS $m^{-1}$ at 25 °C, an exchangeable sodium percentage (ESP) less than 15, and soil pH usually below 8.5 (Richards, 1954). The dominant feature is the high concentration of neutral soluble salts such as NaCl, $CaCl_2$, and $MgSO_4$, which cause osmotic stress and specific ion toxicity in plants (Naorem et al., 2023). In contrast, sodic soils have an ESP greater than 15 and often a pH above 8.5, reflecting the predominance of sodium on the cation exchange complex (Richards, 1954). Excess sodium, usually derived from highly soluble $Na_2CO_3$ and common to many arid areas, leads to soil dispersion due to clay deflocculation, structural breakdown, and reduced permeability, creating severe constraints for plant growth and microbial functioning (Wong et al., 2009; Rengasamy, 2018).

In coastal systems, chlorides (i.e. NaCl and $MgCl_2$) predominate and salinity dynamics are shaped by the balance between freshwater inputs from river discharge and the saltwater inputs from sea water intrusion and marine aerosol (Shrivastava and Kumar, 2015). Climate-driven changes in river flow, groundwater depletion, and sea level rise facilitate the inland advance of saline water in estuaries and aquifers, altering the existing equilibrium (Daliakopoulos et al., 2016; Bellafiore et al., 2021). Wetlands are particularly vulnerable, as storm surges and coastal flooding can determine prolonged flooding which affect soil properties and microbial and plant survival (Herbert et al., 2015). Evidence from South and Southeast Asia, as well as from Mediterranean deltas, illustrates how prolonged droughts combined with sea-level rise have already caused substantial losses of arable land through salinization (García-Ruiz et al., 2011; Smajgl et al., 2015).

Overall, soil salinization represents a major threat to agricultural productivity, ecosystem functioning, and food security in both arid interiors and coastal zones. With climate change expected to exacerbate these pressures, the development and implementation of effective mitigation strategies has become an urgent priority to sustain soil health and ensure long-term land use.

## Mitigation strategies for soil salinization

The severity of salinity's impact on agriculture and ecosystems has moved people to develop a wide array of mitigation and management strategies over the years. Traditional approaches to manage salt-affected soils rely mainly on physical, chemical, and agronomic

interventions. These include improved irrigation management and drainage to leaching salts from the upper horizons, as well as the biological removal of salts by harvest of high salt accumulating aerial plant parts, in areas with negligible irrigation water or rainfall available for leaching (Qadir et al., 2000). Chemical reclamation, especially for sodic soils, involves applying gypsum or other calcium sources to replace sodium on the exchange complex, improving soil structure and permeability (Chhabra, 2017). Sulphur and organic amendments are also used to lower pH and enhance soil aggregation (Wong et al., 2010). On the agronomic side, the growth of salt-tolerant crops, such as barley or cotton, and advances in breeding and biotechnology for stress tolerant varieties represent long-standing strategies (Munns and Tester, 2008). In addition to the traditional approaches, plant biostimulants have gained attention as useful tools to enhance plant tolerance to abiotic stresses, including salinity (Calvo et al., 2014). Biostimulants are defined as non-nutrient substances or microorganisms that, when applied to plants or soils, stimulate natural processes to improve nutrient efficiency, stress tolerance, or crop quality (du Jardin, 2015). They include microbial inoculants such as plant growth-promoting rhizobacteria and arbuscular mycorrhizal fungi, which, for example, can contribute to enhance root development and nutrient uptake (Etesami and Beattie, 2018). Other types are seaweed extracts, protein-based products, inorganic compounds, and specific fractions of the soil organic matter. Notably, organic amendments such as compost and manure, already part of traditional management, overlap conceptually with the biostimulant practices, by improving soil structure, water-holding capacity, and microbial activity (Cherif et al., 2009). Biochar, though less widely tested, also shows potential as a soil conditioner in saline environments (Agegnehu et al., 2017).

Regarding the soil organic matter fractions, there are different ways to fractionate the organic matter, based on size, density, or chemical stability. Physical fractionation by density separates “light” particulate organic matter (POM), relatively fresh plant and microbial debris not bound to minerals, from the heavier mineral-associated organic matter (MAOM), which consists of older, humified compounds stabilized by clay and silt (Six et al., 2002; von Lützow et al., 2007). Similarly, aggregate-size fractionation distinguishes soil organic matter (SOM) associated with macro and microaggregates, relating carbon pools to soil structure and stability (Six et al., 2000). The reason for such approaches is that labile fractions like POM turn over rapidly, fuelling microbial activity and short-term nutrient cycling, whereas stable fractions like MAOM contribute to long-term carbon sequestration,

cation exchange, and aggregate stability (Cotrufo et al., 2013). These distinctions are especially relevant in salt-affected soils, where salinity and sodicity alter soil aggregation and ionic balance. High sodium levels, for instance, can disrupt aggregates and destabilize MAOM, releasing organic matter into solution (Rengasamy, 2006; Wong et al., 2010).

Another important pool is the dissolved organic matter (DOM), soluble in water and composed of small molecules such as sugars, amino acids, phenols, and fulvic acids (Kalbitz et al., 2000). DOM is highly mobile and reactive, playing a critical role in nutrient cycling, microbial metabolism, and the transport and complexation of metals and salts (Aiken et al., 2011). In saline and wetland soils, DOM dynamics are particularly relevant because sodium concentrations and fluctuating redox conditions can alter DOM solubility and stability, thereby modifying microbial activity and interactions with minerals (Herbert et al., 2015).

Chemical fractionation separates SOM into pools defined by solubility and chemical properties, typically fulvic acids, humic acids, and humin (Stevenson, 1994; Piccolo, 2001). Fulvic acids are the most soluble and mobile, of relatively low molecular weight and high oxygen content; they remain soluble across a wide pH range and can interact with metals and nutrients (Tipping, 1986). Humic acids are less soluble, characterized by higher aromaticity and molecular weight. They precipitate under acidic conditions but dissolve at neutral to alkaline pH, contributing to cation exchange and pH buffering (Tan, 2014). Humin is insoluble in both acid and alkali and is strongly associated with minerals, representing the most recalcitrant pool (Piccolo, 2001). These fractions are not only indicators of SOM stability but also play functional roles under elevated salinity. Humic acids can enhance root growth, improve ionic balance, and stimulate antioxidant activity in plants exposed to sodium stress (Nardi et al., 2002; Canellas et al., 2015). Fulvic acids, due to their mobility and their capacity for chelating micronutrients such as Fe and Zn, improve their bioavailability under saline conditions (Chen et al., 2004; Olivares et al., 2015). Altogether, these findings highlight that the effectiveness of soil organic matter in mitigating salt stress depends not only on its overall quantity but also on its composition and stability, which determine whether added or native organic matter contributes to short-term nutrient availability or to long-term improvements in soil structure and ion buffering capacity.

# Iron plaque formation in wetland soils

Wetlands cover between 6% and 9% of the Earth's land surface and store approximately 20–35% of global terrestrial carbon, making them one of the most important ecosystems for climate regulation and biodiversity (Mitsch & Gosselink, 2015; Zhang et al., 2023). Despite this relevance, wetlands are also among the most vulnerable ecosystems to soil salinization and anoxia. Periodic or permanent flooding limits gas exchange and microbial respiration rapidly consumes available oxygen (Pezeshki, 2001; Mitsch & Gosselink, 2015). Under these reduced conditions, soils accumulate reduced chemical species such as $Fe^{2+}$, $Mn^{2+}$, ammonium, and sulphide (Patrick & DeLaune, 1977; Lamers et al., 2013). For plants, oxygen deprivation at the root level represents a severe stress, impairing respiration and nutrient uptake (Colmer and Voesenek, 2009). When salinity and anoxia co-occur, plants face a dual challenge: maintaining oxygen supply to roots while also restricting toxic ion uptake. This trade-off often requires structural modifications, such as increased suberization of root tissues that reduce both sodium entry and radial oxygen loss (Peralta Ogorek et al., 2023).

To cope with prolonged soil anoxia, many wetland species develop aerenchyma, a tissue characterized by intercellular air spaces that facilitate internal diffusion of $O_2$ from shoots to roots (Evans, 2004). Some of this $O_2$ passively diffuses out from roots into the surrounding rhizosphere through a process called radial oxygen loss (ROL) (Colmer, 2003). Through ROL, roots act as localized sources of oxygen in otherwise anaerobic soils, creating steep redox gradients around root surfaces (Armstrong, 1980).

Among the main consequences of oxygen release in the rhizosphere is the precipitation of $Fe^{3+}$ on root surfaces, forming iron plaques (Figure 1). As stated above, under waterlogged conditions $Fe^{3+}$ is reduced to much more soluble $Fe^{2+}$, which diffuses toward roots where is re-oxidized by oxygen from ROL to $Fe^{3+}$ that quickly precipitate as amorphous or poorly crystalline iron oxy(hydr-)oxides (Chen et al., 1980; Hansel et al., 2001). These typically consist of ferrihydrite and lepidocrocite, with possible gradual transformation into more crystalline forms such as goethite, depending on pH, redox dynamics, and aging processes (Hansel et al., 2003). These reddish-brown coatings are a common feature on the roots of rice (*Oryza sativa*), common reed (*Phragmites australis*), and mangroves, often visible as rust-colored deposits (Taylor et al., 1984) and commonly called iron plaques.

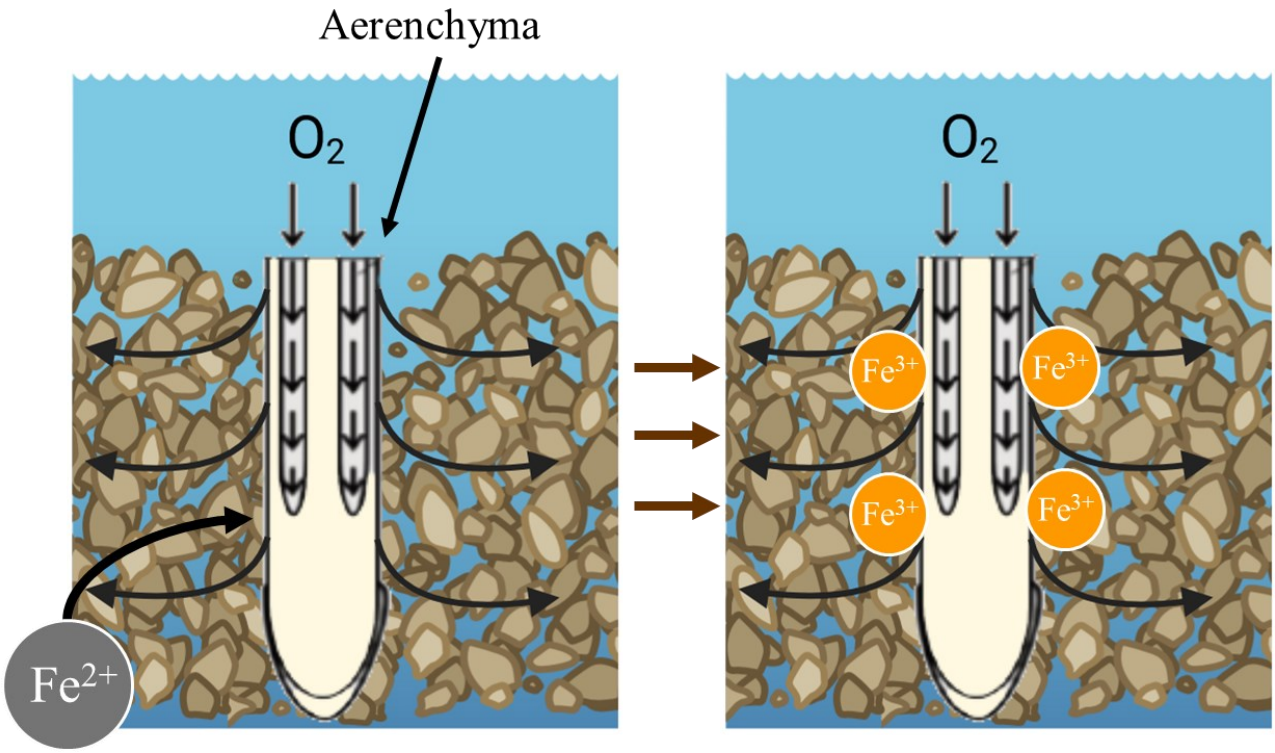


**Figure 1.** Iron plaque formation process in anoxic flooded soils.

Iron plaques play an important role for wetland plants, as they work as a potential sink and second source of nutrients and pollutants (Khan et al., 2016). Due to their high specific area and strong sorptive affinity (Chen et al., 2006), they act as a dynamic barrier, regulating at the same time the fluxes of essential nutrients and toxic elements between the soil solution and plant (Liu et al., 2005). For example, phosphate has a high affinity and is often immobilized in plaques, restricting its immediate availability to plants (Batty et al., 2000). The same is true for toxic elements such as arsenic, cadmium, or copper, which are complexed at the root surface and see their translocation into shoots reduced (Seyfferth et al., 2010; Meharg and Zhao, 2012). Several studies have reported that the development of iron plaque on rice roots significantly reduces arsenic uptake and its translocation to the grain, acting as a key detoxification mechanism in flooded systems (Meharg et al., 2009; Pardo et al., 2016). On the opposite, it is also true that thick $Fe^{3+}$ deposits may result negative for plants, as they may decrease the uptake of beneficial micronutrients like manganese or zinc, and halt root exchange processes (Taylor et al., 1984).

Although ROL is one of the main drivers, the plaque formation process is controlled by multiple abiotic and biotic factors. In fact, ROL intensity depends on root anatomy, age, and species-specific physiology. For example, *Phragmites australis* exhibits high $O_2$ release

along much of the root axis, forming more plaques than *Spartina alterniflora* under similar field conditions (He et al., 2024). From the soil side, plaque development requires adequate $Fe^{2+}$ in solution, which occurs under moderately reducing conditions. If the soil is too oxidizing, $Fe^{2+}$ precipitates before reaching the roots, while under strongly reducing, sulfidic conditions, $Fe^{2+}$ may be immobilized as iron sulphides, limiting plaque formation (Lamers et al., 2013; Neubauer et al., 2007). Soil pH also plays an important role, as Fe plaque formation and sorption capacity are favored at neutral to slightly alkaline pH, whereas under acidic conditions plaques are less stable and metal adsorption capacity is reduced (Zhang et al., 2019). Hydrological dynamics further modulate plaque abundance: flowing water can deliver $Fe^{2+}$ and carbonates that favor precipitation, whereas stagnant or intermittently dry conditions may limit external plaque formation and promote internal iron deposition in roots (St-Cyr & Crowder, 1989).

Biotic interactions also influence plaque dynamics. Iron-oxidizing bacteria can catalyze $Fe^{2+}$ oxidation at the root interface, enhancing plaque deposition, while iron-reducing bacteria may dissolve $Fe^{3+}$ phases, limiting plaque persistence (Emerson et al., 1999; Weiss et al., 2004).

## Interaction between soil organic matter, salinity and iron plaques

Among the many factors influencing iron plaque formation and dissolution dynamics, the role of SOM remains debated in the literature. On one hand, high organic matter inputs stimulate microbial respiration, driving soils into harsh reducing conditions and causing the formation of large amounts of soluble $Fe^{2+}$, which can be exploited as substrate for plaque formation (Roden and Wetzel, 2002; Yuan et al., 2022). This has been studied in organic-rich floodplain sediments, where higher Fe plaque accumulation has been observed on *P. australis* roots compared to mineral soils, consistent with stronger reducing conditions (Roden and Wetzel, 2002). On the other hand, SOM may also suppress plaque deposition by complexing iron, increasing its solubility and thus inhibiting its precipitation onto roots. Low molecular weight organic acids, such as citrate and oxalate can chelate $Fe^{3+}$, keeping it in solution and preventing precipitation on root surfaces (Jones et al., 1996; Liu et al., 2021a).

In rice paddies, root exudation of low molecular weight organic acids can strongly acidify the rhizosphere, and such compounds are also known to increase iron solubility by acting as ligands and chelators (Fox & Comerford, 1990; Mimmo et al., 2014).

Beyond plaque, it has been already discussed that SOM plays an important role in reducing salt stress. Organic amendments such as compost or biochar improve soil aggregation and water-holding capacity, reducing osmotic stress and facilitating nutrient uptake in saline soils (Chaganti and Crohn, 2015; Lakhdar et al., 2009). For instance, Lakhdar et al. (2009) demonstrated that compost addition to saline Tunisian soils enhanced wheat biomass and soil fertility despite high salinity levels. Nevertheless, the chemical mechanism by which SOM reduces salt stress in plants and microorganisms was only partially demonstrated.

The interaction between SOM and plaque becomes more complex under saline conditions. Moderate sulphate inputs can stimulate S and Fe cycling, with sulphides formed under reducing conditions being re-oxidized to $Fe^{3+}$ oxyhydroxides on root surfaces, thereby favouring plaque deposition (van der Welle et al., 2007; Miao et al., 2024). Conversely, high salinity and sulphide accumulation often depress root ROL through enhanced suberization and lignification of root tissues, which inhibits plaque formation (Kotula et al., 2009; Rickard and Morse, 2005). A study in mangrove wetlands reported that salinity induced ROL suppression hence limited Fe plaque formation, shifting iron towards sulphide minerals instead (Peralta Ogorek et al., 2023).

The aim of this thesis is to investigate the interplay between SOM, soil salinity and iron plaque formation, with particular focus on three interconnected aspects: i) elucidating the mechanisms by which SOM may mitigate salt stress in soils and plants; ii) assessing how salinity and soil physicochemical properties influence the development and characteristics of iron plaques; iii) clarifying the role of SOM in promoting or constraining iron plaque formation under different redox and saline conditions.

# *General aims*

The aim of this PhD thesis was to deepen the understanding and provide new insights on the interaction among soil salinity (environmental factor), soil organic matter (soil factor), and iron plaque formation (plant-soil factor). The roles of the soil organic matter (SOM) and soil salinity in the plaque formation dynamics are still under scientific debate, and, even if it is well accepted that SOM plays an important role in contrasting soil salinity stress, the chemical mechanism behind this process is still partially unclear.

As a first step, I investigated these three parameters together, focusing on the combined influence of soil properties (e.g. hydrophobic and hydrophilic organic matter, electrical conductivity) and plant traits (i.e. plant stand density, root exudation and root porosity) on root iron plaque formation along salinity gradients. This was carried out in a field study exploiting *Phragmites australis* as a model plant species. Only few studies in the literature have tried to assess the role of multiple parameters in modulating the dynamics of deposition and dissolution of $Fe^{3+}$ on plant root surfaces, given the difficulty of separating the contribution of each variable to the final result.

Based on the findings of this first study, I decided to focus my attention on the role of specific fractions of soil organic matter, performing two separate experiments in the laboratory. The first aimed to evaluate the mitigation effect of humified organic matter on the increase of electrical conductivity imposed by two salts: i) NaCl, the most common salt in soils of coastal areas; ii) $Na_2CO_3$, mainly present in arid – semiarid habitats. My work was to identify the chemical mechanism through which different humic acids can contrast the increasing osmotic stress in plants following salts dissociation and the subsequent increase in soil $Na^+$ concentration. The second laboratory experiment aimed to clarify the role of SOM in iron plaque formation. I induced plaques on artificial roots in solution under three treatments: absence of soil organic matter, and varying C:Fe molar ratios using two different carbon sources, soil-derived OM and root exudate-like OM.

# *Chapter 1*

# Preface

This work investigated how multiple soil factors and plant traits interact to modulate the formation of root iron plaques in *Phragmites australis* along salinity gradients. The study was carried out in the Grado-Marano Lagoon (NE Italy), an ecosystem increasingly exposed to sea-level rise and saltwater intrusion due to the ongoing climate change affecting coastal habitats. By combining field measurements and statistical modelling, this work explores how salinity affects the formation of iron plaques on *P. australis* roots through its influence on soil conditions and plant traits.

Our findings show that salinity does not directly determine plaque formation but rather acts indirectly by altering soil oxygen levels and vegetation structure, highlighting the complex interactions that link plants and soils in coastal wetlands.

A manuscript on this work is currently under writing process and will be submitted shortly.

# *Soil factors modulating root plaque formation in Phragmites australis along salinity gradients*

## 1. Introduction

It is widely accepted that sea-level rise is one of the most significant effects of the climate change threatening coastal areas worldwide (Nicholls and Cazenave, 2010; Mimura, 2013). The average rate of global sea level rise reached ~ 4.8 mm/year in the last 10 years, and the projections of sea-level increase exceed the 50 cm for the end of the century, with final expected range varying based on the uncertainties related to the different scenarios (Oppenheimer et al., 2019; Griggs and Reguero, 2021). The intensity of this phenomenon varies between areas, triggering different degree of the local impacts, such as flooding frequency and saline water intrusion (Woodruff et al., 2013). In coastal regions, the saltwater intrusion, together with bad management and overuse of available freshwater resources, threatens fresh- and brackish-water ecosystems, potentially harming biota and altering biogeochemical processes (White & Kaplan, 2017; Bhattachan et al., 2018). This is specifically true for river deltas and estuarine systems, recognized as global hotspots of vulnerability to climate change (Shahid et al., 2018a; Alcérreca-Huerta et al., 2019). The degradation and potential loss of these habitats is a critical issue, as they are as productive as tropical forests and coral reefs, provide habitat and shelter for a high diversity of animals and play an essential role in global $CH_4$ and $CO_2$ sequestration (Mitsch and Gosselink, 2015; Cronin et al., 2020). Prolonged flooding and increased salinity affect soil properties and microorganisms by lowering redox potential, enhancing the accumulation of sulphides, destabilizing soil organic matter pools and subsequently alter microbial community composition, favouring sulphate reducers and methanogens (Chambers et al., 2011). Moreover, excess sodium and chloride can disrupt soil aggregation, reduce permeability, and inhibit enzymatic activity, leading to declines in microbial diversity and function (Rath et al., 2019). This can also lead to severe dieback in wetland vegetation due to anoxic soil conditions and osmotic stress, respectively. Prolonged flooding lowers $O_2$ availability in soils, driving anoxia and challenging root access to $O_2$, with consequent growth reduction

and impair nutrient uptake (Pezeshki, 2001). In addition, salinity imposes two related stresses, i.e. the osmotic stress that suppresses plant growth and specific ion toxicity driven mainly by $Na^+$ and $Cl^-$ that accumulate in plant tissues, accelerating leaf senescence and disrupting metabolism (Munns and Tester, 2008). When saline waters flood a soil, the effect is synergic leading to a decline in plant photosynthesis, growth, and survival in wetland habitats (White and Kaplan, 2017).

Among wetlands, common reed stands (*Phragmites australis* [Cav.] Trin. Ex Steudel) represent one of the main, worldwide present, freshwater habitats. *P. australis* is a perennial and cosmopolitan wetland species, with clonal populations covering large surfaces that drive important ecosystem services. Plants are dense and form extensive reed beds that are capable to provide habitat and nesting sites for birds and invertebrates (Valkama et al., 2008), to slow water flow and attenuate waves, trap and stabilize sediments, and store carbon and nutrients, contributing to habitat protection and development (Kiviat, 2013).

During the last decades, common reed stands started to suffer from a widespread process of dieback, particularly in Central and Eastern Europe (van der Putten, 1997), and in North America (Cronin et al., 2020; Hu et al., 2021). The first substantial retreat occurred around several Swiss lakes and was documented by Hürlimann (1951), with subsequent reports confirming the persistent trend (e.g. Klötzli, 1971; Sukopp & Markstein, 1989; Brix, 1999). The main factors identified as causes of this syndrome were initially eutrophication, mechanical damage or erosion (e.g., by waves, boats), and alteration of the water level through regimentation (e.g., Schröder, 1979; Ostendorp, 1989). Only recently, other hypotheses have been suggested in the literature trying to fulfil the gap apparently only partially explained by the previous hypotheses. Extreme flooding is surely an important factor shaping wetlands as it causes an impair oxygen supply to submerged shoots and roots (Koppitz, 2004; Cronin et al., 2020). For instance, Elsey-Quirk et al. (2024) reported that the continuous increase in average flooding elevation along the Mississippi river delta is contributing to a gradual, long-term decline of *P. australis*, with an average 68% reduction in its cover recorded over a 16-year monitoring period. Moreover, in the same study, the ability of *P. australis* to recover from stress events, such as storms, was markedly reduced in individuals exposed to frequent flooding, compared to those under less stressful conditions. Flooding can also indirectly affect common reed stands following the increase in soil sulphide concentrations in anoxic soils exposed to the intrusion of saline waters enriched in sulphate ions (Armstrong et al. 1996). Sulphide phytotoxicity was proved to

affect *P. australis* rhizomes with bud and root death occurring within 3-7 days at sulphide concentrations of ~1 mM. Both flooding and salinity were therefore considered, at some point, as other possible triggers of the common reed die back syndrome. Elevated salinity (combined with flooding) suppresses growth and survival of *P. australis* and affect its distribution also following the increase in soil sulphides (Hellings & Gallagher, 1992; Lissner & Schierup, 1997; Chambers et al., 1998). Recent landscape experiments in the Mississippi River Delta further stressed the link between saltwater intrusion and extensive dieback and poor recovery of the species (Cronin et al., 2020; Elsey-Quirk et al., 2024).

The negative impacts on *P. australis* are typically characterized by symptoms such as smaller size of plants, dead rhizomes, abnormal lignification and an evident retreat especially from deep waters (Hartog et al., 1989; van der Putten, 1997), providing several plant traits to be used to assess the impacts of abiotic these stresses. Gigante et al. (2011) reported how common reed populations affected by dieback exhibited reductions down to ~45% in several morphological traits, including stem height, stem diameter, lateral root diameter, and stem density, compared to healthy stands. One trait that has received relatively little attention despite largely occurring in flood-tolerant species is root plaque formation. Plaques are mainly iron precipitates (oxyhydroxides) that form by root oxygen release from roots into the rhizosphere and the consequent oxidation of the reduced $Fe^{2+}$ to $Fe^{3+}$ (Maisch et al., 2020; Khan et al., 2016). Iron plaques play an important role for wetland plants, as they work as a potential sink and second source of nutrients and pollutants (Khan et al., 2016). However, the presence and thickness of plaques are defined by many triggers, often interacting each other. Plaques are in fact the result of both rhizosphere chemistry and plant physiology, representing a possible key trait for the assessment of plant stand fitness, such as that of *P. australis* stands.

Among plaque triggers, completely neglected is the direct or indirect role of flood and salt stresses. A very little step forward was done by Liu et al. (2021b), which showed a direct, non-linear salinity effect on plaque abundance working in mesocosms, more specifically with oligohaline conditions (2.4‰) increasing plaque amount and mesohaline conditions (8.2‰) suppressing it. Yet, no study has unravelled the direct and indirect pathways through which salinity, potentially mediated by soil chemistry and plant traits, determines plaque abundance on *P. australis*.

Therefore, the aim of our study was to investigate the combined influence of key soil properties of flooded soils and plant traits of *P. australis* on root plaque development along salinity gradients. Specifically, we focused on common reed stands located in two delta rivers, i.e. Stella and Cormor rivers, in the Northern Adriatic Sea, selected as they present clear salinity gradients over short distances and evidence of a declining population. We hypothesized that elevated salinity and flooding will negatively influence iron plaque formation, either by altering the chemistry of the plant rhizosphere and the Fe cycle (e.g. more chlorinated forms of Fe), or by inhibiting plant ability to release oxygen or exudates from roots, thereby limiting $Fe^{2+}$ oxidation in the rhizosphere or boosting root exudation.

# 2. Materials and methods

## 2.1 The study area

The Stella and Cormor rivers are spring rivers that flow into the Grado and Marano Lagoon (4SPA/SAC Natura 2000 IT3320037), the second largest lagoon in Italy after the Venice lagoon. Spanning about 160 $km^2$, the lagoon is enclosed by the Tagliamento River delta to the west and the Isonzo River delta to the east. The salinity reaches average levels of 28.5 PSU (~ 30 g $L^{-1}$) in the eastern basin, and of 21.5 PSU (~ 22 g $L^{-1}$) in the western basin due to the fresh water discharged from the Stella, Turgnano, and Cormor rivers (Gatto & Marocco, 1993; Ferrarin et al., 2010). Specifically, the Stella and Cormor estuarine systems have an average combined discharge of approximately 45 $m^3$ $s^{-1}$ (Ferrarin et al., 2010; Fontolan et al., 2012), with the Stella River counting for about half of the freshwater entering the lagoon from the Friulian plain. Both systems support a range of valuable natural habitats, and the Stella River delta has been designated as a regional protected area, covering about 1,377 hectares. The freshwater contributions of the Stella, Turgnano and Cormor rivers have shaped over 300 ha of common reed beds (*P. australis*), bulrush stands and brackish marshes (Cosolo et al., 2015).

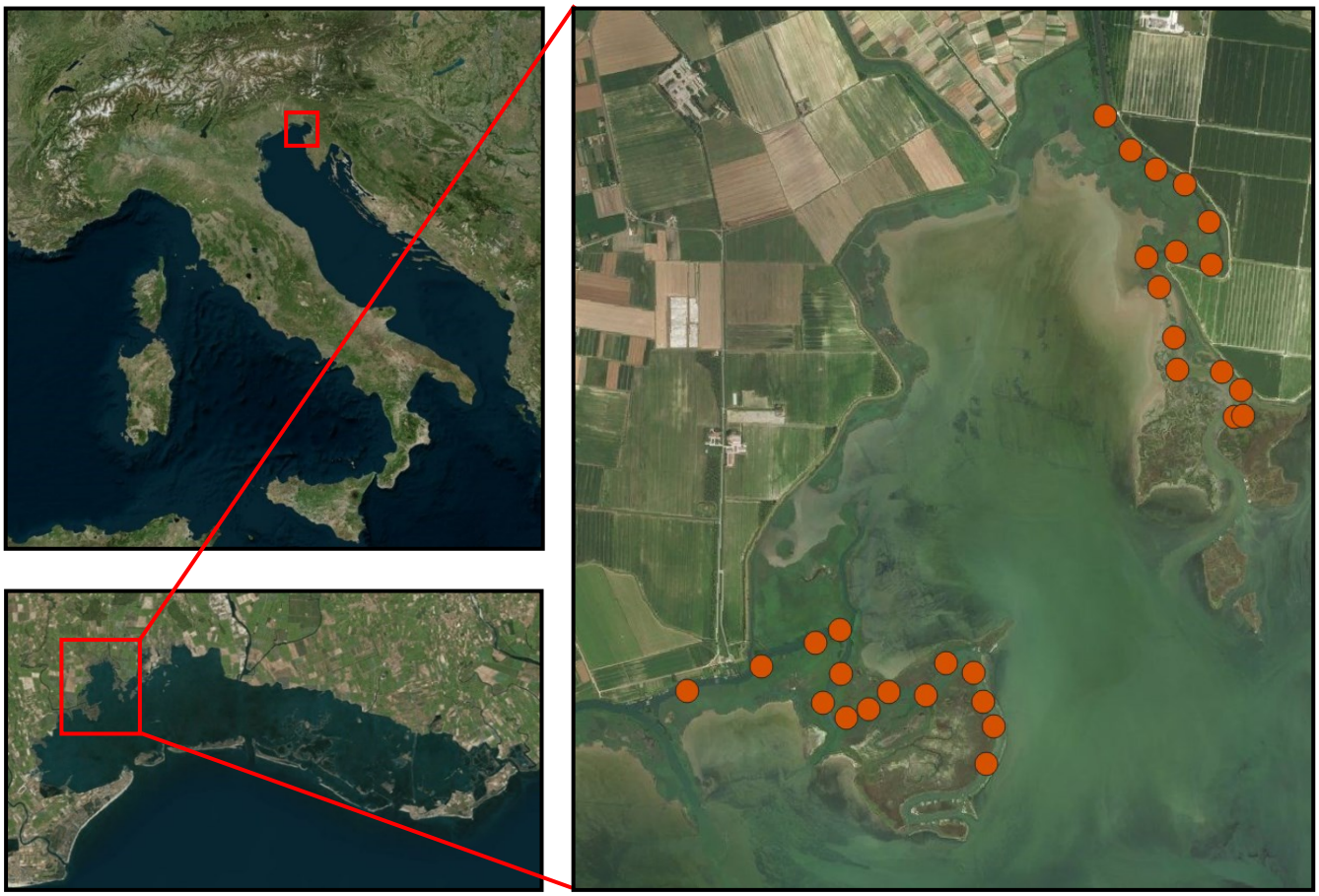

**Figure 1.** Study Satellite images of the geographical positions of Grado – Marano Lagoon and Cormor and Stella Rivers, and of the 30 sampling sites chosen for the experiment.

## 2.2 Sampling plan and field measurements

A total of 30 sampling sites covering about 6 Km of the two systems were selected for the present work (15 sampling sites per each river) (Figure 1; Supplementary material Figure S1). These were chosen along the edges of the main river channel, following the distribution range of *P. australis* as defined in Poldini et al. (1999) and verified in the field during the surveys. Sampling sites were initially identified using the software QGis (QGIs.org, 2025), with a distance within each of ~ 200 m. Real sampling positions were then acquired through a GNSS device (Mobile Mapper50, Spectra Precision).

Soil redox potential (Eh), plant stand density and average plant height were measured at each sampling site. Soil Eh was measured using a redox probe connected to a portable voltmeter (Crison Instruments, Barcelona, Spain), following standard procedures (ISO 11271:2022),

and corrected using Zobell's solution as reference. The probe was inserted directly into the topsoil for about 5 cm.

Plant density of *P. australis* stands was assessed counting the number of shoots within a square plot of 0.25 m². The plant density was then expressed as the number of stems per m² (Warren et al., 2001). Within the sampling site, five plants were randomly selected for measuring the average plant height. The height of each plant shoot was recorded from the base of the collar to the base of the last internode. Fieldwork was conducted between June and July 2024 during neap tides.

From the same plants used for height measurements, the sixth fully expanded leaf from the apex was collected for determination of specific leaf area (SLA). Roots of *P. australis* were also collected, and water from the same station was sampled for subsequent root exudation rate determination. At each sampling site, a soil sample of about ~100 cm² of surface area and 25 cm depth was collected for laboratory analysis. All materials were sealed in plastic bags, transported to the laboratory in a portable refrigerator, and stored at 4 °C until processing. The soil subsample designated for acid-volatile sulphide (AVS) quantification was processed immediately, as well as root porosity and root exudation of citric and malic acids. The remaining roots were air-dried for later iron-plaque quantification.

## 2.3 Physicochemical characterisation of soil samples

Within 24 h from sampling, the soil sample collected in the field was used for acid volatile sulphides (AVS) determination, using a modified version of the procedure outlined by Pellegrini et al. (2018). Specifically, a portion of each soil sample was fresh-weighed and placed into a 250 mL screw-cap jar. Filter paper strips (Whatman No. 1) impregnated with 1.5 M $Pb(NO_3)_2$ solution were clipped to the jar cap. Samples were acidified (6 M HCl), sealed, gently swirled (~ 15 s), and left for ~3 min; the strip colour was then matched to $Na_2S_9H_2O$ reference charts to determine AVS molar concentrations. Additionally, another aliquot of the soil sample was used to determine soil moisture content. Sulphide concentrations were then expressed as μmol of acid volatile sulphides (AVS) per gram of dry soil.

Remaining soil samples were air dried for measuring soil pH and EC, the content of carbonate and of soil organic matter fractions, i.e. the hydrophilic and the hydrophobic

fractions. Soil pH was measured in water suspension 1:2.5 *w/v* (soil to DI water ratio) using a glass probe (Crison Instruments, Barcelona, Spain), while soil EC was determined on a 1:5 w/v ratio (soil to DI water extract) with a Xs Cond 7 Vio conductivity meter (Crison Instruments, Barcelona, Spain). Soil carbonate content was determined using the Scheibler-Dietrich calcimeter (Austrian Standards International, 1999). Total organic carbon and the hydrophilic organic fraction were determined after alkaline extraction and subsequent PVP-adsorption fractionation, respectively (Lowe, 1975; IHSS protocol). Specifically, soil samples were treated with a 0.1 M NaOH in a 1:10 ratio (soil to extractant). The mixture was shaken for 4 h, with 0.3 M KCl added during the last hour for facilitating the settling of clay overnight. Samples were then centrifuged at 10,000 rpm for 30 minutes. The supernatant was collected and one aliquot for each sample was taken and stored for Total Organic Carbon (TOC) analysis (pH adjusted to 7 prior to analysis). This represents the sum of hydrophilic and hydrophobic organic fractions of soil samples. The pH of the remaining supernatant was then adjusted to 1, left to settle overnight, and centrifuged to collect the supernatant. Again, the supernatant was collected and one aliquot for each sample was taken and stored for TOC analysis, in order to exactly quantify the organic carbon in solution and successively being able to calculate the abundance of the hydrophobic fraction. Fractionation was performed on the supernatant using polyvinylpyrrolidone (PVP) columns. The columns were sequentially washed with Milli-Q water, 0.5 M NaOH, Milli-Q water (twice), and 0.05 M $H_2SO_4$ (twice), and successively samples were passed through, followed by 5 mL of Milli-Q water. The eluate, representing the hydrophilic organic fraction, was adjusted to a neutral pH just prior the analyses at a TOC analyzer (Shimadzu, Kyoto, Japan). At this point, the hydrophobic fraction was determined by difference.

## 2.4 Plant morphological and physiological traits

Within 24 h of sampling, about five roots were processed for citric and malic acid leakage and for tissue porosity analyses. Approximately 100 mg of intact tips of adventitious roots were collected and placed in 50 mL tubes filled with filtered water collected from the corresponding sampling site. After mechanical shake for 24 h, the root tips removed and the solution stored in a freezer for subsequent analysis of citric and malic acid contents. The roots were oven-dried at 60 °C for 2 days, and successively weighted. Citrate concentration in solution was measured as NADH oxidation (Bergmeyer, 1974) using the Megazyme Citric

acid assay kit (Bray Business Park, Bray, Co.). The decrease in absorbance was detected at 340 nm by a VICTOR3 Multilabel Counter Plate Reader (Perkin-Elmer, USA). The citrate concentration in the samples was calculated using a calibration curve obtained with the standard solution provided with the enzymatic kit and by correcting the values obtained for the samples dry weight. Root leakage was assessed for both citric and malic acids; however, malic acid was consistently below the detection limit, and only citrate was quantifiable. This outcome was consistent with reports for marsh species, including *P. australis*, in which the low-molecular-weight organic acid spectrum is dominated by oxalate and citrate, while malate is frequently not detected (Mucha et al., 2010; Rocha et al., 2015).

Tissue porosity of adventitious roots of *P. australis* was measured using the pycnometer method described by Jensen et al. (1969). A 25 mL pycnometer (Isolab GmbH, Germany) was filled with DI water and weighed. Plant roots (~ 0.05 g fresh mass) were gently rinsed and wiped before weighing. The root tissue was then placed into the water-filled pycnometer, and the combined weight was recorded. Successively, the roots were retrieved and ground with a mortar and pestle, and the resulting homogenate was weighed in the pycnometer filled with DI water. The water temperature was maintained constant at 20 °C throughout all measurements. Root porosity was calculated using the formula provided by Jensen et al. (1969), which considers the changing in weight in presence or absence of air in the intact or squeezed plant tissue, respectively.

The remaining roots were air dried at room temperature and used to quantify Fe amount in the plaque following the cold dithionite – citrate – bicarbonate extraction (DCB) method by Crowder & Taylor (1983). The total Fe content was measured on filtered solutions by inductively coupled plasma-optical emission spectrometry (ICP-OES). Data were reported as μg Fe $g^{-1}$ dry root biomass.

To calculate SLA, five leaves from each station were press-dried and scanned. Images were analysed with ImageJ Fiji software (Schindelin et al., 2012) to determine leaf area and length. The leaves were oven-dried at 70 °C for 72 hours to measure their dry weight, then SLA was calculated as the ratio of the one-sided leaf area to its oven-dry mass. Data were presented as $cm^2$ $g^{-1}$.

## 2.5 Statistical analysis

Structured equation models (SEM) were performed to assess the influence of plant and soil properties on root plaque formation along salinity gradients. These models are a multivariate statistical framework integrating multiple regression equations to evaluate networks of direct and indirect causal relationships among observed and latent variables (Bollen, 1989; Grace, 2006). SEM allow the simultaneous testing of pathways hypothesized from prior knowledge, quantifying both the strength and direction of interactions within a system. In this approach, relationships are represented as a path diagram, which is then evaluated against empirical data using goodness-of-fit criteria and information-theoretic metrics. Specifically, piecewise SEM enable the inclusion of mixed-effects models, non-normal data structures, and hierarchical designs commonly encountered in ecological studies (Shipley, 2009; Lefcheck, 2016).

In our case, the model was run using the "piecewiseSEM" package v. 2.3.0.1 (Lefcheck, 2016) after assessing data normality and variables collinearity by the variance inflation factor ("performance" R package, Lüdecke et al., 2021), with highly correlated and redundant predictors screened out by excluding variables with high variance inflation factor (VIF>2) to minimize multicollinearity within the selected variables. River location (2 stations) and sampling day (4 days) were included as random factors to avoid scale and site dependent effects. Specifically, this approach considers that samples collected along the same transect and within the same river are more likely to be similar each other than with samples from the different river. The Akaike information criterion corrected for small sample sizes (AICc), was preliminary used for the best model selection (Supplementary material Figure S2): the final model showed the lowest AICc (Burnham and Anderson 2004). The tested relationships of the selected model are reported as a graphical path in Figure 2. To visualize the statistically significant relationships of each model within the SEM network, plots were generated using the visreg function from the "visreg" package (Breheny and Burchett, 2017).

In constructing the *a priori* model, decisions were made regarding the direction of each relationship to be tested (SEM constrain). We primarily hypothesized that saltwater could affect iron plaque deposition directly, following the stabilization of $Fe^{3+}$ in solution by chloride and organic ligands (Liu and Millero, 2002). EC can also work indirectly through osmotic stress and specific ion toxicity, triggering variations in the root exudation processes

(Abdel-Latef & Chaoxing, 2014; Rohrbacher and St-Arnaud, 2016), reducing functional root porosity and radial oxygen loss from roots, or causing plant death and therefore lowering the stand density, further decreasing the plant-mediated $O_2$ supply (Amsberry et al., 2000; Vasquez et al., 2005) and $Fe^{2+}$ oxidation. Moreover, seawater intrusion raises $SO_4^{2-}$ inputs, stimulating sulphate reduction, lowering Eh, and increasing AVS microbial production (Howard & Mendelssohn, 1999; Chambers et al., 2014).

Eh can directly influence Fe mobility by reducing the $Fe^{3+}$ to $Fe^{2+}$ at increasing flooding stress (Reddy et al., 2022). Low Eh also promotes AVS formation in brackish wetlands richer in sulphate compared to freshwaters (Howard & Mendelssohn, 1999). Conversely, soil anoxia induces root aerenchyma formation, increasing root porosity and root oxygen loss (ROL) under flood stress (Pedersen et al., 2021), although extreme reducing conditions can still constrain plant growth (Pezeshki, 2001). Calcium carbonate is known to buffer soil pH (Brambati, 1968), which, at subalkaline values and under soil anoxic conditions, favours $Fe^{2+}$ as the stable phase in solution and therefore the potential formation of plaque. Soil carbonates may have a direct influence on plaque abundance, since St-Cyr & Crowder (1988) reported that the iron plaque formation was strictly related to the iron bound to carbonate in soil, hypothesizing that the oxidation of siderite ($FeCO_3$) in the rhizosphere resulted in the precipitation of goethite on the roots. Root exudation (citric acid used as a proxy) was expected to directly cause a reduction in plaque formation through the complexation of hydroxyl groups with Fe that causes the migration of Fe oxides (Gutteridge, 1991; Chen et al., 2016), or indirectly following the rhizosphere acidification and the favoured reduction of $Fe^{3+}$ to $Fe^{2+}$ (Guo and Cutright, 2014). Soil sulphides can form FeS and compete with plaque formation (Rickard and Luther, 2007), and, at high concentration, can reduce root exudation by impairing root tip vitality, being $H_2S$ a phytotoxin (Lamers et al., 2013). Increases in root porosity help plant survival, and both plant density and root porosity were expected to favour the amount of oxygen released in the rhizosphere, hence enhancing the amount of iron deposition on root surfaces. The organic matter fractions were included in the model for their potential to influence iron availability in the soil by reducing it through metal complexation or, in the case of the hydrophobic fraction, by indirectly increasing it via boosting microbial activity and oxygen demand, thus lowering soil Eh (Jones et al., 1996; Christensen & Sand – Jensen, 1998). Conversely, hydrophilic organic C may indirectly favour plaque abundance by supporting plant growth and density, given its

documented positive effects on nutrient recycling by microorganisms and element availability for plants (Li et al., 2018).

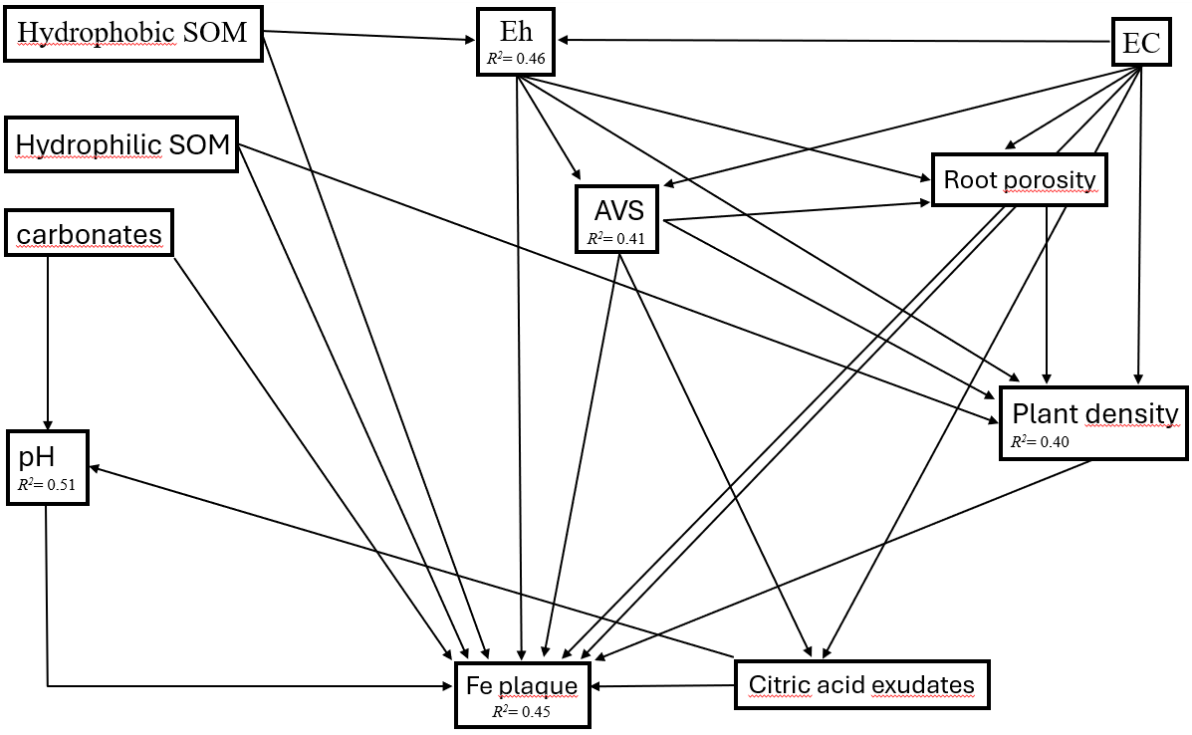


**Figure 2.** Structural equation model (SEM) illustrating the hypothesized direct and indirect relationships among soil and plant variables influencing root iron plaque formation in *P. australis*.

# 3. Results

## 3.1 Salinity effects on soil properties

Data regarding chemical properties variations inside the sampling area are shown in Table 1 and detailed for the 30 stations in Supplementary Tables S2, S3. Soil electrical conductivity (EC) held consistent variations along the Cormor and Stella rivers, ranging from ~0.1 to 20.0 dS $m^{-1}$ across the sampling sites. As expected, EC values gradually decreased moving upstream from the river mouth, with some notable exceptions recorded at upstream stations for both rivers (Supplementary material Table S2, 8.45 dS $m^{-1}$ and 8.71 dS $m^{-1}$, respectively) along Cormor River and another example (Supplementary material Table S3, 1.53 dS $m^{-1}$) along Stella River. Soil Eh values showed a variation trend which was opposite than those

regarding soil EC, going from strong reducing values near the river mouths (below −400 mV) to positive values upstream (Table 1). This trend was more consistent along Stella River than along Cormor River, where some upstream stations appeared to be subjected to soil anoxic conditions (Supplementary material Table S2).

High concentrations of AVS were measured at stations with high EC, particularly near the river mouths, with concentrations more than 50% higher than in upstream stations for both rivers (Supplementary material Tables S2, S3).

Soil pH in the sampling area was overall neutral to neutral-alkaline (Table 1), following an increasing trend along the systems, from slightly acidic conditions downstream to neutral–alkaline conditions upstream (Supplementary material S2, S3). In three stations along Stella River values were lower (~ 5.5, Supplementary material Table S3), and in two of these stations no carbonates were measured in the soil. Soil carbonates pattern kept following that of soil pH, with upstream stations showing higher carbonate contents (Supplementary material Tables S2, S3). Notably, soil content of carbonates was significantly different between the two rivers, with Cormor River having about 5 times more carbonates (Table 1).

Regarding organic matter fractions, there were not large differences between the two rivers (Table 1). For both, hydrophobic OM tended to be more abundant at upstream freshwater stations, whereas the hydrophilic fraction showed no clear longitudinal trend (Supplementary material Tables S2, S3).

**Table 1.** Mean values of the variables studied, based on 30 sampling sites at the Cormor – Stella delta system. Data are presented as mean ± standard deviation for each parameter. OM stands for organic matter.

| Variable | Unit | Cormor river mouth | Stella river mouth |
|---|---|---|---|
| Carbonate content | g $Kg^{-1}$ | 213.2 ± 78.0 | 41.5 ± 32.2 |
| Soil conductivity (EC) | dS $m^{-1}$ | 5.7 ± 5.6 | 6.4 ± 6.1 |
| Soil pH | | 7. 6 ± 0.4 | 7.0 ± 0.7 |
| Soil redox potential | mV | -176.7 ± 162.5 | -230.1 ± 200.7 |
| Acid Volatile Sulphides (AVS) | μmol $g^{-1}$ dry soil | 15.3 ± 17.9 | 24.4 ± 59.8 |
| Hydrophobic OM | mg $g^{-1}$ dry root | 5.0 ± 2.0 | 6.9 ± 3.5 |
| Hydrophilic OM | mg $g^{-1}$ dry root | 2.4 ± 0.5 | 3.16 ± 1.1 |
| Plant stand density | plants $m^{-2}$ | 161.1 ± 68.7 | 149.1 ± 71.0 |
| Plant height | cm | 191.27 ± 76.6 | 122.86 ± 73.54 |
| Specific Leaf Area (SLA) | $cm^2\ g^{-1}$ | 114.41 ± 14.6 | 122.86 ± 17.59 |
| Root citric acid leakage | mg $mg^{-1}$ dry root | 0.01 ± 0.0008 | 0.01 ± 0.001 |
| Root malic acid leakage | mg $mg^{-1}$ dry root | b.d.l. | |
| Root porosity | % | 42.8 ± 6.9 | 35.1 ± 8.2 |
| Root iron plaque | mg Fe $g^{-1}$ dry root | 5.34 ± 6.49 | 3.34 ± 2.51 |

## 3.2 Plant traits responses across the salinity gradient

*P. australis* traits varied along the salinity gradient. Mean data are shown in Table 1, while their spatial variation along Cormor River and Stella River is reported in Supplementary Tables S2, S3. Across the 30 stations, plant stand density showed clear spatial variability and tended to peak at intermediate positions along both transects (Supplementary mat Tables S2, S3, 316 plants $m^{-2}$ in Cormor and 236 plants $m^{-2}$ in Stella). These values fall within published ranges for dense *P. australis* stands. High densities of about 200 plants $m^{-2}$ were reported for natural dense canopies in northern Poland (Hardej and Ozimek, 2002), while studies in

North America reported ranges between 13-125 plants $m^{-2}$ (Meyerson et al., 2000) and studies documenting reed-bed decline ~ 46 stems $m^{-2}$ in Central Italy (Gigante et al., 2011).

Plant height also varied across stations broadly mirroring the density peaks at some mid-downstream stations (Supplementary mat Tables S2, S3). Mean values of stations near the river mouths (~1.2-1.9 m) lie within the more typical ~ 2-3.5 m range reported for European stands (Čížková et al., 2023). SLA values were more consistent along the transects, not following a specific changing pattern.

For belowground traits, root porosity ranged from ~20% to ~55% with no consistent longitudinal trend (Table 1; S2–S3). Root leakage was monitored for citric and malic acids. Results revealed that malate was consistently below the detection limit in our samples, whereas citrate was quantifiable, so we hereafter refer to root citric acid exudation (values in Table 1; S2–S3). Yet, its values remained relatively stable across the sampling area, with only minor fluctuations (Supplementary mat Tables S2, S3).

## 3.3 Direct and indirect effects of salinity and soil–plant relationships on iron plaque formation

Across the 30 stations, the amount of iron plaque on *Phragmites australis* roots spanned from 0.52 mg Fe $g^{-1}$ dry root to 9.39 mg Fe $g^{-1}$, with a maximum of 26.89 mg Fe $g^{-1}$ recorded in the most downward station along Cormor River. The distribution of values per station and per river is reported in Table 1 and Supplementary Tables S2, S3. We then used structural equation modelling (Figure 3) to relate this observed variability in plaque to soil and plant variables across the gradient.

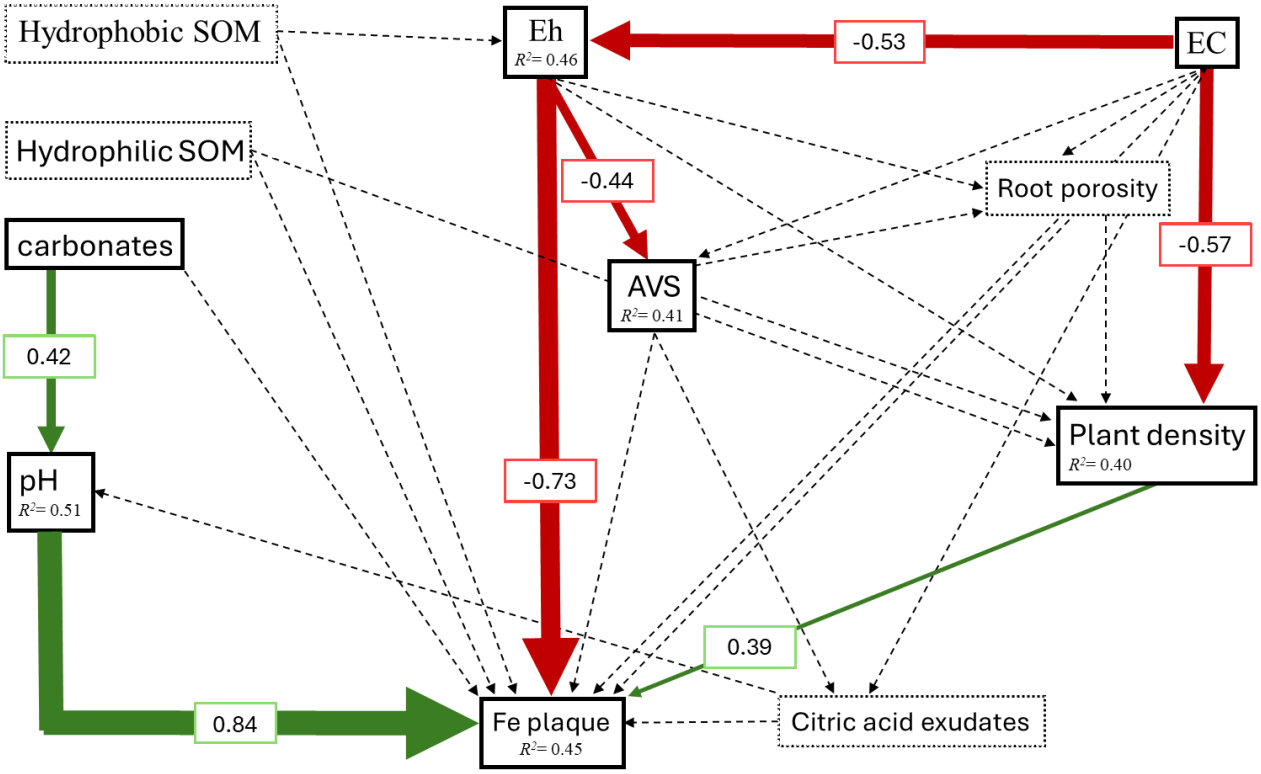


**Figure 3.** Results of the tested structural equation modelling. Green and red arrows respectively refer to statistically significant positive and negative relationships. Arrow width is proportional to the size of the correlation, reported in the text box. Dashed lines refer to non-significant relationships. Conditional $R^2$ values of models are shown within boxes.

Within the model, three relationships resulted statistically significant in describing how plaque abundance varied along the two rivers. First, plaque increased with soil pH, as displayed in Figure 4a. The regression model accounted for a $R^2$ of 0.45 and reported for a positive influence of pH in plaque abundance. Second, plaque held a negative relation with soil redox potential, as shown in Figure 4b, indicating higher plaque values associated with more anoxic conditions. Third, plaque responded non-linearly to plant stand density, with a second-order trend that peaked at intermediate plant densities around ~230 plants $m^{-2}$ (Figure 4c).

Although soil EC did not affect directly iron plaque (Figure 3), it had an indirect effect through both the soil and plant branches of the model. Specifically, EC was negatively related both to soil Eh (Supplementary mat Figure S7) and to plant stand density in the model (Supplementary Figure S6), with $R^2$ of 0.46 and 0.40, respectively. Both these variables

were, in turn, related to plaque variation trends along the two rivers, as already stated (Figure 3). Two further relationships emerged as significant paths inside the model, which however did not directly involve the plaque amounts measured in the 30 sampling sites. Carbonate content was positively related to soil pH (Supplementary material Figure S8) with a correlation value of 0.42 and a $R^2 = 0.51$, while soil Eh was negatively related to AVS with a correlation value of -0.44 and a $R^2 = 0.41$ (Supplementary material Figure S5).

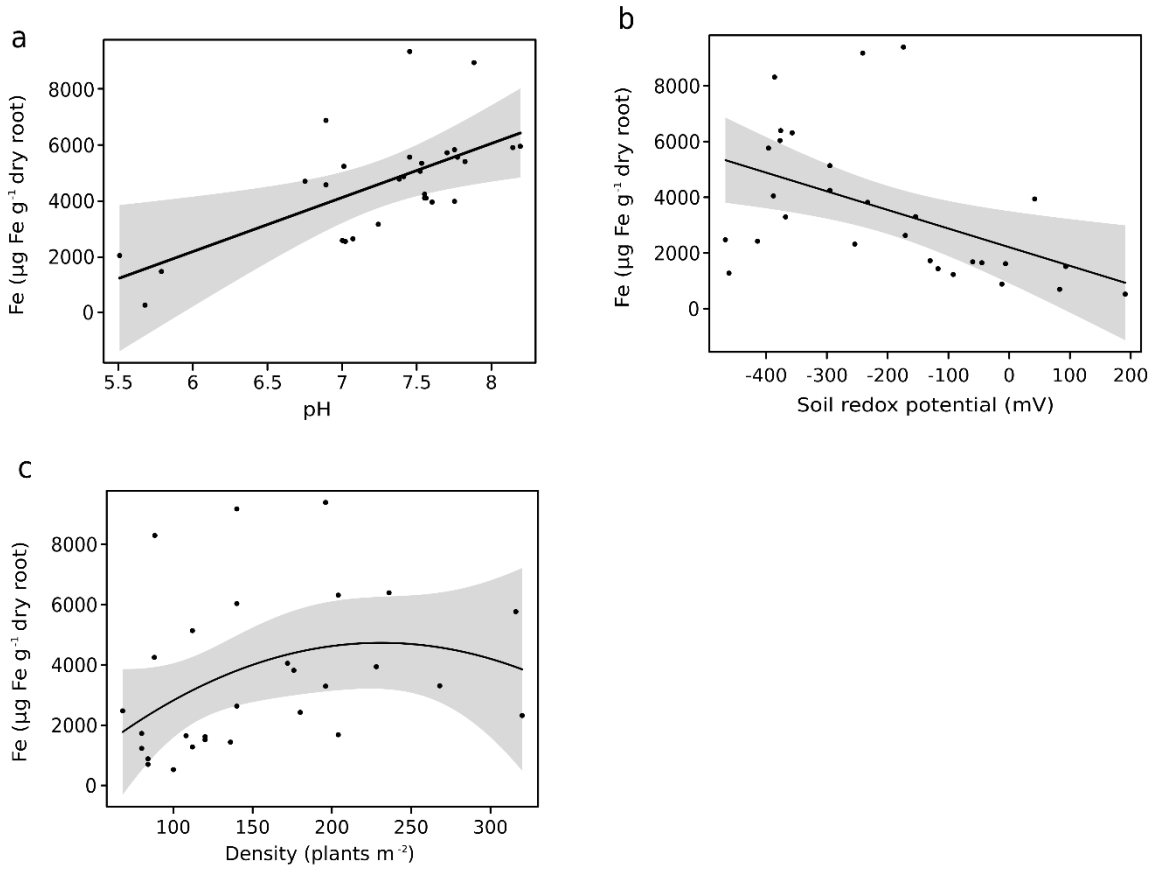


**Figure 4.** Effect plots of the relations between Fe deposition and pH (a), soil Eh (b) and plant stand density (c) calculated with the linear mixed-effects model included in the piecewise structural equation modelling analysis. The solid black line represents a smoothed regression fit. Confidence intervals (95%) are shown as the shaded areas.

# 4. Discussion

## 4.1 Impacts of salinity and soil properties on plaque abundance

The aim of this study was to assess how multiple soil physicochemical properties and plant traits of *Phragmites australis* influenced iron plaque abundance along salinity gradients. From SEM model outcomes, salinity did not have a direct effect on iron plaque abundance but acted indirectly by negatively influencing both soil Eh and plant density. In the case of soil Eh, two are the possible concurring mechanisms. The first refers to the sulphate enrichment in brackish waters compared to river freshwaters, increasing the occurrence of this alternative electron acceptor for anaerobic microbial respiration processes in anoxic sediments inhabited by the common reed, implying the lowering of the soil redox potential (Giblin & Howarth, 1984; Pezeshki & DeLaune, 2012). The second mechanism is related to the increasing ionic strength associated to the increased salinity. As described by Bethke (2007), a change in ionic strength affects soil potential because it influences the activity of enzymes used by microorganisms in electron transfer reactions, as it alters their conformation. The activity of these enzymes, and consequently the energy yield from the reactions they catalyse, is negatively affected by ionic strength. In addition, salinity indirectly influenced plaque abundance by reducing plant density, a process widely described in literature, thus reducing rhizosphere aeration. High salt concentrations impose osmotic stress in plants, leading to impaired growth and mortality of less adapted species (Munns & Tester, 2008; Gharsallah et al., 2016). This is common in wetland habitats, where vegetation composition is highly subjected to variations in soil anoxia and salinity (Achenbach et al., 2013; Herbert et al., 2015).

Among the physicochemical factors measured, soil Eh had a direct influence on plaque abundance, confirming that more reducing conditions increase the abundance of $Fe^{2+}$ in the soil solution and, therefore, the potential oxidation to $Fe^{3+}$ driven by root ROL (Zhang et al., 2020). Soil Eh acts together with pH to control iron speciation, as at neutral or subalkaline pH values, increasing Eh promotes $Fe^{2+}$ in soil solution and the subsequent formation of ferric oxyhydroxides, whereas under strong reducing and acidic conditions Fe remains in solution (Morgan & Lahav, 2007). The significant role of pH, as arisen from the SEM model, is also consistent with previous studies showing that alkaline or carbonate-rich soils enhance Fe precipitation and plaque formation (Crowder & Macfie, 2011).

Although organic matter is often reported to affect Fe cycling, by favouring the plaque formation through microbial-driven oxygen consumption (Liu et al., 2021) or by contrasting the process through organic complexation of Fe (Jones et al., 1996), in our experiment neither of the two organic matter fractions resulted in any significant effect on plaque abundance. Its influence may have been masked by the dominant effects of salinity, as described by Morrissey et al. (2014). They reported that even a modest salinity increase in wetlands can enhance microbial decomposition rates and can strongly reduce soil organic matter accumulation, which could also explain the low variability for both fractions in our dataset. Similarly, AVS content, although negatively affected by soil Eh, did not show any direct relationship with plaque abundance. High AVS concentrations refer to strong reducing conditions and large sulphate reduction. In such environments, $Fe^{2+}$ can partially precipitate onto the roots as FeS rather than as $Fe^{3+}$ oxides, resulting in the formation of FeS coatings instead of Fe plaques (LaFond-Hudson et al., 2018). In our experiment, we did not discern between iron plaques and FeS deposits on root surfaces. Nevertheless, some of the older roots appeared very dark which is a typical sign of the occurrence of these black deposits (Seyfferth et al., 2010).

## 4.2 Role of *P. australis* in modulating iron plaque abundance

The density of *P. australis* individuals along Cormor and Stella rivers resulted as the only plant trait significantly influencing root iron plaque formation. Here, the relation between the two variables followed a non-linear pattern (Fig. 4c), with plaque amount increasing from low to intermediate densities and then declining at the highest plant stand densities. A possible explanation relies on the greater resulting root biomass enhancing root radial oxygen loss to the rhizosphere at increasing densities that turns to competition for space and nutrients above a certain threshold of stand density. The accelerated $Fe^{2+}$ oxidation and plaque formation at increasing soil aeration, due to root ROL (Chen et al., 1980; Colmer, 2003; Khan et al., 2016), slow down when interspecific competition occurs. In fact, competition for belowground resources has been reported to limit root development and reduce the capacity of wetland plants to transport oxygen to the rhizosphere, thereby altering soil redox conditions (Wetzel & van der Valk, 1998; Pezeshki & DeLaune, 2012).

By contrast, belowground plant traits did not play a significant role in determining plaque abundance in our study. The fact that root porosity did not emerge as a significant parameter

could be related to the presence and modulation in tightness of root apoplastic barriers. These refer to depositions of lignin, suberin and waxes in root apoplast, which limit oxygen diffusion from roots to rhizosphere. Apoplastic barriers strongly influence root ROL ability (Ejiri & Shiono, 2019; Peralta Ogorek et al., 2023) and are constitutively formed in common reed roots (Armstrong et al., 2000). Literature reports that environmental conditions, such as anoxia and the presence of organic acids, can increase the tightness of this barrier by inducing suberin and lignin deposition in the exodermis and endodermis (Colmer, 2003; Armstrong & Armstrong, 2005), the increase observed instead in root porosity resulting from aerenchyma formation (Malik et al., 2003; Konnerup et al., 2016). This entails a counterbalance of root ROL ability that might be responsible of the non-significant output of our model.

Similarly to root porosity, the root exudation of citric acid did not significantly influence plaque abundance. Levels remained stable across the sampling area, and while it is known that low molecular weight organic acids can influence Fe cycling by chelation and driving changes in soil pH (Guo & Cutright, 2014; Adeleke et al., 2017), here their effect appears secondary compared to other plant and soil parameters. Citric acid concentration measured in our extracts had values ranging between 3.0 μM and 3.5 μM, that corresponded to the lower levels reported for di- and tricarboxylic acids in wetland soils (0–50 μM; Adeleke et al., 2017). Studies highlighting significant impacts of organic acids on Fe cycle have instead applied exogenous organic acids with concentrations between 0.5 mM and 2.0 mM (Meng et al., 2022; Yang et al., 2023), therefore two to three orders of magnitude higher than those quantified in our work. This difference suggests that the concentration of root-derived organic acids in our case was insufficient to substantially alter rhizosphere redox equilibria and consequently iron plaque formation.

# 5. Conclusions

Our study demonstrates that salinity exerts a strong indirect influence on iron plaque formation on *P. australis* roots, by negatively controlling soil redox potential and plant density. Among the soil parameters, soil Eh and pH emerged as the main physicochemical factors controlling plaque abundance. More reducing conditions were associated with greater plaque accumulation, due to high availability of $Fe^{2+}$ in the rhizosphere. Likewise, higher pH values favoured $Fe^{3+}$ precipitation, confirming the coupled control of Eh and pH on iron speciation in flooded sediments. Organic matter and AVS did not show a detectable effect on plaque abundance, likely due to their limited variability across the study area. This may be related to salinity driven mineralization processes and the formation of FeS under reducing conditions, which can mask their influence on iron plaque formation.

Plant stand density significantly influenced plaque abundance, showing an increase up to intermediate densities followed by a decline at higher ones. On the contrary, root porosity and citric acid exudation did not show any significant relationship with plaque abundance, which effect can be hidden by a major role of root ROL barriers, limiting the $O_2$ passive flow outside the root, or the prevailing effect of other more effective organic acid excluded from our initial hypothesis. Overall, these results highlight how salinity can indirectly modulate multiple biogeochemical equilibria in brackish water systems, with some (i.e. Eh and stand density) working as the main driving factors for iron plaque formation.

# *Chapter 2*

# Preface

The work focused deeper on elucidating the mechanism behind the mitigation effect of salt stress brought by soil organic matter, a process that so far has been only partially demonstrated. Specifically, a laboratory experiment was conducted with model solutions exploiting four natural derived humic acids and one artificial polyelectrolyte to test their capacity to counteract the increase in electrical conductivity and pH values imposed by $Na_2CO_3$ and NaCl, respectively.

Our results showed that all the humic or humic-like substances could effectively mitigate the osmotic effects of $Na_2CO_3$, while showing negligible influence under NaCl. We proposed a mechanism for the contrasting behaviour between the two salts, attributed to the different chemical equilibria involved, involving the pH-dependent dissociation of humic functional groups.

This work was published on 25 September 2025 in the "*Sustainability"* journal. (**https://doi.org/10.3390/su17198621**).

# *The potential role of humic substances in the amelioration of saline soils and its affecting factors*

## 1. Introduction

Soil salinization is a major driver of agricultural land degradation worldwide (Daliakopoulos et al., 2016; Shahid et al., 2018b; Sahab et al., 2021): it is estimated that salt-affected soils occupy more than 20% of global irrigated land, with an estimated annual economic loss of US$ 27.3 billion (Qadir et al., 2014). Salinization, in fact, reduces crop yields causing osmotic stress and specific ion toxicity (Zörb et al., 2019). In salt-affected soils, plant growth is highly affected by the reduced water potential that induces osmotic stress and ion imbalance in plants (Abd El-Samad & Shadad, 1996; Xiong & Zhu, 2002; Betzen et al., 2019). Future projections forecast an increase of up to 1.5 million ha of soils experiencing worsening salt accumulation within a few decades (FAO, 2021).

Coastal and sub-arid regions are both susceptible to salt accumulation but differ both for the causes of salinization and for the composition of soluble salts. In arid and semi-arid regions, excess soluble salts predominantly arise from rock weathering and paucity of precipitations combined with high evapotranspiration rates (Jordán et al., 2004; Qadir et al., 2014). Here, carbonates predominate and because of the low solubility of calcium carbonate which precipitates, sodium carbonate often prevails in the soil solution with other salts represented by calcium and magnesium chlorides and sulphates (Naorem et al., 2023). Saline-alkali soils (Richards, 1954) are typically strongly affected by the high solubility of Na2CO3 and the high level of exchangeable sodium (Choudhary & Kharche, 2018), so that their scarce buffering capacity causes a dramatic increase in soil pH, which can easily reach pH values above 10 (Chhabra, 2004).

Conversely, in coastal soils, salinization is primarily driven by marine aerosol and saline water intrusion (Bates et al., 2008; Shrivastava & Kumar, 2015). The soluble salts present in these soils are dominated by chlorides, with NaCl and MgCl2 reaching about 83% of total dissolved salts. In this case, as in the sodic saline soils, the high exchangeable sodium (>15%

Cation Exchange Capacity) results in unbalanced nutrient uptake for soil microorganisms and plants (Mazhar et al., 2022).

A wide variety of approaches is currently applied to alleviate the negative effects of high salinity levels: besides the removal of salts by leaching with good quality irrigation water (Shahid et al., 2018b; Wu et al., 2024) combined with the correction of soil pH, the use of organic amendments such as compost or manure, which seem to efficiently mitigate the alkalinity of sodic soils (Lakhdar et al., 2009) and the adverse effects on crop yields, is a valuable and sustainable strategy. The application of organic amendments remediates nutrient imbalance (Lakhdar et al., 2009; Ait-El-Mokhtar et al., 2020) and improves soil water retention and cation exchange capacity, sustaining plant growth and soil microbial activity (Ouni et al., 2014), but can also have positive effects on salt stress.

The application of organic amendments was often reported to successfully ameliorate saline soils (Li et al., 2022). Although debates persist on the possible increase in Na+ and Cl- concentrations after the application of some salt-rich organic amendments (Gondek et al., 2020), multiple studies have highlighted the benefits of organic amendments on salinity tolerance in plants (Ha-Tran et al., 2021; Kerbab et al., 2021; Hoque et al., 2023). Addition of organic materials to soil, especially the more humified sources including animal manure and compost, but also biochar, straw, and other amendments, has been proven to be beneficial against salt stress and the consequent reduction in crop yields. For instance, Shukry et al. (Shukry et al., 2023) reported that rice growing in a saline soil treated with 40 mg L-1 of humic acids (HA) exhibited increased plant height and dry weight. Atero-Calvo et al. (Atero-Calvo et al., 2024) documented a consistent reduction in the oxidative stress of lettuce plants after treatment with a commercial leonardite based product, while Vitti et al. (Vitti et al., 2024) observed a strong increase in the germination capacity and root growth of Lepidium sativum after application of humic substances (HS) extracted from compost. These results were imputed to a possible enhanced ionic balance caused by a lower Na uptake and to an improved potassium level, together with the activation of plant antioxidant defenses or hormone-like activity of HS (Abu-Ria et al., 2023; Malik et al., 2023; Atero-Calvo et al., 2024).

The complex positive impact of organic matter addition on saline soil productivity and in particular, its mechanisms of action have been so far, scarcely investigated. Apart from the well-known positive effects on soil physical characteristics and nutrient availability, the

effecting factors involved in the amelioration of saline soils by organic amendments are still largely unknown. Among the components contained in organic amendments, or formed within the soil as a consequence of their application, humic substances have been proven to enhance resistance to osmotic stress in plants and to increase the availability of nutrients (Delgado et al., 2002; Yang et al., 2021). Many studies have shown that HA, which also stimulate germination and growth by increasing membrane permeability and facilitating nutrient uptake (Dell'Amico et al., 1994; Saidimoradi et al., 2019), can be used as biostimulants and alleviate stress to seeds and seedlings (Mahdy & Fathi, 2012; Mahmood et al., 2017; Kaya et al., 2018; Maiwan et al., 2023). However, it is reasonable to presume that there are other ways by which humic substances can reduce the impact of large concentrations of dissolved salts.

This study aims at elucidating the mechanism by which humic substances, by acting directly on the osmolarity of the soil solution, can alleviate its effects on plants and microorganisms. We hypothesized that this mechanism cannot be only ascribed to the biostimulant action of HS on plants metabolism, that alleviates salinity stress symptoms, but that it also resides in an abiotic direct effect on the osmolarity of the soil solution. In fact, the ionisable functional groups on the HS molecules can potentially interact with the dissolved osmolytes, reducing their concentration and thereby their mobility, exerting a direct mitigation on the osmotic potential experienced by roots. Specifically, humic acids (HA), which are composed of less polar and less soluble molecules (Olk et al., 2019), but have their ionizable moieties solvated and in dynamic equilibrium with the soil solution, may be particularly effective. Upon dissociation, these moieties release protons that are neutralized by the alkalinity of the soil solution. The negative charges, thus left uncompensated, are able to attract cationic osmolytes within the electrostatic double layer, thereby virtually subtracting them from the soil solution and the contact with plant roots. Our hypothesis is therefore that HA can have a stronger effect towards Na2CO3 than towards NaCl because the more alkaline pH supports the further dissociation of HA acidic functional groups and the released protons may shift the equilibrium of carbonate ions towards the formation of carbon dioxide.

In this work, we performed a series of laboratory experiments in which micro-additions of the two salts, namely $Na_2CO_3$ and NaCl, that typically predominate in the soil solution of saline soils, were added to de-aerated solutions containing or not different types of HA, monitoring pH and electrical conductivity (EC) to quantify the effects of HA on the osmolarity of solutions. We also tested the effect of HA on the germinability and root

elongation of *Zea mays* L., by growing seeds and seedlings in $Na_2CO_3$ or NaCl solutions in absence or presence of HA, in order to evaluate the potential mitigation ability of HA on germination and root growth of seedlings.

# 2. Materials and Methods

## 2.1 HA sources

Four HA and an anionic synthetic polyelectrolyte: polyacrylic acid (PAA), were used to investigate mechanisms of potential mitigation effects on salt stress. PAA was chosen because it has a well characterized chemical structure and properties and, as a potassium salt, it is used in agriculture to improve soil structure (Teodorescu et al., 2009; Wilske et al., 2014). PAA and Aldrich HA were purchased from Sigma Aldrich, whereas soil (EHA) and peat humic acids (PHA) were extracted following the procedure suggested by the IHSS from, respectively, the Elliott silt loam soil and the Pahokee (Florida) Peat materials provided by the IHSS. Compost humic acids (CHA) were obtained from a well matured sample of compost obtained from the anaerobically digested separately collected organic fraction of municipal solid waste, provided by Bioman SpA (Maniago, Italy). The compost was shaken for one hour in 0.1 M NaOH plus 0.1 M Na4P2O7 at a 1:10 ratio (w:v), under N2; to obtain the HA the extract was acidified to pH 1 using concentrated H2SO4. Leonardite humic acids (LHA) purchased from Sigma Aldrich (H16752, Sigma Aldrich), were purified by dissolution in 0.1 M KOH and re-precipitation by adding 6 M HCl. All HA were purified by re-suspension in milliQ water followed by dialysis and freeze-drying in a Scanvac CoolSafe 55 – 4 (LaboGene, Denmark).

## 2.2 Mitigation capacity

The capacity of humic acids to mitigate salinity was tested by means of a DL50 automatic Graphix Titrator (Mettler Toledo, USA), adding stepwise microvolumes (30 µL) of 0.167 M NaCl and 0.213 M Na2CO3 solutions to a cell equipped with a pH electrode connected to the titrator and a conductivity cell connected to a Cond 7 Vio portable conductimeter (XS Instruments, Italy). At the beginning of the experiments the cell was filled with de-aerated milliQ water or solutions containing HA or PAA.

Sodium carbonate (anhydrous, ≥99.5%, Carlo Erba Reagents, Cornaredo, Italy) was oven-dried at 105 °C for 24 h and stored in a desiccator before being used to prepare solutions. Solutions containing HA were prepared by dissolving 50 mg of freeze-dried preparation in a minimum amount of NaOH solution, then adding de-aerated MilliQ water to reach a final concentration of 2.5 mg mL-1. All solutions were then acidified with Amberlite IR-120 H+ resin (39389-20-3, Sigma Aldrich), under a nitrogen atmosphere to prevent $CO_2$ interference, until the lowest possible pH value, which differed for each HA solution, was reached. Before the experiment, solutions were filtered through a 0.2 µm cellulose syringe filter. The final concentrations of dissolved C in the resin treated solutions were quantified with a Shimadzu TOC-V CPN analyzer (Shimadzu, Japan). In the case of NaCl, pH was afterwards corrected to pH ~ 6, to simulate pH levels commonly found in saline coastal soils (e.g. (Chabreck, 1972; Weaver et al., 2004).

The micro-additions were performed every 5 minutes, to allow the pH electrode to reach equilibrium. For sodium carbonate, the endpoint was set to pH ~ 10, which is commonly adopted as the endpoint of ionization for all acidic groups of HA (Pettersson et al., 1989). All experiments were performed in triplicates.

From the obtained graphs, the slopes of EC for solutions without or with HA were retrieved for comparison. In addition, the capability of the HA and PAA to reduce the concentration of free dissolved ions in solution of a given soil was calculated by subtracting the difference between the EC of a solution containing Na2CO3 only and that of a Na2CO3 + HA solution measured at the pH 7.5, from that of the conductivity of a Na2CO3 solution and that of a Na2CO3 + HA solution measured at pH 8.5.

## 2.3 Acid-base titrations

Solutions were prepared by dissolving each HA and the PAA in a minimum volume of 0.1 M NaOH solution, followed by the addition of de-aerated MilliQ water to achieve a final concentration of 2.5 mg $mL^{-1}$. The solution was then acidified to pH 3 using 1 M HCl and immediately titrated. From titration curves, the negative charge from strong (Q1) and weak (Q2) acidic functional groups were calculated following the procedure proposed by Ritchie and Perdue (Ritchie & Perdue, 2003). They represent respectively the total number of negative charge sites developed by an organic polyelectrolyte at pH 8 (Q1) and twice the difference between the number of total negative charge sites at pH 11 and pH 8 (Q2). In

addition, the total amount of ionized groups at pH 7, pH 8.5 and 10 were graphically retrieved.

## 2.4 1H-NMR spectroscopy

$^{1}$H-NMR spectra were acquired using a Bruker Advance III 400 spectrometer equipped with a 5 mm Iprobe operating at 400.13 MHz. The samples were prepared by dissolving 2 mg of each humic or humic-like substance in 0.6 mL of deuterium oxide ($D_2O$) and placed in NMR tubes for analysis.

Spectra were recorded using the zgesgp sequence for selective saturation of the HDO resonance. Experimental parameters were selected as following: relaxation time 2 s, acquisition time 1.39 s, and number of scans 1280, for a total acquisition time of 75 min. The spectra were divided into the following five regions: 0–1.7 ppm, corresponding to terminal methyl and methylene groups of methylene chains, methylene of alicyclic groups and CH2 and CH groups at least two carbons away from aromatic rings or polar functional groups; 1.7–3.0 ppm, corresponding to protons of methyl and methylene groups α to aromatic or carboxylic acid groups; 3.0–5.0 ppm, corresponding to protons α to carbon attached to oxygen groups (polysaccharides or carbohydrates); 5.0–6.5 ppm, corresponding to protons of olefins; and 6.5–9.0 ppm, corresponding to aromatic protons (Wilson, 1981; Gigliotti et al., 1997). The relative intensity of each region was calculated by integrating the areas under the corresponding peaks and expressing them as percentages of the total spectral area.

## 2.5 Germination test

Germination rates and root elongation rates were tested on *Zea mays* seeds (P0423, Pioneer) exposing them to agarose media with increasing levels of salts and humic acids. Aqueous solution containing 1% agarose and three levels of NaCl or $Na_2CO_3$, without or with increasing HA concentrations were prepared in a total of 60 Petri dishes and let to solidify. The three salt levels were, respectively, 0.05 M, 0.1 M, 0.15 M for NaCl and 0.025 M, 0.05 M, 0.125 M for $Na_2CO_3$. CHA quantities were as following: 3 µg $L^{-1}$, 6 µg $L^{-1}$, 12 µg $L^{-1}$, 25 µg $L^{-1}$,50 µg $L^{-1}$, 100 µg $L^{-1}$, 200 µg $L^{-1}$, 400 µg $L^{-1}$, 800 µg $L^{-1}$. The final pH of solutions was set to 6. Mayze seeds were rinsed with distilled water and left to soak overnight in

aerated distilled water and in darkness. About 10 seeds were positioned in each Petri dishes and these were placed on a black background desk. An automated system for image collection (Panasonic Lumix GH5 camera) was set for 72 hours, collecting images every hour (time-lapse mode). Seeds with a visible protruding radicle, at least 1 mm in length, were counted as germinated. The root length was measured on the first four germinated seeds in each plate, after 12 hours from germination. All images were analysed using ImageJ software (Schneider et al., 2012).

The number of germinated seeds was recorded every 3 hours over the 72-hour experimental period.

## 2.6 Statistical analysis

All statistical analyses were conducted using R studio v4.4.3 (R Core Team, 2025).

One-way ANOVA was performed to evaluate significant differences in EC trends slopes between control and experimental treatments. Data normality (Shapiro-Wilk test) and homogeneity of variances (Bartlett's test) were tested across all experimental groups. ANOVA was conducted to determine the effects of HA from different origins and PAA on EC in solutions titrated with Na2CO3 or NaCl. Post-hoc comparisons using Tukey's HSD test was exploited to identify pairwise differences between treatment groups. Data analyses were conducted using the 'aov' and 'TukeyHSD' functions of the 'multcomp' package (Hothorn et al., 2008).

Germination data was computed using the "germinationmetrics" package in R (Aravind et al., 2023). Two-way ANOVA was used to assess significant differences of humic acids concentrations of salt levels on seed germination and root elongation rates, for each salt type ($Na_2CO_3$ or NaCl). Data normality was assessed based on the distribution of model residues. Tukey's post hoc test was used for pairs comparisons. Data analyses were conducted using "lm", 'anova' and 'TukeyHSD' functions of the "stats" (R Core Team, 2025) and 'multcomp' (Hothorn et al., 2008) packages.

# 3. Results

## 3.1 The effect of the type of salt

In Figure 1 we report changes in EC and pH in water and water plus HA solutions during stepwise micro-additions of $Na_2CO_3$. The data obtained from these graphs allowed us to compare the behaviour of HA from different origins and to calculate, by means of specifically devised equations the salinity neutralized by a unit addition of each HA at any given change in pH. A polyelectrolyte of known structure, PAA, which is also sometimes used in agriculture as a salt (potassium polyacrylate) to improve soil structure, was also considered to better understand the mechanisms involved.

Addition of a weak electrolyte such as $Na_2CO_3$ to water (Figure 1) determines a steep immediate increase in pH from about 6 to ~ 9, already after the addition of 6.4 mg of the salt, because of the hydrolysis of the carbonate ions, which tend to associate with protons, thereby increasing the equilibrium concentration of $OH^-$ ions. Afterwards in the absence of PAA and HA, the pH of the solution increases only slightly, whereas as expected its EC increases linearly ($a= 0.072$, $p< 0.001$) with salt additions.

All HA and even more the PAA, buffered the solution pH and strongly counteracted the pH increase imposed by $Na_2CO_3$ additions (Figure 1). Polyacrylic acid (PAA) exhibited the strongest buffering effect, with pH values increased by only 1.85 units at the end of the experiment (Figure 1a). In the presence of HA, after a brief initial decrease in conductivity, caused by the neutralization of protons derived from the dissociation of the stronger acidic groups, the EC increases steadily, displaying again a linear positive trend. However, the increase rates measured per unit salt addition were, in all cases, significantly lower than that of the control solution (Figure 2). Therefore, in the case of salinity caused by $Na_2CO_3$, all tested HA and the synthetic polyelectrolyte PAA resulted effective in contrasting the increase in conductivity of the solutions at increasing salt levels, as confirmed by the significant statistical differences among EC slopes calculated from experimental data (Figure 2).

Among the tested HA, CHA and EHA were the most effective at mitigating the $Na_2CO_3$-induced increase in EC, yielding final EC values nearly 50% lower than those of the control (Figure 2a). LHA and PAA also reduced the EC increase rate, whereas PHA resulted as the least effective (Figure 2a).

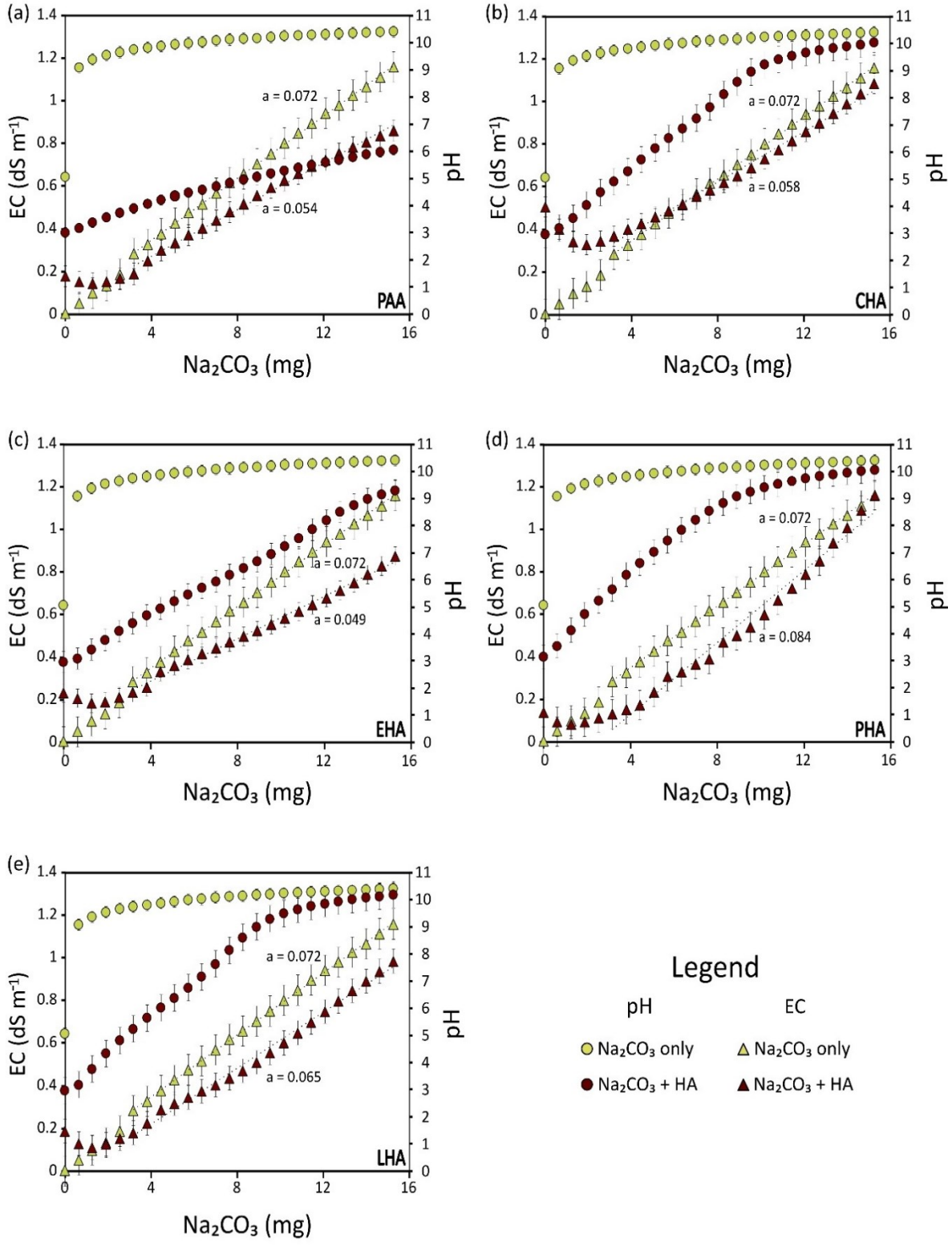


**Figure 1.** Changes in pH and EC registered following micro-additions of 0.2 M Na2CO3 to de-aerated water and to solutions containing polyacrylic acid PAA (a) or HA of different origin, i.e. compost CHA (b), soil EHA (c), peat PHA (d) and leonardite LHA (e). Data points represent the mean of three independent replicates and bars represent the standard deviation.

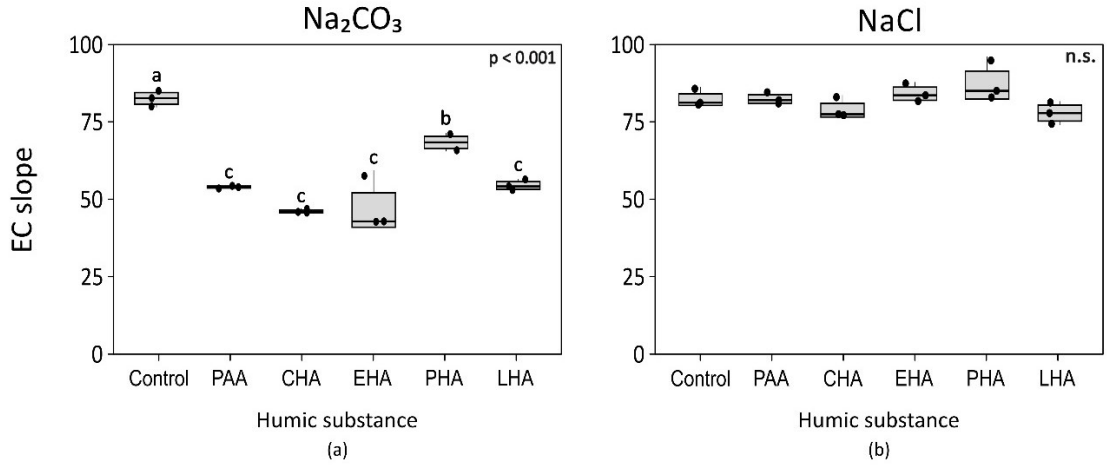


**Figure 2.** Effect of HA on EC increments (dEC/dmg) measured per unit $Na_2CO_3$ addition in (left) and NaCl (right) up to pH values of 7. ANOVA analysis highlights the statistical differences in EC slopes between the control (no PAA or HA) and the PAA and HA treatments. Different letters refer to statistically significant differences based on Tukey's post hoc test ($Na_2CO_3$ and NaCl: $p < 0.001$ and n.s. respectively).

Conversely, when the same experiment was performed with NaCl, which is a strong electrolyte and does not cause hydrolysis of water, additions did not have any significant effect on the pH of the solutions either in the absence or in the presence of HA or PAA (Figure 3). The presence of the latter, however, strongly acidified the solution and the pH remained around 3 throughout the experiment. In this situation the EC of the solution containing PAA remained always well above that measured in the NaCl only control (Figure 3).

Considering the fact that HA cannot be expected to possess any dissociated, negatively charged acid group to attract free sodium ions at the equilibrium pH attained after treatment with the cation exchange resin, which differed slightly for each type of HA (see Figure 1), the solutions were adjusted to pH 6.0 before starting adding NaCl (Figure 3).

This allowed us to better compare the eventual effects of their presence, because in the NaCl only control the pH remains around pH 6 throughout the experiment. Under these conditions (initial pH raised to 6.0) and in the presence of HA, the pH slightly decreases after the addition of 6 mg of the salt, due to a minor cation exchange reaction driven by the increase in ionic strength and concentration of sodium ions. However, in this case, ANOVA did not

detect statistical differences among the slopes of the control, of the PAA and of any of the HA (Figure 2b).

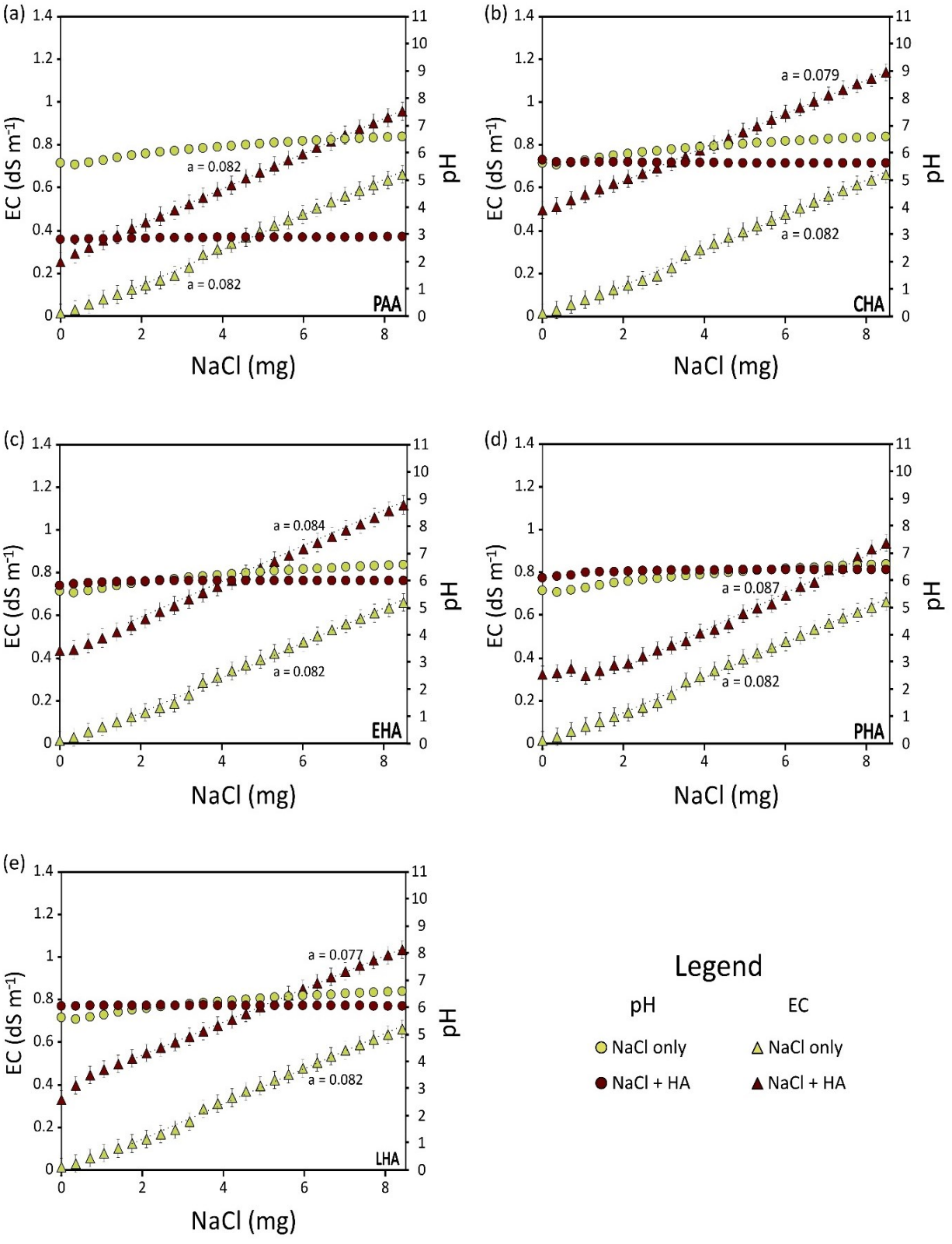

**Figure 3.** Changes in pH and EC following micro additions of 0.2 M NaCl to de-aerated water and solutions containing polyacrylic acid PAA (a) or HA of different origin, i.e. compost CHA (b), soil EHA (c), peat PHA (d) and leonardite LHA (e). Data points represent the mean of three independent replicates and bars represent the standard deviation.

## 3.2 The effect of the type of HA

The EC data, measured during the experiments, allow to evaluate and compare the ability of each HA to mitigate salinity when this is caused by dissolved $Na_2CO_3$. The overall salinity amelioration potential ($SAP_{HA}$) of each HA at a given pH can then expressed as the amount of $Na_2CO_3$ neutralized per unit of weight of HA and can be calculated as from the values read in graphs of Figure 1 using the following equation:

$$SAP_{HA} = \frac{(\mathrm{A} - \mathrm{A}')}{W_{HA}} \bullet 1000 \qquad (1)$$

where:

- A is the amount of $Na_2CO_3$ that in the water + HA solution yields the pH experienced by the HA in the soil;
- A' is the amount of $Na_2CO_3$ that if added to water would produce a solution with the same conductivity as A;
- WHA is the weight of HA expressed in mg.

Considering that HA are generally not applied in their fully protonated form, the effective SAP ($SAP_{HA\ eff}$) of the HA contained in an amendment added to a certain soil can still be calculated (equation 2) from the graph, by subtracting the amount $Na_2CO_3$ added to HA to bring the acid saturated HA to the pH at which it is actually applied:

$$SAP_{HA\,eff} = \frac{(\mathrm{A} - \mathrm{A}') - (\mathrm{B} - \mathrm{B}')}{W_{HA}} \bullet 1000 \qquad (2)$$

Where:

- A is the amount of $Na_2CO_3$ that in the water+HA solution yields the pH experienced by the HA in the soil;
- A' is the amount of $Na_2CO_3$ that if added to water would produce a solution with the same conductivity as A;
- B is the quantity of $Na_2CO_3$ added to HA to bring the acid saturated HA to the pH at which it is actually applied;
- B' the quantity added to water to get a solution that, at the original pH of HA has the same conductivity of B.

**Table 1.** Salinity amelioration potential (SAP) of HA and PAA at pH 7 towards osmolarity caused by $Na_2CO_3$. The table shows the effectiveness of the different HA in mitigating EC rise in terms of mg of $Na_2CO_3$ neutralized per gram of HA following a change in pH from the fully protonated form to pH 7 ($SAP_{HA}$) and from pH 7.0 to 8.5 ($SAP_{eff}$).

| Humic acid | Origin | $SAP_{HA}$ (mg $Na_2CO_3$ $g^{-1}$ HA) | $SAP_{eff}$ (mg $Na_2CO_3$ $g^{-1}$ HA) |
|---|---|---|---|
| PAA | Polyacrylic Acid | 142.59 | 49.86 |
| CHA | Compost | 28.56 | 25.10 |
| PHA | Peat Soil | 155.65 | 43.60 |
| EHA | Elliott Soil | 164.55 | 44.35 |
| LHA | Leonardite | 142.62 | 46.44 |

As an example, and to underline the dependence of SAP on the pH variation experienced by HA, we calculated the SAP of each of the examined HA (Table 1) and their capability to neutralise the increase of EC corresponding to the maximum change in pH (i.e. from 7 to 8.5) that can likely occur to the HA contained in an organic amendment, such as compost, when incorporated in a typical saline soil. When results were normalised per g of HA, PAA showed the highest potential capacity of mitigation, corresponding to 49.9 mg $Na_2CO_3$ $g^{-1}$, followed by LHA, EHA and PHA, whose calculated $SAP_{eff}$ values were only slightly lower and very close to each other (i.e. ~ 45 mg $Na_2CO_3$ g $HA^{-1}$), and with CHA recording the lowest potential, i.e. 25.1 mg $Na_2CO_3$ g $HA^{-1}$ (Table 1).

The mitigation effect of PAA is somewhat lower that could be expected by its high content of carboxyl groups, which significantly influence its surface charges at increasing pH levels (Table 2).

## 3.3 HA characterisation

The characterisation of the selected HA, which were chosen in order to examine the behaviour of HA of widely different origin and humification degrees, was performed in order to understand which structural factors determine the different capabilities displayed. To highlight the range of structural variations of the different HA employed the percent distribution of proton types was obtained from $^{1}$H-NMR spectra and the quantitation of the negative charge density development following pH changes was calculated based on acid-base titrations.

According to the respective $^{1}$H-NMR spectra (Supplementary material Figure S1), LHA have the highest percentage of aromatic protons (Table 2), about twice that of CHA, indicating, in the latter, a lower degree of aromaticity. The amount of aromatic protons in EHA was lower than that of LHA, but 50% higher than that of CHA. The percentage of olefinic protons (protons directly bound to double bonds) was low in all compounds, never exceeding 4%. Protons bound to oxygen in polysaccharides and carbohydrates were abundant in PHA and EHA (~ 29% and ~ 25% respectively), while they were poorly represented in LHA (5.4%).

On the contrary, as expected from the polymer's composition, PAA shows, in the $^{1}$H-NMR spectrum and proton type distribution (retrieved from literature, (Chollakup et al., 2013), the highest percentages of methyl and methylene protons associated to terminal aliphatic groups and to carboxylic and aromatic groups, at least 1.6 times higher than those of the other HA considered, which on the contrary showed similar values between each other. Regarding aliphatic structures, EHA had the lowest amount of alkyl protons.

**Table 2.** Relative abundance of protons in functional groups of PAA and HA determined by $^{1}$H-NMR analysis. The table displays the percentage distribution of protons bound to different structural units across the following chemical shift regions: aromatic-H (9.0–9.5 ppm), α to double bonds H (6.5–5.0 ppm), H in α to carbons bound to oxygen (5.0–3.0 ppm), methyl and methylene H associated to carboxyl groups (3.0–1.7 ppm) and methyl and methylene H in terminal aliphatic groups (1.7–0 ppm). Data are normalized to a total area of 100% for each substance.

| | Aromatic-H | H in α to double bonds | H in α to carbons bound to oxygen | methylene H associated to carboxyl groups | H in terminal methyl and methylene groups |
|---|---|---|---|---|---|
| PAA * | 0.31 | 0.00 | 61.58 | 36.92 | 1.19 |
| CHA | 10.43 | 0.16 | 21.86 | 30.64 | 37.19 |
| PHA | 11.82 | 2.79 | 29.25 | 19.50 | 36.62 |
| EHA | 14.70 | 1.64 | 25.53 | 23.82 | 34.30 |
| LHA | 19.15 | 3.54 | 5.38 | 33.56 | 38.35 |

* Deduced from Chollakup et al. (Chollakup et al., 2013)

In order to obtain information on the charge density and charge pH dependence, we calculated the Q1 and Q2 parameters (Table 3) of the examined HA from their acid-base titration curves (Supplementary material Figure S2). According to Ritchie and Purdue (Ritchie & Perdue, 2003) these parameters respectively provide a quantitative estimation of carboxyl and phenolic groups. The model substance, PAA has the highest concentration of carboxyls, i.e. Q1, (17.0 meq $g^{-1}$ C). The HA that have the largest quantity of ionizable groups that can be assimilated to carboxyls, being dissociated at pH 8 are PHA and EHA (~ 10 meq $g^{-1}$ C) followed by LHA and CHA (~ 9 meq $g^{-1}$ C). As for Q2, which has been considered to correspond to phenolic groups, the larger values were recorded for CHA and PHA (5.50 meq $g^{-1}$ C) followed by EHA (4.0 meq $g^{-1}$ C) while the lowest was recorded for LHA (2.45 meq $g^{-1}$ C). The limits of this assumption are highlighted by the Q2 value of PAA (3.50 meq $g^{-1}$ C): PAA does not actually contain any phenolic group, only carboxyls. These groups were made progressively weaker by the build-up of the negative charge density on the polymer molecules, during titration.

**Table 3.** Calculated maximum charge densities for the first (Q1) and second (Q2) types of negatively charged binding sites at pH 8 and 10 respectively, total ionized groups at pH 7, 8.5 and 10 and ionization increase from pH 7 to pH 8.5 and from pH 8.5 to pH 10.

| | Q1 (mmol $g^{-1}$ C) | Q2 (mmol $g^{-1}$ C) | Total ionized groups at pH 7 (mmol $g^{-1}$ C) | Total ionized groups at pH 8.5 (mmol $g^{-1}$ C) | Total ionized groups at pH 10 (mmol $g^{-1}$ C) | Charge increments from pH 7 to 8.5 (mmol $g^{-1}$ C) | Charge increments from pH 8.5 to 10 (mmol $g^{-1}$ C) |
|---|---|---|---|---|---|---|---|
| PAA | 17.00 | 3.50 | 15.25 | 17.50 | 17.75 | 2.50 | 0.25 |
| CHA | 8.80 | 5.50 | 9.20 | 10.10 | 11.55 | 2.35 | 1.45 |
| EHA | 10.20 | 4.00 | 9.60 | 10.50 | 12.25 | 2.67 | 1.75 |
| PHA | 10.13 | 5.50 | 9.63 | 10.50 | 12.88 | 3.25 | 2.38 |
| LHA | 9.03 | 2.45 | 8.55 | 9.33 | 10.25 | 1.70 | 0.92 |

The numbers of total ionized groups at pH 7, which represents the average pH of good quality composts, and at pH 8.5, which is considered the upper limit for saline soils according to the U.S. Salinity Laboratory (Richards, 1954), is reported in table 3. The numbers of total ionized groups at pH 10, a representative pH for alkaline saline soils (Chhabra, 2004), was also calculated. In this way, the negative charge increment corresponding to the lower (7 to 8.5) and upper extremes (7 to 10, in the case of alkaline saline soils) of the pH change that may be experienced by HA contained in an organic amendment when added to soil was also calculated and reported (Table 3), to evaluate the effect of soil pH on the amelioration potential of HA. Total ionized groups were always highest in PAA but, although the synthetic polymer, between 7 and 8.5, a negative charge increment similar to those of the HA, only a negligible further increment occurred from pH 8.5 to 10. This is reasonable, considering that PAA does not possess acidic groups weaker than carboxyls. On the contrary the contribution of phenolic groups is sizeable in the case of HA. At pH 8.5, EHA PHA and CHA displayed about the same amount of total ionized groups (10.50 ÷ 10.10 meq $g^{-1}$ C). However, differences were displayed at pH 10, with EHA and PHA showing the highest number of ionized groups, around 30% more than CHA. At all the examined pH values, the lowest amount of ionized groups was that of LHA (8.55, 9.33 and 10.25 meq $g^{-1}$ C at pH 7, 8.5 and 10, respectively) which is coherent with the strong aromatic nature revealed by $^{1}$H-NMR spectra (Table 2).

## 3.4 Seed germination and root growth of seedlings

Germination of maize was monitored for three days (Figure 4). After 24 h, the percent germination rate was lowest at the highest salt concentration (i.e. 7.31 and 13.25 mg $L^{-1}$ for NaCl and $Na_2CO_3$) for both salts, with mean percent germination falling below 20%. The lower salinity level applied (i.e. 2.92 and 2.65 mg $L^{-1}$ for NaCl and $Na_2CO_3$), yielded germinations of 47% for the NaCl treatment and of 70% for $Na_2CO_3$.

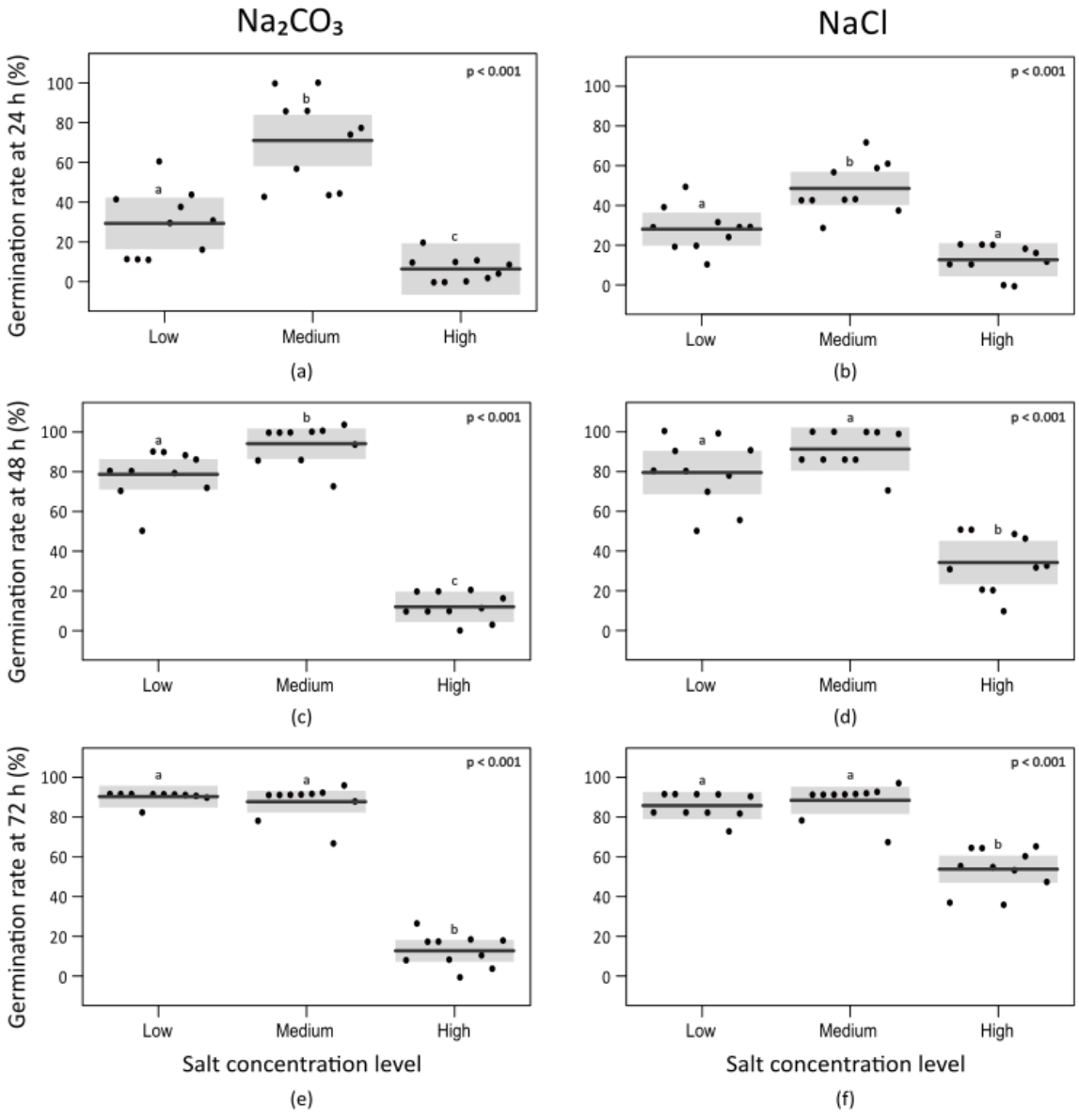


**Figure 4.** Percent germination rates of *Zea mays* seeds that were exposed to solutions of two different salts ($Na_2CO_3$ and NaCl) at three concentrations levels after 24 (a,b), 48 (c,d) and 72 (e,f) h. "Low", "Medium", "High" correspond to the three concentration levels of the salts tested. Dots represent rates of germination at increasing concentrations of CHA. Different letters refer to statistically significant differences based on Tukey's post hoc test ($p < 0.001$).

At the examined lower and medium salt concentration however, salinity only delayed germination. In fact, after 48 h, germination rates increased remarkably reaching mean percent rates above 80%, that did not significantly differ from the control. These high levels remained after 72 hours, in the lower and medium salinity treatment, but were markedly reduced in the higher salinity treatment. A lower germination was observed in the $Na_2CO_3$ compared to the NaCl treatment.

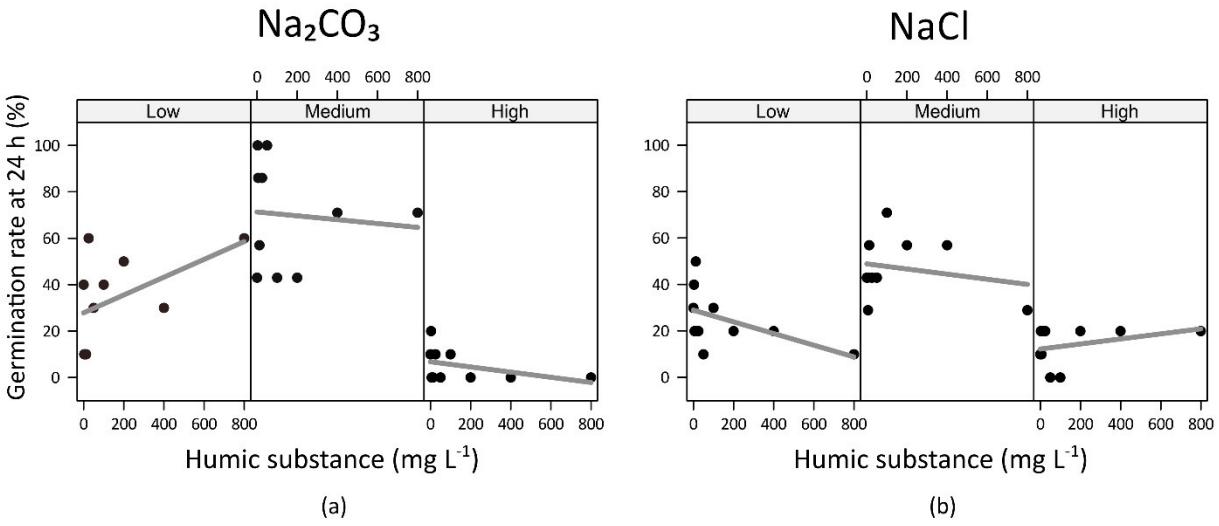


**Figure 5.** Germination rate of *Zea mays* seeds after 24 hours in the presence of different CHA concentrations. "Low", "Medium", "High" correspond to the three concentration levels of the salts tested. Dots represent the percentage of seeds germinated at increasing concentrations of CHA. Grey bars refer to the trends

Based on ANOVA, salinity significantly affected seed germination (Figure 4) whereas the presence and concentration of humic substances did not have a significant effect (Supplementary material Table S3).

Despite the absence of an effect related to the presence of HA, we observed a contrasting trend in germination comparing the two salts at 24 h and at the lowest salt concentration (Figures 5 a, b). In the NaCl treatment, increasing CHA concentrations progressively reduced germination, suggesting an exacerbation of the inhibitory effect of the salt. Conversely, in the $Na_2CO_3$ treatment, increasing CHA concentrations tended to enhance germination, with a 20% increase at 800 µg $L^{-1}$ compared to the control. Despite the high variability of data, maize germination at 800 µg $L^{-1}$ CHA was 50% higher in the presence of $Na_2CO_3$ compared

to the same CHA concentration than in the presence of NaCl, confirming a stronger possible mitigation effect mediated by humic substances in the case of $Na_2CO_3$.

Salt concentration also showed a statistically significant effect on root elongation of maize seedlings for both NaCl and $Na_2CO_3$ whereas the concentration of CHA had no effects (Supplementary material Figure S4, Table S5). Contrary to seed germination, root growth was already inhibited by the lower level of salt, whereas, at no salinity, mean root elongation for NaCl and $Na_2CO_3$ was about 0.43 mm $h^{-1}$ and 0.53 mm $h^{-1}$ respectively, which means they were on average ~ 2 and ~ 3 times those measured in the low and high salinity levels.

# 4. Discussion

Among the different strategies that have shown some potential for enhancing the productivity of saline soils, the use of organic amendments has been often reported to improve soil conditions (Daba, 2025). This work does not aim to recommend any specific strategy, but only to explain how, humic substances, can act to alleviate the osmolarity stress caused by dissolved salts. Addition of HA to soil may occur not only through the use of commercial humate products but, more frequently, through addition of compost, sewage sludge or crop residues, which either contain HA or will generate them during their decomposition in soil. Several studies assessed a reduction of EC after the application of organic amendments in saline soils where pH values exceeded 8.0 (Tejada et al., 2006; Wang et al., 2014; Chaganti et al., 2015). Based on our hypothesis, which was confirmed by the results of salt addition experiments, this action is driven by the increase in pH experienced by HA that causes ionisable weak acid groups to dissociate (Pertusatti & Prado, 2007). The increased negative charge on the humic molecules causes more cations to become attracted within the diffuse double layer (Cooke et al., 2007; Brady & Weil, 2016). At the same time, the release of protons shifts the equilibrium among carbonate, bicarbonate ions and dissolved $CO_2$ in the solution. Being the $CO_2$ a gas, in a non-equilibrium condition, it may be lost by diffusion into the gas phase. This means that in the field, the amelioration that can be achieved, depends on the actual pH difference between the original pH of the HA, contained in a commercial product or in an organic amendment such as compost and the pH of the soil. The larger the difference, the stronger will be the decrease in osmolarity (EC) of the soil solution produced by a given amendment. Our work also shows that, as an undesirable side effect, the addition of organic amendments to ameliorate saline soils, may trigger the release

of $CO_2$ from soluble carbonates and therefore mobilise $CO_2$ trapped in mineral soil components. This effect however is not long lasting, but limited to a short pulse.

The fact that HA and PAA fail to display any SAP, when NaCl is the only salt present and at constant pH, is actually not surprising. It is well known in fact, that sodium ions are very weakly retained within the diffuse double layer and would never be able to cause the displacement of $H^+$ from acid groups which has been observed in the presence of divalent metals (Stevenson, 1982).

Strongly alkaline saline soils are therefore likely to profit more and in particular saline sodic soils, whose pH is bound to increase when excess salts are amended (Brady & Weil, 2016), may particularly benefit from addition of organic materials containing, or producing HA through their humification in soil. The addition of non-humified substrates may be potentially more beneficial. In fact, in this case HS would be produced in the soil in their acid form and not added together with the stoichiometric amount of positive counter ions, as when compost is added to soil.

The decrease in osmolarity, testified by the decrease in EC, also strongly depends on the anionic composition of the soil solution. In fact, no amelioration was observed in our experiments in the presence of NaCl. In fact, in this case, besides the lack of change in pH, that does not allow the formation of novel negative charges, chloride ions, contrary to carbonate ions, which may be removed from the solution as gaseous carbon dioxide by a shift in their acid-base equilibrium, are never lost from the solution.

## 4.1 Dependence of SAP on the structural traits of HA

Nevertheless, the density of acid groups on HS molecules and their strength (see Table 3) seems to explain only partially the documented reduction in EC. In fact, PAA, in spite of the much larger number of carboxyls displayed a similar $SAP_{eff}$ than the rest of the HA, with the only exception of CHA (Table 1).

It is likely that other structural factors may concur in determining the amelioration potential of HA. Other structural differences, such as molecular size and tendency to aggregation may in fact contribute to the observed decrease in osmolarity. Molecular size, in fact promotes the aggregation of humic molecules, occluding attracted counter-ions with-in a supramolecular structure and further decreasing the number of free molecules in the soil

solution (Jovanović et al., 2013). Flocculation of HA, although impaired by Na is at the same time driven by the shielding of the negative charge at increasing ionic strength and is a phenomenon normally observed in saline sodic soils (Rengasamy & Olsson, 1991).

Total ionized groups were calculated at pH 7 and 10 which respectively represent the pH generally exhibited by compost and the pH frequently measured in salt-affected soil of high sodicity. Total ionized groups density was highest in PAA at both pH levels, which is consistent with the high amount of calculated strong acidic groups. While this specific aspect of HS performance in salt-affected soils with different initial pH levels has not been extensively investigated, numerous studies have confirmed the effectiveness of HS in efficiently reducing soil pH in saline-sodic and sodic soils (Shaaban & El-Fouly, 2002; Bai et al., 2017; Mahmood et al., 2017).

Despite LHA exhibit the lowest number of dissociated groups at both pH 8.5 and 10, our salt addition experiment showed that leonardite has potentially an ability to mitigate the increase of EC following $Na_2CO_3$ additions which is comparable to those of the other HA. This could be explained considering that phenolic groups become increasingly relevant in retaining cations at alkaline pH (pKa ~ 10) (Rai et al., 2021).

## 4.2 Potential practical applications

These findings can have practical application. In fact, knowing the content of HA, or the amount of HA potentially produced in the soil, of a given compost or amendment and the salinity amelioration potential ($SAP_{HA\ eff}$) of its HA, the quantity to be applied in the field can be easily calculated for the specific soil considered, by applying Equation 2. As an example, knowing that, for instance, from the $SAP_{HA\ eff}$ of CHA, approximately 25 mg of $Na_2CO_3$ can be neutralized per gram of compost HA when the pH increases from 7.0 to 8.5 (Table 1), we can assess the amount of compost that should be applied in the field in order to alleviate salinity. If we consider, for instance, a soil with a EC of 4 dS $m^{-1}$, a moisture content of 25% and a bulk density of 1.3 g $cm^{-3}$ (Villalobos et al., 2024), and the aim to reduce EC to 2 dS $m^{-1}$ in the top 5 cm layer, the amount of good quality mature compost to be applied will be about 40 t per hectare. This is a quite reasonable quantity for arable crops also considering the content of plant nutrients (Supplementary material S6 for details on calculations). It must be noted that the amount required may be much larger in case of compost that is not well humified: the HA content of the compost and their $SAP_{HA\ eff}$ must

be both known in order to obtain reliable predictions on short term effects of the application. From $SAP_{HA\ eff}$ data reported in table 1, it is also evident that PAA may represent a possible alternative to compost in the amelioration of salinity.

Regarding the germination and root elongation rates of *Zea mays*, our data confirmed the stronger toxicity of $Na_2CO_3$ compared to NaCl (Figure 4), recording a decrease in seed germination of about 90% for $Na_2CO_3$ and 45% for NaCl, after 72 h from the beginning of seed exposure to the salt and at the highest salt level tested (i.e. 0.125 M and 0.15 M for $Na_2CO_3$ and NaCl, respectively). Moreover, root elongation decreased by more than 50% in both treatments within 12 hours from germination (Supplementary material Figure S4). Interestingly, a moderate salt concentration instead stimulated maize germination (24 – 48 hours). This evidence is consistent with the common use of saline solutions to boost seed germination: it includes salts such as $CaCl_2$ but also NaCl, the latter with concentrations up to 5 mg $L^{-1}$ (Gebreegziabher & Qufa, 2017) that aligns to the medium salt level applied in our experiment (for both $Na_2CO_3$ and NaCl).

In our experiment, the effect of humic substances on seed germination was not statistically significant. However, at the lowest salt concentration applied, a contrasting trend was observed after 24 hours comparing $Na_2CO_3$ and NaCl exposed seeds. Seed germination tended to increase with increasing levels of HA in the case of $Na_2CO_3$ but decreased in that of NaCl (Figure 5). This contrasting behaviour supports our hypothesis for which HS can be effective in reducing the osmotic stress for the plant only if the pH of the soil solution causes the HA to dissociate (Oades, 1989; Tülp et al., 2009).

# 5. Conclusions

Our results unraveled the plausible mechanism behind the salt stress relief driven by application of organic amendments to salt-affected soils and showed that it depends on: i) the nature of salts, ii) the pH of the soil and iii) the quantity and properties of HA in the organic amendment. The mechanism is based on, but not only limited to, the electrostatic interaction of the excess negative charges, that are generated by the dissociation of acidic ionizable groups on HA molecules, with the cations dissolved in the soil solution of saline soils. The dissociation of acid groups that occurs when HA are eventually exposed to the more alkaline soil pH will produce an excess of negative charges that will attract and hold more cations in the diffuse double layer of HA. Because of the very slow diffusion of HA

and of their tendency to aggregate in saline solutions, it is expected that the concentration of free ions in the bulk soil solution will be lowered. This will reduce the osmolarity of the soil solution and potentially mitigate salinity stress to plants and microorganisms.

Consistently with this mechanism, the germination assays further confirmed the greater stress by $Na_2CO_3$ compared to NaCl. Moreover, although not statistically significant, a slight improvement in germination was observed at low $Na_2CO_3$ concentration in the presence of humic acids, suggesting a potential role of HA in alleviating stress under alkaline conditions.

An essential part of the mechanism is, however, the concomitant neutralization of carbonate ions and the consequent non-equilibrium release of $CO_2$. In fact, when the amendment has a pH lower than the soil, then the weak acid functional groups of the humic substances contained in it will dissociate and release $H^+$ in solution. These will then react with carbonate or bicarbonate ions, shifting the equilibrium towards gaseous $CO_2$. This situation is highly likely to occur, as good quality composts have generally a pH around 7, whereas the pH of many soils where salts have been accumulated are alkaline or even, in some cases (saline sodic soils), extremely alkaline.

The calculated $SAP_{HA\ eff}$ that can be obtained in the laboratory from easy EC and pH measures also provides a mean to obtain preliminary information the minimum amount of amendment to be applied under field conditions to a given soil. Extrapolation of outcomes from laboratory experiments to field conditions, however, is never straightforward and needs to be validated with field research. Further research is also needed to advance our insight into concomitant factors, such as aggregation and precipitation, that may also contribute to the amelioration potential of humic substances towards soil salinity.

# *Chapter 3*

# Preface

This chapter focuses on understanding how dissolved organic matter (DOM) modulates the formation of iron plaques under controlled experimental conditions. While the dynamics and ecological role of iron plaque formation have been widely investigated, the specific influence of DOM on iron cycling remains controversial. Some studies suggest that DOM can promote Fe precipitation by establishing very harsh anoxic conditions and boosting microbial respiration, favouring a large availability of $Fe^{2+}$ and potentially larger plaque deposition, whereas others report that it inhibits plaque formation by stabilizing Fe in soluble organic complexes.

To disentangle this issue and provide new insights into the chemical control exerted by organic matter on iron cycling and root–soil interfaces, we developed an experimental setup based on artificial roots, allowing control over oxygen diffusion and $Fe^{2+}$ availability. Two organic carbon sources, i.e. soil-derived DOM and malic acid, representing root exudates, were tested at increasing C:Fe ratios to evaluate their effects on iron oxidation and precipitation. The results demonstrated that DOM can markedly suppress plaque deposition by complexing $Fe^{3+}$ in solution, with the extent of inhibition depending on both the carbon source and its concentration. These findings support the hypothesis that the organic matter negatively control $Fe^{3+}$ precipitation and reduce plaque formation on plant roots, at least in a controlled environment.

# *Role of dissolved organic matter in modelling iron plaque formation on artificial roots*

## 1. Introduction

Under flooded soil conditions, hydrophytes develop aerenchyma tissue to sustain internal aeration upon hypoxia/anoxia. This acclimation derives from the need of ensuring sufficient oxygen to root tips for cell division and root growth. Aerenchyma is a special tissue where air spaces are longitudinally connected and allow the passive and quick diffusion of oxygen acquired from leaves that are in contact with air. This oxygen travels along the aerenchyma down to the root tip. Nevertheless, some of it passively diffuses out into the surrounding anoxic rhizosphere through a process commonly named root radial oxygen loss (ROL), altering the soil redox potential (Eh) and oxidizing the soluble $Fe^{2+}$ present close to root surfaces to $Fe^{3+}$ (Khan et al., 2016). The $Fe^{3+}$ precipitates as insoluble iron oxyhydroxides on root surfaces, forming reddish-brown deposits called iron plaques (He et al., 2024). This process is the primary mechanism of iron plaque formation, and it is considered one of the most important biological factors controlling their development (Fu et al., 2016; Khan et al., 2016).

Iron plaques have been widely investigated following their environmental role as both sinks for pollutants and secondary sources of nutrients (e.g. Greipsson, 1994; Batty et al., 2000; Liu et al., 2005). This is mainly due to their high specific surface area and strong sorptive affinity for multiple ions (Chen et al., 2006), such as toxic metal(loid)s including arsenic, cadmium, and lead that can be immobilized on plaque surfaces reducing their bioavailability to the plant (Dixit & Hering, 2003; Liu et al., 2011; Sebastian & Prasad, 2016). For example, in paddy soils, iron plaques play a crucial role in regulating the uptake of both toxic and essential elements. They can immobilize contaminants such as arsenic and cadmium, thereby reducing their translocation to aboveground tissues (Hu et al., 2005; Fu et al., 2018), while simultaneously adsorbing nutrients like phosphate and acting as a temporary nutrient reservoir on the root surface (Greipsson & Crowder, 1992; Zhang et al., 1999). Under certain

conditions, the plaque can also release nutrients back to the plant, functioning as a dynamic pool of beneficial elements in wetland environments (Zhong et al., 2009; Jia et al., 2018).

Over the past decades, numerous studies have examined the drivers of plaque formation (e.g. Crowder & Macfie, 1986; St-Cyr & Crowder, 1989). As already stated, ROL is considered one of the most important biotic factors, while soil Fe availability is identified as the primary abiotic control (Mendelssohn et al., 1995). Furthermore, pH, redox potential, texture, soil carbonate content and organic matter are known to alter Fe solubility and microbial oxygen demand, modulating plaque abundance (St-Cyr & Crowder, 1989; Mendelssohn et al., 1995). Plant species and genotypes also differ for their thickness of formed plaques, owing to differences in root anatomy and ROL (Armstrong, 1971; Wright & Hossner, 1984). Nevertheless, the role of several parameters concurring in plaque formation, especially those related to soil properties, remain still unclear. Much of the understanding derives from simplified pot or hydroponic systems focusing on single factors and thus neglecting the complexity of field surveys. For example, solution experiments with *Typha latifolia* showed plaque increasing with increasing $Fe^{2+}$ and within a narrow pH range, while chelated Fe translated into little plaque formation (Taylor et al., 1984). Conversely, other studies linked plaque formation to the Fe bound to carbonates fraction rather than the exchangeable Fe, highlighting carbonate buffering and water movement as key driving factors (St-Cyr & Crowder, 1988, 1989). Moreover, field seasonal surveys reported mid-summer peaks in iron precipitation coincident with plant growth, highlighting that plant phenological stage is increasing variability to the process of plaque formation (Crowder & Macfie, 1986).

One of the still controversial soil factors is probably soil organic matter. On one hand, dissolved organic compounds can complex $Fe^{2+}$ and $Fe^{3+}$ in the rhizosphere solution, increasing iron solubility and thus inhibiting its precipitation onto roots. Jones et al. (1996) reported that organic acids like citrate and malate extruded by roots significantly enhanced Fe dissolution in the rhizosphere, and Liu et al. (2021c) had similar results working with dissolved organic matter in hydroponics. On the other hand, high levels of organic matter in flooded soils can intensify microbial respiration and oxygen consumption, creating strongly reducing environments and a concurrent increase in $Fe^{2+}$ oxidation, followed by the subsequent precipitation of $Fe^{3+}$. Christensen et al. (1998) observed that in an oligotrophic lake, plaque abundance on *Lobelia dortmanna* roots rose significantly with increasing organic content of the sediment, due to more pronounced anoxia (larger microbial activity) and $Fe^{2+}$ availability. Moreover, different organic matter types can modulate plaque

dynamics. Low molecular weight organic acids acidify and chelate Fe, promoting dissolution of $Fe^{3+}$ oxides and Fe complexation, thus suppressing plaque formation (Jones et al., 1996). A recent study found that adding exogenous organic acids to mangrove seedlings markedly decreased iron plaque accumulation via rhizosphere acidification and chemical reduction of $Fe^{3+}$ to $Fe^{2+}$ (Meng et al., 2022).

A further challenge in studying iron plaques is their heterogeneous distribution on root systems. Iron plaque does not form uniformly along roots but follows ROL spatial variations, with localized Fe oxidation and plaque accumulation near ROL 'hotspots' (Seyfferth et al., 2010). Differences in root type, age, and anatomy lead to further irregular plaque deposition patterns (Gilbert & Frenzen, 1998). Typically, plaque is mainly observed in the elongation and root-hair zones of primary roots and is rarely present on very young lateral or newly formed roots. This spatial pattern reflects continuous root growth, in contrast to older segments experiencing longer exposure to oxic conditions and accumulating thicker deposits (Evans, 2004; Povidisa et al., 2009). Armstrong (1967) showed how the apex of submerged plant roots remained free of Fe precipitate, with plaques forming a ring just behind the actively oxidizing tip before diminishing behind the root tip. Such microscale variability can potentially complicate both sampling and result interpretation in plaque experiments (Limmer et al., 2021).

Given these complexities, our study aims to clarify the effect of organic matter on iron plaque formation under controlled conditions, overcoming some of the experimental challenges using living plants. In fact, we monitored plaque development in absence or presence of dissolved organic matter using artificial roots to standardize oxygen delivery along their length and to minimize the heterogeneity derived from the use of living plants. The roots consisted of silicone tubes of root-like dimensions (i.e. 1.19 mm of external diameter). Sealed bottles were used to force anoxic conditions and allow oxygen diffusion only through the artificial root. We induced the formation of iron plaques by preparing $Fe^{2+}$ enriched solutions (about 1 mM $Fe^{2+}$), either without organic matter or with dissolved organic matter from two sources: (1) a paddy soil-derived fraction and (2) malic acid purchased from Sigma Aldrich to mimic root exudatation. Organic matter was added to the solution in a 2:1 or 12:1 C to Fe molar ratio. Through this setup, and by using silicon tubes as a proxy for living roots, we could monitor the single effect of organic matter on the amount of Fe precipitated within the iron plaque.

We hypothesized that dissolved organic matter would reduce plaque deposition by complexing Fe, with different effects based on the source of the organic matter exploited.

# 2. Materials and Methods

## 2.1 Fe plaque–induction system

A silicone tube of the size of a root (external diameter of 1.19 mm) was mounted vertically through the cap of a 500 mL glass bottle fitted with multiple inlets, out of which two were exploited for positioning the artificial roots (i.e. silicone tubes) and one allowing access to the solution for temporal monitoring. A fourth inlet was kept tightly closed (Figure 1). The tube was immersed in 500 mL of a 15 mM MES-buffered solution to ı 6 containing 1 mM $Fe^{2+}$ ($Fe_2SO_4 \cdot 7H_2O$), prepared either without dissolved organic matter (DOM) or with DOM adjusted to C:Fe molar ratios of 2 and 12. All solutions were deaerated by purging $N_2$ prior to $Fe^{2+}$ addition, and all handling was performed in an anaerobic glove box under $N_2$. All equipment was pre-cleaned with 1% HCl to minimize any metal contamination. Prior research supports the feasibility of such systems demonstrating that $O_2$ permeability of artificial roots is comparable to that of living roots lacking root apoplastic barriers (Peralta et al., 2021).

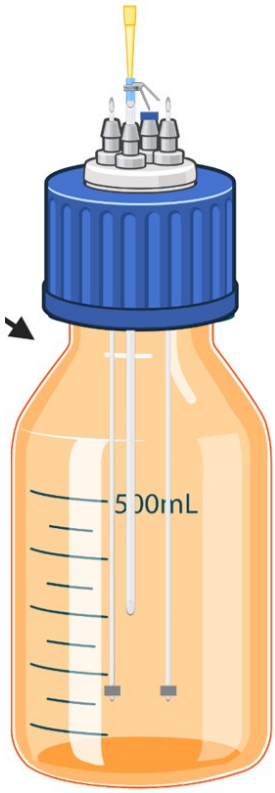


**Figure 1.** Sketch of the experimental setup. Two artificial roots are inserted in a tight-closed glass bottle: roots represent the only pathway for $O_2$ entrance. A third inlet is used for time monitoring of Fe dynamics on the solution.

## 2.2 Dissolved organic matter types

Two DOM sources were employed in this experiment. First, malic acid (MC) (97-67-6, Sigma-Aldrich) was used as a low molecular weight organic acid to simulate root exudation, considering that it is one of the most abundant acid exudates from rice roots (Jones, 1998). Second, soil-derived DOM (SC) was extracted from a paddy soil by adding 0.1 M NaOH at a 1:5 ratio (w soil/v solution). The suspension was shaken for 4h and allowed to settle overnight, after which the supernatant was collected, acidified to pH 6 with dilute HCl, and filtered before use.

## 2.3 $Fe^{2+}$ temporal dynamics and Fe plaque quantification

Temporal monitoring of $Fe^{2+}$ and $Fe^{3+}$ concentrations was conducted to follow Fe oxidation and precipitation dynamics during iron plaque induction. Daily measurements were

performed by withdrawing small solution aliquots (~ 300 µL) from the incubation system and immediately analysing them for dissolved Fe species using the ferrozine colorimetric method. Absorbance readings were taken at a microwell plate reader (TECAN, Switzerland) at a wavelength of 562 nm. $Fe^{2+}$ and total Fe concentrations were measured, while the concentration of $Fe^{3+}$ was calculated by difference. This allowed us to verify that $Fe^{2+}$ oxidation proceeded consistently across treatments and enabled identification of the endpoint of the plaque formation, defined by a > 90% decrease in dissolved $Fe^{2+}$. This approach ensured that iron plaque quantification was performed only after the precipitation process had reached almost completion and steady-state conditions were achieved. After 7 days (MC) or 12 days (SC) of induction, when this concentration threshold were reached, bottles were opened and iron plaque formed on the artificial roots was extracted with the cold dithionite–citrate–bicarbonate (DCB) method (Crowder & Taylor, 1983). Extracts were filtered through 0.22 µm paper membranes and stored at −20 °C until quantification by ICP–OES (Agilent, CA, United States).

## 2.4. Statistical analysis

All statistical analyses were conducted using R studio v4.4.3 (R Core Team, 2025).

A two-way ANOVA was performed to evaluate the effects of DOM type (malic acid, soil-derived C, or control without DOM) and C:Fe molar ratio (2:1 and 12:1) on the amount of Fe accumulated in the plaque. Data normality (Shapiro-Wilk test) and homogeneity of variances (Bartlett's test) were tested across all experimental groups. Post-hoc comparisons using Tukey's HSD test were exploited to identify pairwise differences between treatment groups. Data analyses were conducted using the 'aov' and 'TukeyHSD' functions of the 'multcomp' package (Hothorn et al., 2008).

# 3. Results

## 3.1 Iron plaque formation

Results on plaque formation at the end of the experiment are shown in Figure 2. Significant differences resulted between all the treatments studied. The greatest amount of iron plaque formed on the artificial roots was observed in absence of DOM, while additions of MC or

SC markedly reduced $Fe^{3+}$ deposition. Across experimental treatments, plaque formation was highest in SC at 2:1 C:Fe, followed by SC at 12:1 C:Fe, MC at 2:1 C:Fe, and lowest in MC at 12:1 C:Fe. Thus, both the type of organic carbon and the C:Fe molar ratio controlled plaque abundance. Malic acid suppressed plaque more strongly than soil-derived DOM, and a higher C:Fe ratio further decreased plaque formation, which is consistent with our hypothesis of a stronger Fe complexation and stabilization in solution.

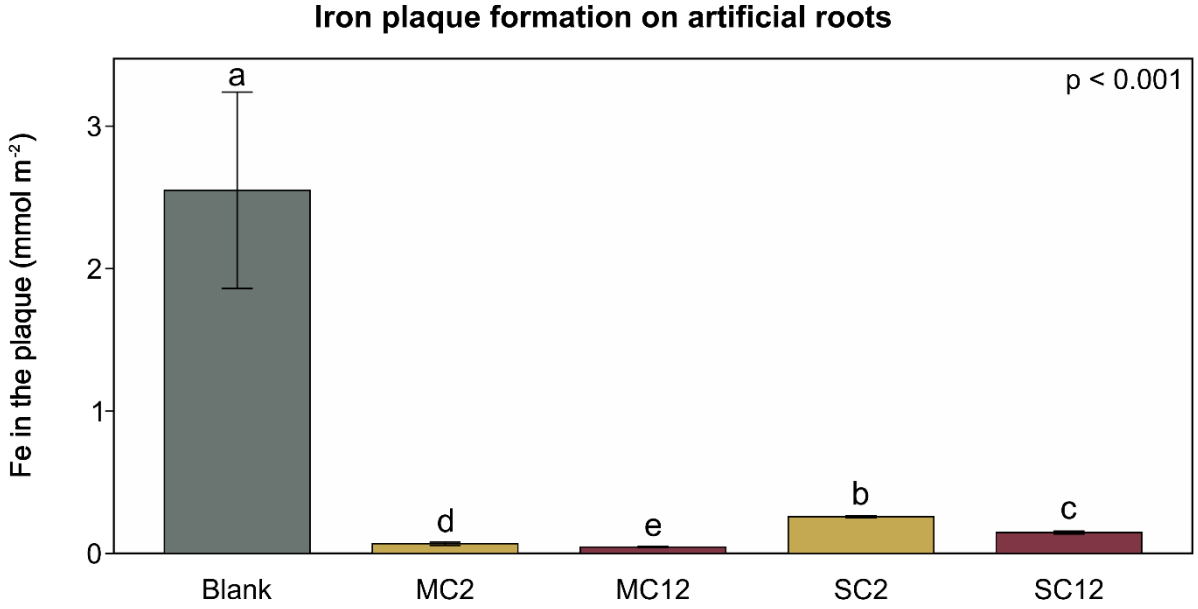


**Figure 2.** Abundance of iron plaque formed at the end of the incubation on artificial roots. Colours refer to different treatments: grey (no DOM), yellow (MC) at C:Fe molar ratios of 2:1 and 12:1, and red (SC) at C:Fe molar ratios of 2:1 and 12:1. Bars show means ± SD. Different letters indicate significant differences among treatments as retrieved from ANOVA and Tukey's post hoc test.

## 3.2 Temporal dynamics of dissolved $Fe^{2+}$ and $Fe^{3+}$

Variations of $Fe^{2+}$ and $Fe^{3+}$ concentrations in solution across treatments during plaque induction are shown in Figure 3. $Fe^{2+}$ concentrations declined over time in all treatments, with minor variations between each other, reflecting progressive oxidation to $Fe^{3+}$ as the experiment progressed. Regarding $Fe^{3+}$, in absence of organic matter its concentration in solution remained low because the newly oxidized $Fe^{3+}$ was progressively and rapidly removed from solution precipitating on the artificial roots. In contrast, both DOM types accelerated $Fe^{2+}$ oxidation and produced much higher $Fe^{3+}$ concentrations in solution,

indicating ligand-assisted oxidation and stabilization of $Fe^{3+}$. The effect was strongest with MC and at the 12:1 C:Fe ratio, where $Fe^{3+}$ rose quickly during the first days of experiment. With SC, $Fe^{3+}$ also increased initially. However, at SC 2:1 it peaked around day ~3 and then dropped to ~0, which is consistent with saturation of available binding sites and subsequent removal of $Fe^{3+}$ as plaque.

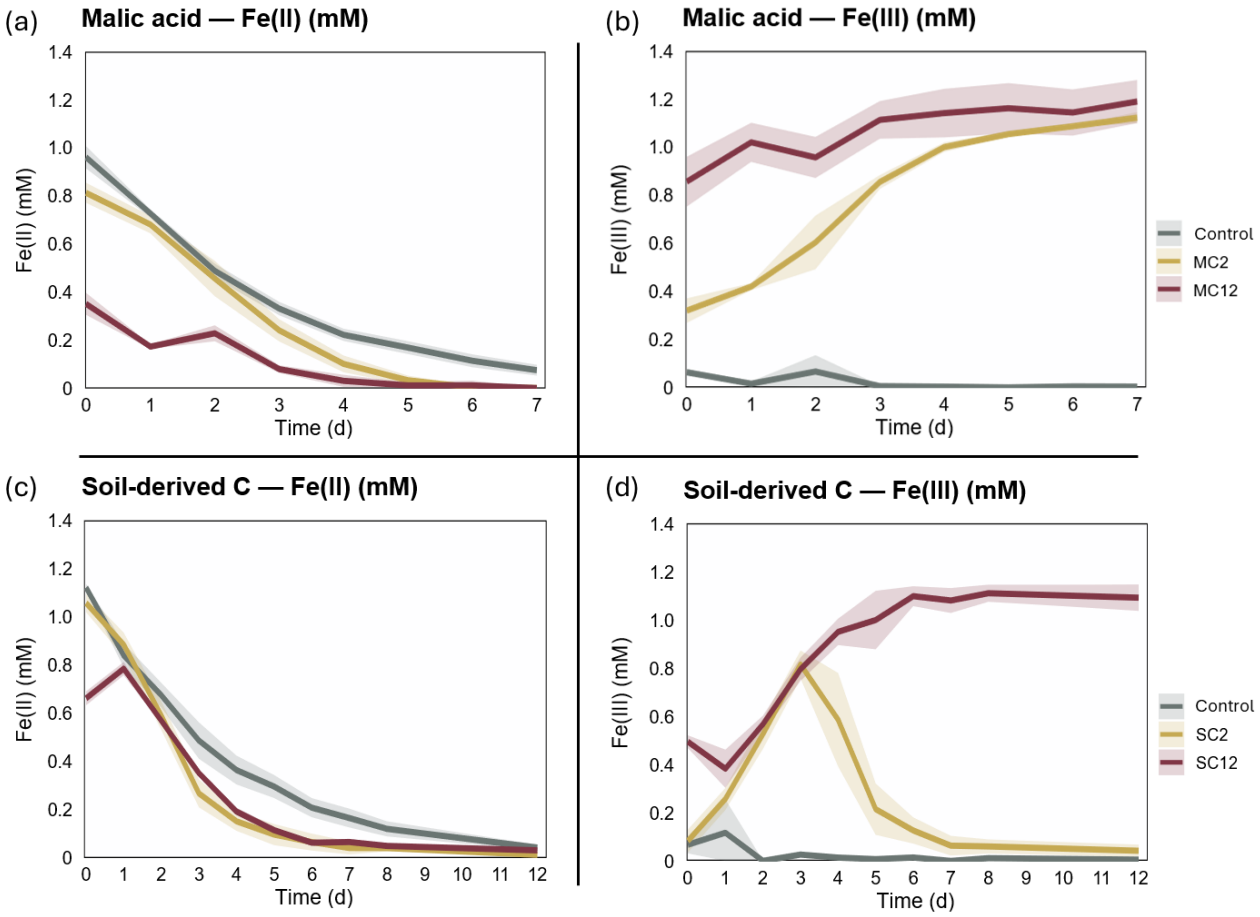


**Figure 3.** Temporal monitoring of $Fe^{2+}$ and $Fe^{3+}$ concentrations in solution in the absence and presence of DOM. (a) MC: $Fe^{2+}$, (b) MC: $Fe^{3+}$, (c) SC: $Fe^{2+}$, and (d) SC: $Fe^{3+}$. Colours indicate treatments: grey = no DOM, yellow = MC or SC at a C:Fe molar ratio of 2:1, and red = MC or SC at a C:Fe molar ratio of 12:1. Lines represent mean values, and shaded areas indicate variability.

# 4. Discussion

This study explored the process on how dissolved organic matter (DOM) modulates iron plaque formation, by exploiting two carbon sources at different C:Fe molar ratios and by using artificial roots. Temporal monitoring showed that DOM promoted rapid $Fe^{2+}$ oxidation

and stabilized $Fe^{3+}$ in solution, while plaque formation at the end of the experiment was strongly suppressed in presence of DOM. The largest inhibition was reported being under MC and at the higher C:Fe ratio (Figures 2, 3).

The declining concentration of $Fe^{2+}$, consistent with its oxidation to $Fe^{3+}$ reported across all samples, reflects the kinetics in natural waters at circumneutral pH, where oxidation rates increase steeply with pH, possibly further modulated by temperature and ionic strength (Millero, 1987; Santana-Casiano et al., 2005; Morgan & Lahav, 2007). In absence of DOM, dissolved $Fe^{3+}$ remained low following its rapidly removal from solution by precipitation, which again is in line with the natural behaviour at circumneutral pH range (Pham & Waite, 2006). By contrast, both MC and SC kept the concentration of dissolved $Fe^{3+}$ in solution remarkably high from the beginning of the experiment (Figure 3), suggesting that Fe-binding organic ligands can accelerate the $Fe^{3+}$ oxidation rate in aqueous phase (Rose & Waite, 2003; Lee et al., 2016). The stronger effect reported for MC is consistent with experimental evidence that citrate and malate can rapidly dissolve $Fe(OH)_3$ and form stable complexes with $Fe^{3+}$, possibly following the high density of ionizable carboxyl groups typical of low molecular weight organic acids (Jones et al., 1996; Adeleke et al., 2017). The DOM amount further played an important role. With soil-derived DOM at 2:1 C:Fe, $Fe^{3+}$ concentration in solution dropped after ~3 days, whereas at 12:1 C:Fe it remained high (Figure 3), a pattern consistent with limited binding capacity at low C:Fe and sustained complexation when binding sites are abundant (Gledhill & Buck, 2012; Lee et al., 2016).

These trends were reflected in plaque formation at the end of the experiment (Figure 2). When $Fe^{3+}$ was complexed in solution by organic molecules, especially under MC and the higher C:Fe ratios of both MC and SC, less Fe was available for precipitation onto the artificial root surfaces, determining significant reduction in plaque abundance relative to the control treatment (absence of DOM). Plaque decreased by ~9 times with SC at 2:1 C:Fe and by ~22 times with MC at 12:1 C:Fe, highlighting that even low DOM levels can strongly suppress plaque deposition by keeping Fe complexed in solution.

DOM apparently covers opposing roles in plaque formation. On one side, it promotes oxidation chemically and, in field conditions, by fuelling microbial $O_2$ demand. This enhances plaque deposition if sufficient $Fe^{2+}$ is available (Laufer et al., 2016; Yuan et al., 2022). On the other side, our findings report how DOM competes with plaque formation by stabilizing $Fe^{3+}$ as soluble complexes that persist in solution and prevent Fe precipitation on

root surfaces (Anderson et al., 2021; Logozzo et al., 2023). Fieldwork with *Lobelia dortmanna* linked higher sediment organic matter to greater plaque, suggesting a main role of anoxia, microbial activity, and $Fe^{2+}$ supply (Christensen & Sand-Jensen, 1998), whereas pot and hydroponic studies showed that DOM can reduce metal availability by its interaction with Fe in the bulk soil and in the rhizosphere, aligning with our complexation and stabilization explanation (Liu et al., 2021c; Meng et al., 2022). In our controlled environment, the complexation mechanism seemed to prevail, as the DOM accelerated $Fe^{2+}$ oxidation in the solution yet halted Fe deposition on the artificial roots, with malic acid and higher C:Fe producing the strongest suppression. Nevertheless, our system was sterile and we cannot exclude the possible contrasting effect in presence of microorganisms, which is advisable to test in the future. Our setup can easily accommodate an increase of complexity by the use of additional organic sources or the inoculation of specific bacterial taxa.

Despite organic matter has been considered only a minor affecting factor within the plaque formation process, our results show that even low amounts of DOM can reduce down to 9 times the plaque formation in presence of soil-derived C, or even to 22 times close to maximum exudation spots of roots. The combination of temporal monitoring and plaque formation at the end of the experiment supports a coherent mechanism: DOM, especially low molecular weight organic acids, accelerates $Fe^{2+}$ oxidation but stabilizes $Fe^{3+}$ as soluble complexes, thereby limiting plaque deposition. This helps unravelling the direct role of organic matter in iron plaque formation and its dynamics.

# 5. Conclusions

This preliminary study with artificial roots shows that dissolved organic matter strongly modulates the Fe cycle and the formation of root iron plaque. Temporal monitoring revealed rapid $Fe^{2+}$ oxidation and sustained $Fe^{3+}$ in solution in the presence of DOM, whereas plaque formation at the end of the experiment was markedly lower than in the absence of organic matter, with different magnitude of inhibition depending on the type of the carbon source and its abundance.

Early oxidation can favour deposition when it occurs near the root surface. However, in our study DOM predominantly competed with plaque formation by complexing $Fe^{2+}$ or $Fe^{3+}$ and stabilising it in solution, far away from the artificial root surface. The type of DOM mattered, as low molecular weight organic acids with a high density of carboxyl groups formed

stronger $Fe^{3+}$ complexes and markedly suppressed plaque formation. Despite our plaque-induction system simplifies the complexity of the real environment, it enabled a controlled and precise reproducibility, allowing a mechanistic comprehension of the plaque formation process and highlighting the direct control mechanism of DOM on iron plaque formation. Moreover, our plaque-induction system can be easily implemented in the future to further deepen our knowledge on basic mechanisms influencing Fe and C dynamics in soils.

# *General discussion*

Coastal wetlands are undergoing rapid shifts due to sea level rise, altered river discharge, and saltwater intrusion, with subsequent effects on soil chemistry, plant communities, and biogeochemical cycling (Herbert et al., 2015; IPCC, 2023). This thesis investigated how soil salinity, soil organic matter (SOM), and related soil and plant traits interact to regulate the root iron plaques formation and to shape rhizosphere processes under flooded soil conditions, where elevated salinity may co-occur (Daliakopoulos et al., 2016; Mitsch & Gosselink, 2015). To achieve this, field observations along a natural salinity gradient were integrated with controlled laboratory experiments designed to isolate the specific roles of humic substances (HS) and dissolved organic matter (DOM) in mitigating salt stress and modulating iron deposition.

Regarding the role of soil salinity and SOM to control plaque formation at field scale, my results demonstrated that salinity regulates iron plaque formation on *Phragmites australis* roots prevalently through indirect mechanisms, and specifically through soil redox potential (Eh) and pH, which emerged as the main physicochemical drivers of plaque abundance, with more reducing conditions promoting $Fe^{2+}$ availability in the rhizosphere and higher pH favouring $Fe^{3+}$ precipitation at the root surface. In anoxic soils, $Fe^{3+}$ is converted to soluble $Fe^{2+}$, and where roots leak oxygen, the $Fe^{2+}$ is re-oxidized at the root-soil interface to Fe oxy(hydr)oxides forming the plaque (Chen et al., 1980; Khan et al., 2016). High salinity contributes to impose harsher conditions, as the abundance of sulphates in the soil, which fuels microbial reduction to sulphide, is strongly related to low Eh values and can divert $Fe^{2+}$ into FeS phases, so that plaque formation ultimately depends on whether root $O_2$ flux can re-oxidize Fe (Lamers et al., 2013; Povidisa et al., 2009). Moreover, plant stand density also significantly influenced plaque abundance, showing a non-linear response with maximum plaque formation at intermediate densities. This pattern likely shows how very high plant densities may reduce rhizosphere oxygen availability due to competition for belowground resources and space. Therefore, these findings suggest that salinity affects plaque formation principally by altering redox potential and plant-driven oxygen supply, rather than exerting a direct inhibition on iron deposition processes. This improved understanding may contribute in the future to more effective management and conservation strategies for wetlands, particularly to the growth dynamics of populations of hydrophytes, such as *P. australis*,

which are likely to experience increasing salinity stress in the coming decades due to sea level rise and more severe seawater intrusions.

One critical point remaining unsolved in my work is the lack of a direct effect of SOM on plaque abundance, which was instead observed by previous studies (e.g. Jones et al., 1996). The basic SOM fractionation performed in this study may have masked a potential role of specific SOM fractions in the processes involved. Some recent studies (Liu et al., 2021c; Xie et al., 2024) have shown that iron plaque formation is not controlled by the total amount of organic matter, but rather by its chemical composition. Specifically, humic-like and high molecular weight DOM fractions have been positively associated with plaque formation, whereas more labile fractions exerted weaker or contrasting effects. Another possibility is that the lack of an effect of the SOM in our study may have been caused by the dominant influence of salinity, which also regulates SOM mineralization. In fact, modest increases in salinity can stimulate microbial decomposition and strongly reduce SOM accumulation in wetland soils (Morrissey et al., 2014), also potentially explaining the low variability of organic fractions in the dataset. Moreover, although root porosity did not show a significant relationship with plaque abundance, my results may instead point to the importance of structural barriers regulating oxygen leakage to the rhizosphere. Many wetland species develop suberized or lignified barriers to cope with prolonged anoxic conditions (Colmer & Flowers, 2008; He et al., 2024), limiting or suppressing radial oxygen loss (ROL). The extent of exodermal suberization and the efficiency of ROL barriers could therefore play a more critical role in determining plaque development under saline conditions than the root porosity itself. However, since direct data on ROL barriers were not acquired in my study, this hypothesis remains to be tested in future work.

Since in this first part I found that salinity affected plaque abundance indirectly through soil redox potential and plant density, but no relationship was observed between DOM and salinity or between DOM and plaque formation, I decided to conduct two controlled laboratory experiments to gain a better mechanistic understanding of the role of SOM.

First, the mitigation capacity of humic substances against salt stress proved to be conditional on both the salt type and the chemical nature of the humic material. In my experiments, humic and humic-like substances effectively alleviated the stress induced by sodium carbonate ($Na_2CO_3$), whereas they showed limited to negligible effects with sodium chloride (NaCl). This response reflects the stronger pH buffering capacity and higher degree of

functional group dissociation in $Na_2CO_3$ affected soils, which promote greater cation exchange and ion complexation compared with the neutral NaCl soils. Such interactions are consistent with the broader view of humic substances as polyelectrolytes capable of regulating ion activity and pH balance in saline environments (Canellas et al., 2015).

These findings confirmed that humic substances differ in their ability to mitigate salt stress, and the $^1$H-NMR analysis and charge density measurements provided evidence for differences in the relative abundance of functional groups, supporting the observed variability in mitigation efficiency. However, other structural characteristics, including molecular size, aromaticity, and supramolecular organization, which have been shown to influence humic reactivity in previous studies (Chen et al., 2004; Piccolo, 2001), remained unaccounted for in my study and may have contributed to the observed variability. In addition, the calculated $SAP_{HA\ eff}$ offers a preliminary quantitative tool to estimate the minimum amount of amendment required for field application, highlighting the practical applicability of these findings. However, extrapolation of outcomes from laboratory experiments to field conditions is never straightforward and needs to be validated with field research. Further research is also needed to advance the insight into concomitant factors, such as aggregation and precipitation, which may also contribute to the amelioration potential of humic substances towards soil salinity.

In an artificial system, the experiments revealed that DOM can markedly suppress iron plaque formation by stabilizing $Fe^{3+}$ in solution through complexation. Temporal monitoring confirmed that DOM not only delayed Fe precipitation but maintained $Fe^{3+}$ in soluble form throughout the experiment, resulting in a significantly lower plaque accumulation at the end of the incubation compared to treatment without DOM addition. This result supports findings from other authors showing that DOM, particularly its low molecular weight fractions, can inhibit Fe precipitation processes, delaying or even preventing plaque formation (Karlsson & Persson, 2010; Aiken et al., 2011), and provides experimental evidence of this mechanism under strictly controlled conditions using an artificial root system. My results further demonstrated that the degree of suppression was dependent on the chemical nature and concentration of the DOM source, with low molecular weight organic acids containing a high density of carboxyl groups exerting the strongest inhibitory effect. As already discussed, other recent studies (e.g. Liu et al., 2021c; Yu et al., 2024; Xie et al., 2024) showed how the DOM composition can affect heavy metals uptake and iron plaque formation by plants, and this could potentially lead in the future to the development of strategies to

modulate nutrient and heavy metal immobilization and plant uptake through targeted management of DOM inputs in the field.

However, despite the mechanistic insights gained from this experiment, some limitations remain. The experiments were conducted under simplified and short-term, solution-phase conditions, designed to isolate the direct effects of DOM but necessarily reducing environmental complexity. In addition, the DOM sources tested represented only a limited range of chemical compositions, which facilitated mechanistic interpretation but may not capture the full variability present in natural wetlands. Future research should therefore aim to scale-up laboratory experiments to field conditions by extending experimental duration and incorporating both natural and artificial substrates that better simulate rhizosphere processes. Incorporating living plants would allow assessing how plant-mediated oxygen release interacts with DOM complexation over time. Moreover, comparing DOM of different origins, such as soil extracts, root exudates, and soil porewaters, could suggest which DOM fractions most strongly influence iron precipitation dynamics and plaque stability.

# *Further research activities*

During my PhD, I took part in several complementary research projects and academic activities.

In collaboration with the University of Verona, I contributed to a study on iron plaque formation in rice paddies exposed to climate change–related stressors (i.e. warming, flooding, organic amendment), with plant elemental analyses conducted through ICP–OES (University of Udine) and Fe speciation by synchrotron-based XRF at the Elettra Synchrotron facility (Trieste, Italy). We hypothesized that warming-induced alterations in iron plaque mineralogy may enhance SOM mineralization, while the application of exogenous organic matter and reduced flooding levels could mitigate this effect. We further expect that both controlled flooding regimes and exogenous organic matter inputs may inhibit SOM degradation and promote the formation of iron plaques, thereby contributing to SOM stabilization.

From October to December 2024, I carried out an Erasmus traineeship at the University of Ljubljana (SLO), focusing on the effects of pH and salinity on iron plaque mineralogy and their elemental composition. My work included sample preparation, XRF imaging, and data analysis of synchrotron-based XRF/XAS measurements on both silicon tubes, used as a proxy for living roots, and on roots of *Puccinellia festuciformis*. A manuscript is under preparation and will be shortly submitted for publication to a peer review journal.

Finally, I collaborated with the Botany Group of the University of Udine on a study conducted in the Grado-Marano Lagoon. The study aimed to assess the impact of saltwater intrusion on one of the largest estuarine reed bed ecosystems in Europe by integrating field-based functional trait analysis with satellite remote sensing. Specifically, it sought to i) characterize *Phragmites australis* responses along salinity and flooding gradients through a trait-based approach, ii) identify key plant traits suitable for satellite monitoring, and iii) detect long-term ecosystem trends using multispectral Sentinel-2 data. My role in the study involved supporting the field sampling campaigns and conducting laboratory analyses of the soil parameters considered, i.e. in-situ measurements of soil redox potential and determinations of soil electrical conductivity and acid volatile sulphides. A paper with the results of this study, to which I contributed as a co-author, has been recently published in Ecological Indicators journal, with the title of “Integrating remote sensing and functional

traits to elucidate estuarine common reed beds decline driven by soil salinity and anoxia" (https://doi.org/10.1016/j.ecolind.2025.114294).

# *References*

**Abd El-Samad, H.M., Shaddad, M.A.K., 1996.** *Comparative effect of sodium carbonate, sodium sulphate, and sodium chloride on the growth and related metabolic activities of pea plants. Journal of Plant Nutrition* **19**, 717–728. https://doi.org/10.1080/01904169609365155.

**Abdel Latef, A.A.H., Chaoxing, H., 2014.** *Does inoculation with Glomus mosseae improve salt tolerance in pepper plants? Journal of Plant Growth Regulation* **33**, 644–653. https://doi.org/10.1007/s00344-014-9414-4.

**Abu-Ria, M., Shukry, W., Abo-Hamed, S., Albaqami, M., Almuqadam, L., Ibraheem, F., 2023.** *Humic acid modulates ionic homeostasis, osmolytes content, and antioxidant defence to improve salt tolerance in rice. Plants* **12**, 1834. https://doi.org/10.3390/plants12091834.

**Achenbach, L., Eller, F., Nguyen, L.X., Brix, H., 2013.** *Differences in salinity tolerance of genetically distinct Phragmites australis clones. AoB PLANTS* **5**, plt019. https://doi.org/10.1093/aobpla/plt019.

**Adams, K.H., Reager, J.T., Buzzanga, B.A., David, C.H., Sawyer, A.H., Hamlington, B.D., 2024.** *Climate-Induced Saltwater Intrusion in 2100: Recharge-Driven Severity, Sea Level-Driven Prevalence. Geophysical Research Letters* **51**, e2024GL110359. https://doi.org/10.1029/2024GL110359.

**Adeleke, R., Nwangburuka, C., Oboirien, B., 2017.** *Origins, roles and fate of organic acids in soils: A review. South African Journal of Botany* **108**, 393–406. https://doi.org/10.1016/j.sajb.2016.09.002.

**Agegnehu, G., Srivastava, A.K., Bird, M.I., 2017.** *The role of biochar and biochar-compost in improving soil quality and crop performance: A review. Applied Soil Ecology* **119**, 156–170. https://doi.org/10.1016/j.apsoil.2017.06.008.

**Aiken, G.R., Hsu-Kim, H., Ryan, J.N., 2011.** *Influence of dissolved organic matter on the environmental fate of metals, nanoparticles, and colloids. Environmental Science & Technology* **45**, 3196–3201. https://doi.org/10.1021/es103992s.

**Ait-El-Mokhtar, M., Baslam, M., Ben-Laouane, R., Anli, M., Boutasknit, A., Mitsui, T., Wahbi, S., Meddich, A., 2020.** *Alleviation of detrimental effects of salt stress on date*

*palm (Phoenix dactylifera L.) by the application of arbuscular mycorrhizal fungi and/or compost. Frontiers in Sustainable Food Systems* **4**, 131. https://doi.org/10.3389/fsufs.2020.00131.

**Alcérreca-Huerta, J.C., Callejas-Jiménez, M.E., Carrillo, L., Castillo, M.M., 2019.** *Dam implications on salt-water intrusion and land use within a tropical estuarine environment of the Gulf of Mexico. Science of The Total Environment* **652**, 1102–1112. https://doi.org/10.1016/j.scitotenv.2018.10.288.

**Allan, R.P., Barlow, M., Byrne, M.P., Cherchi, A., Douville, H., Fowler, H.J., Gan, T.Y., Pendergrass, A.G., Rosenfeld, D., Swann, A.L.S., Wilcox, L.J., Zolina, O., 2020.** *Advances in understanding large-scale responses of the water cycle to climate change. Annals of the New York Academy of Sciences* **1472**, 49–75. https://doi.org/10.1111/nyas.14337.

**Amsberry, L., Baker, M.A., Ewanchuk, P.J., Bertness, M.D., 2000.** *Clonal integration and the expansion of Phragmites australis. Ecological Applications* **10**, 1110–1118. https://doi.org/10.1890/1051-0761(2000)010%255B1110:CIATEO%255D2.0.CO;2.

**Anderson, L.E., Trueman, B.F., Dunnington, D.W., Gagnon, G.A., 2021.** *Relative importance of organic- and iron-based colloids in six Nova Scotian lakes. npj Clean Water* **4**, 26. https://doi.org/10.1038/s41545-021-00115-4.

**Aravind, J., Vimala Devi, S., Radhamani, J., Jacob, S.R., Srinivasan, K., 2023.** *germinationmetrics: Seed Germination Indices and Curve Fitting.* Zenodo. https://doi.org/10.5281/zenodo.8267035.

**Armstrong, W., 1967.** *The oxidising activity of roots in waterlogged soils. Physiologia Plantarum* **20**, 920–926. https://doi.org/10.1111/j.1399-3054.1967.tb08379.x.

**Armstrong, W., 1971.** *Radial oxygen losses from intact rice roots as affected by distance from the apex, respiration and waterlogging. Physiologia Plantarum* **25**, 192–197. https://doi.org/10.1111/j.1399-3054.1971.tb01427.x.

**Armstrong, W., 1980.** *Aeration in higher plants.* In: Woolhouse, H.W. (Ed.), *Advances in Botanical Research.* Academic Press, pp. 225–332. https://doi.org/10.1016/S0065-2296(08)60089-0.

**Armstrong, J., Afreen-Zobayed, F., Armstrong, W., 1996.** *Phragmites die-back: sulphide- and acetic acid-induced bud and root death, lignifications, and blockages within aeration and vascular systems. New Phytologist* **134**, 601–614. https://doi.org/10.1111/j.1469-8137.1996.tb04925.x.

**Armstrong, W., Cousins, D., Armstrong, J., Turner, D., Beckett, P.M., 2000.** *Oxygen distribution in wetland plant roots and permeability barriers to gas-exchange with the rhizosphere: a microelectrode and modelling study with Phragmites australis*. *Annals of Botany* **86**, 687–703. https://doi.org/10.1006/anbo.2000.1236.

**Armstrong, J., & Armstrong, W., 2005.** *Rice: sulfide-induced barriers to root radial oxygen loss, $Fe^{2+}$ and water uptake, and lateral root emergence*. *Annals of Botany* **96**, 625–638. https://doi.org/10.1093/aob/mci215.

**Atero-Calvo, S., Magro, F., Masetti, G., Navarro-León, E., Blasco, B., Ruiz, J.M., 2024.** *Salinity stress mitigation by radicular and foliar humic substances application in lettuce plants. Plant Growth Regulation* **104**, 151–167. https://doi.org/10.1007/s10725-024-01151-z.

**Austrian Standards International (ASI), 1999.** *ÖNORM L 1084-99: Bodenuntersuchung – Bestimmung des Carbonatgehaltes – Volumetrisches (Scheibler) Verfahren.* Austrian Standards International, Wien.

**Bai, Y., Yan, Y., Zuo, W., Gu, C., Xue, W., Mei, L., Shan, Y., Feng, K., 2017.** *Coastal mudflat saline soil amendment by dairy manure and green manuring. International Journal of Agronomy* **2017**, 4635964:1–4635964:9. https://doi.org/10.1155/2017/4635964.

**Bates, B.C., Kundzewicz, Z.W., Wu, S., Palutikof, J.P. (Eds.), 2008.** *Climate Change and Water. IPCC Technical Paper VI.* IPCC Secretariat, Geneva, 210 pp. Available online: https://archive.ipcc.ch/pdf/technical-papers/climate-change-water-en.pdf.

**Batty, L.C., Baker, A.J.M., Wheeler, B.D., Curtis, C.D., 2000.** *The effect of pH and plaque on the uptake of Cu and Mn in Phragmites australis (Cav.) Trin ex. Steudel. Annals of Botany* **86**, 647–653. https://doi.org/10.1006/anbo.2000.1191.

**Bellafiore, D., Ferrarin, C., Maicu, F., Manfè, G., Lorenzetti, G., Umgiesser, G., Zaggia, L., Levinson, A.V., 2021.** *Saltwater intrusion in a Mediterranean delta under a changing climate. Journal of Geophysical Research: Oceans* **126**, e2020JC016437. https://doi.org/10.1029/2020JC016437.

**Bergmeyer, H.U. (Ed.), 1974.** *Methods of Enzymatic Analysis.* 2nd ed., Vol. 3. Academic Press, New York, pp. 1464–1468.

**Bethke, C.M., 2007.** *Microbial kinetics*. In: *Geochemical and Biogeochemical Reaction Modeling*. Elsevier, 257–268. https://doi.org/10.1017/CBO9780511619670.

**Betzen, B.M., Smart, C.M., Maricle, K.L., Maricle, B.R., 2019.** *Effects of increasing salinity on photosynthesis and plant water potential in Kansas salt marsh species. Transactions of the Kansas Academy of Science* **122**, 49–58. https://doi.org/10.1660/062.122.0105.

**Bhattachan, A., Jurjonas, M.D., Moody, A.C., Morris, P.R., Sanchez, G.M., Smart, L.S., Taillie, P.J., Emanuel, R.E., Seekamp, E.L., 2018.** *Sea level rise impacts on rural coastal social-ecological systems and the implications for decision making. Environmental Science & Policy* **90**, 122–134. https://doi.org/10.1016/j.envsci.2018.10.006.

**Bollen, K. A., 1989.** *Structural equations with latent variables.* John Wiley & Sons.

**Brady, N.C., Weil, R.R., 2016.** *The Nature and Properties of Soils.* 15th ed. Pearson, Columbus, OH, USA. https://doi.org/10.2136/sssaj2016.0005br.

**Brambati, A., 1968.** *Sedimenti e litofacies della Laguna di Marano e di Grado. Memorie degli Istituti di Geologia e Mineralogia dell'Università di Padova* **28**, 1–108.

**Breheny, P., Burchett, W., 2017.** *Visualization of regression models using visreg. The R Journal* **9**, 56–71. https://doi.org/10.32614/RJ-2017-046.

**Brix, H., 1999.** *The European research project on reed die-back and progression (EUREED). Limnologica* **29**, 5–10. https://doi.org/10.1016/S0075-9511(99)80033-4.

**Buckley, B.M., Anchukaitis, K.J., Penny, D., Fletcher, R., Cook, E.R., Sano, M., Nam, L.C., Wichienkeeo, A., Minh, T.T., Hong, T.M., 2010.** *Climate as a contributing factor in the demise of Angkor, Cambodia. Proceedings of the National Academy of Sciences* **107**, 6748–6752. https://doi.org/10.1073/pnas.0910827107.

**Burnham, K.P., Anderson, D.R., 2004.** *Multimodel inference: Understanding AIC and BIC in model selection. Sociological Methods & Research* **33**, 261–304. https://doi.org/10.1177/0049124104268644.

**Calvo, P., Nelson, L., Kloepper, J.W., 2014.** *Agricultural uses of plant biostimulants. Plant and Soil* **383**, 3–41. https://doi.org/10.1007/s11104-014-2131-8.

**Canellas, L.P., Olivares, F.L., Aguiar, N.O., Jones, D.L., Nebbioso, A., Mazzei, P., Piccolo, A., 2015.** *Humic and fulvic acids as biostimulants in horticulture. Scientia Horticulturae* **196**, 15–27. https://doi.org/10.1016/j.scienta.2015.09.013.

**Chabreck, R.H., 1972.** *Vegetation, water and soil characteristics of the Louisiana coastal region.* Louisiana Agricultural Experiment Station Bulletin 664, Louisiana State University, Baton Rouge, LA, USA, 72 pp. Available online: https://repository.lsu.edu/agexp/147.

**Chaganti, V.N., Crohn, D.M., 2015.** *Evaluating the relative contribution of physiochemical and biological factors in ameliorating a saline–sodic soil amended with composts and biochar and leached with reclaimed water. Geoderma* **259–260**, 45–55. https://doi.org/10.1016/j.geoderma.2015.05.005.

**Chaganti, V.N., Crohn, D.M., Šimůnek, J., 2015.** *Leaching and reclamation of a biochar and compost amended saline–sodic soil with moderate SAR reclaimed water. Agricultural Water Management* **158**, 255–265. https://doi.org/10.1016/j.agwat.2015.05.016.

**Chambers, R.M., Mozdzer, T.J., Ambrose, J.C., 1998.** *Effects of salinity and sulfide on the distribution of Phragmites australis and Spartina alterniflora in a tidal saltmarsh. Aquatic Botany* **62**, 161–169. https://doi.org/10.1016/S0304-3770(98)00095-3.

**Chambers, L.G., Reddy, K.R., Osborne, T.Z., 2011.** *Short-term response of carbon cycling to salinity pulses in a freshwater wetland. Soil Science Society of America Journal* **75**, 2000–2007. https://doi.org/10.2136/sssaj2011.0026.

**Chambers, L.G., Davis, S.E., Troxler, T., Boyer, J.N., Downey-Wall, A., Scinto, L.J., 2014.** *Biogeochemical effects of simulated sea level rise on carbon loss in an Everglades mangrove peat soil. Hydrobiologia* **726**, 195–211. https://doi.org/10.1007/s10750-013-1764-6.

**Chen, C.C., Dixon, J.B., Turner, F.T., 1980.** *Iron coatings on rice roots: Morphology and models of development. Soil Science Society of America Journal* **44**, 1113–1119. https://doi.org/10.2136/sssaj1980.03615995004400050046x.

**Chen, Y., Clapp, C.E., Magen, H., 2004.** *Mechanisms of plant growth stimulation by humic substances: the role of organo-iron complexes. Soil Science and Plant Nutrition* **50**, 1089–1095. https://doi.org/10.1080/00380768.2004.10408579.

**Chen, R.F., Shen, R.F., Gu, P., Dong, X.Y., Du, C.W., Ma, J.F., 2006.** *Response of rice (Oryza sativa) with root surface iron plaque under aluminium stress. Annals of Botany* **98**, 389–395. https://doi.org/10.1093/aob/mcl110.

**Chen, Z., Liu, F., Bu, T., Liu, Y., Zhu, J., 2016.** *Effects of organic acids on dissolution of Fe and Mn from weathering coal gangue. Acta Geochimica* **35**, 316–328. https://doi.org/10.1007/s11631-016-0104-8.

**Cherif, H., Ayari, F., Ouzari, H., Marzorati, M., Brusetti, L., Jedidi, N., Hassen, A., Daffonchio, D., 2009.** *Effects of municipal solid waste compost, farmyard manure and chemical fertilizers on wheat growth, soil composition and soil bacterial characteristics under Tunisian arid climate. European Journal of Soil Biology* **45**, 138–145. https://doi.org/10.1016/j.ejsobi.2008.11.003.

**Chhabra, R., 2004.** *Classification of salt-affected soils. Arid Land Research and Management* **19**, 61–79. https://doi.org/10.1080/15324980590887344.

**Chhabra, R., 2017.** *Soil salinity and water quality.* Routledge, London. https://doi.org/10.1201/9780203739242.

**Chollakup, R., Beck, J.B., Dirnberger, K., Tirrell, M., Eisenbach, C.D., 2013.** *Polyelectrolyte molecular weight and salt effects on the phase behaviour and coacervation of aqueous solutions of poly(acrylic acid) sodium salt and poly(allylamine) hydrochloride. Macromolecules* **46**, 2376–2390. https://doi.org/10.1021/ma202172q.

**Choudhary, O.P., Kharche, V.K., 2018.** *Soil salinity and sodicity.* In: *Soil Science: An Introduction.* Indian Society of Soil Science, New Delhi, India, pp. 353–384.

**Christensen, K.K., Sand-Jensen, K., 1998.** *Precipitated iron and manganese plaques restrict root uptake of phosphorus in Lobelia dortmanna. Canadian Journal of Botany* **76**, 2158–2163. https://doi.org/10.1139/b98-181.

**Čížková, H., Kučera, T., Poulin, B., Květ, J., 2023.** *Ecological basis of ecosystem services and management of wetlands dominated by common reed (Phragmites australis): European perspective. Diversity* **15**, 629. https://doi.org/10.3390/d15050629.

**Colmer, T.D., 2003.** *Long-distance transport of gases in plants: a perspective on internal aeration and radial oxygen loss from roots. Plant, Cell & Environment* **26**, 17–36. https://doi.org/10.1046/j.1365-3040.2003.00846.x.

**Colmer, T.D., Flowers, T.J., 2008.** *Flooding tolerance in halophytes. New Phytologist* **179**, 964–974. https://doi.org/10.1111/j.1469-8137.2008.02483.x.

**Colmer, T.D., Voesenek, L.A.C.J., 2009.** *Flooding tolerance: suites of plant traits in variable environments. Functional Plant Biology* **36**, 665–681. https://doi.org/10.1071/FP09144.

**Cook, B.I., Mankin, J.S., Marvel, K., Williams, A.P., Smerdon, J.E., Anchukaitis, K.J., 2020.** *Twenty-first century drought projections in the CMIP6 forcing scenarios. Earth's Future* **8**, e2019EF001461. https://doi.org/10.1029/2019EF001461.

**Cooke, J.D., Hamilton-Taylor, J., Tipping, E., 2007.** *On the acid–base properties of humic acid in soil. Environmental Science & Technology* **41**, 465–470. https://doi.org/10.1021/es061424h.

**Cosolo, M., Sponza, S., Fattori, U., 2015.** *La laguna di Marano e Grado: un mosaico di biodiversità – un patrimonio da preservare.* Regione Autonoma Friuli Venezia Giulia, Udine, 52 pp.

**Cotrufo, M.F., Wallenstein, M.D., Boot, C.M., Denef, K., Paul, E., 2013.** *The Microbial Efficiency-Matrix Stabilization (MEMS) framework integrates plant litter decomposition with soil organic matter stabilization: do labile plant inputs form stable soil organic matter? Global Change Biology* **19**, 988–995. https://doi.org/10.1111/gcb.12113.

**Cronin, J.T., Johnston, J., Diaz, R., 2020.** *Multiple potential stressors and dieback of Phragmites australis in the Mississippi River Delta, USA: Implications for restoration. Wetlands* **40**, 2247–2261. https://doi.org/10.1007/s13157-020-01356-8.

**Crowder, A.A., Taylor, G.J., 1983.** *Use of the DCB technique for extraction of hydrous iron oxides from roots of wetland plants. Amer. J. Bot.* **70**(8): 1254-1257.

**Crowder, A.A., Macfie, S.M., 1986.** *Seasonal deposition of ferric hydroxide plaque on roots of wetland plants. Canadian Journal of Botany* **64**, 2120–2124. https://doi.org/10.1139/b86-279.

**Daba, A.W., 2025.** *Rehabilitation of soil salinity and sodicity using diverse amendments and plants: a critical review. Discover Environment* **3**, 53. https://doi.org/10.1007/s44274-025-00199-6.

**Dai, A., 2013.** *Increasing drought under global warming in observations and models. Nature Climate Change* **3**, 52–58. https://doi.org/10.1038/nclimate1633.

**Daliakopoulos, I.N., Tsanis, I.K., Koutroulis, A., Kourgialas, N.N., Varouchakis, A.E., Karatzas, G.P., Ritsema, C.J., 2016.** *The threat of soil salinity: A European scale review. Science of The Total Environment* **573**, 727–739. https://doi.org/10.1016/j.scitotenv.2016.08.177.

**Delgado, A., Madrid, A., Kassem, S., Andreu, L., del Campillo, M.C., 2002.** *Phosphorus fertilizer recovery from calcareous soils amended with humic and fulvic acids. Plant and Soil* **245**, 277–286. https://doi.org/10.1023/A:1020445710584.

**Dell'Amico, C., Masciandaro, G., Ganni, A., Ceccanti, B., Garcia, C., Hernandez, T., Costa, F., 1994.** *Effects of specific humic fractions on plant growth.* In: Senesi, N., Miano, T.M. (Eds.), *Humic Substances in the Global Environment and Implications on Human Health.* Elsevier, Amsterdam, pp. 563–566.

**Dixit, S., Hering, J.G., 2003.** *Comparison of arsenic(V) and arsenic(III) sorption onto iron oxide minerals: implications for arsenic mobility. Environmental Science & Technology* **37**, 4182–4189. https://doi.org/10.1021/es030309t.

**du Jardin, P., 2015.** *Plant biostimulants: definition, concept, main categories and regulation. Scientia Horticulturae* **196**, 3–14. https://doi.org/10.1016/j.scienta.2015.09.021.

**Ejiri, M., Shiono, K., 2019.** *Prevention of radial oxygen loss is associated with exodermal suberin along adventitious roots of annual wild species of Echinochloa. Frontiers in Plant Science* **10**, 254. https://doi.org/10.3389/fpls.2019.00254.

**Elsey-Quirk, T., Lynn, A., Jacobs, M.D., Diaz, R., Cronin, J.T., Wang, L., Huang, H., Justic, D., 2024.** *Vegetation dieback in the Mississippi River Delta triggered by acute drought and chronic relative sea-level rise. Nature Communications* **15**, 3518. https://doi.org/10.1038/s41467-024-47828-x.

**Emerson, D., Weiss, J.V., Megonigal, J.P., 1999.** *Iron-oxidizing bacteria are associated with ferric hydroxide precipitates (Fe-plaque) on the roots of wetland plants. Applied and Environmental Microbiology*. https://doi.org/10.1128/AEM.65.6.2758-2761.1999.

**Etesami, H., Beattie, G.A., 2018.** *Mining halophytes for plant growth-promoting halotolerant bacteria to enhance the salinity tolerance of non-halophytic crops. Frontiers in Microbiology* **9**, 148. https://doi.org/10.3389/fmicb.2018.00148.

**Evans, D.E., 2004.** *Aerenchyma formation. New Phytologist* **161**, 35–49. https://doi.org/10.1046/j.1469-8137.2003.00907.x.

**FAO, 2021.** *The State of the World's Land and Water Resources for Food and Agriculture – Systems at breaking point. Synthesis report 2021.* FAO, Rome. https://doi.org/10.4060/cb7654en.

**Ferrarin, C., Umgiesser, G., Bajo, M., Bellafiore, D., De Pascalis, F., Ghezzo, M., Mattassi, G., Scroccaro, I., 2010.** *Hydraulic zonation of the lagoons of Marano and Grado, Italy. A modelling approach. Estuarine, Coastal and Shelf Science* **87**, 561–572. https://doi.org/10.1016/j.ecss.2010.02.012.

**Fontolan, G., Pillon, S., Bezzi, A., Villalta, R., Lipizer, M., Triches, A., D'Aietti, A., 2012.** *Human impact and the historical transformation of saltmarshes in the Marano and Grado Lagoon, northern Adriatic Sea. Estuarine, Coastal and Shelf Science* **113**, 41–56. https://doi.org/10.1016/j.ecss.2012.02.007.

**Fox, T.R., Comerford, N.B., 1990.** *Low-molecular-weight organic acids in selected forest soils of the southeastern USA. Soil Science Society of America Journal* **54**, 1139–1144. https://doi.org/10.2136/sssaj1990.03615995005400040037x.

**Fu, Y.-Q., Yang, X.-J., Ye, Z.-H., Shen, H., 2016.** *Identification, separation and component analysis of reddish brown and non-reddish brown iron plaque on rice (Oryza sativa) root surface. Plant and Soil* **402**, 277–290. https://doi.org/10.1007/s11104-016-2802-8.

**Fu, Y., Yang, X., Shen, H., 2018.** *Root iron plaque alleviates cadmium toxicity to rice (Oryza sativa) seedlings. Ecotoxicology and Environmental Safety* **161**, 534–541. https://doi.org/10.1016/j.ecoenv.2018.06.015.

**García-Ruiz, J.M., López-Moreno, J.I., Vicente-Serrano, S.M., Lasanta–Martínez, T., Beguería, S., 2011.** *Mediterranean water resources in a global change scenario. Earth-Science Reviews* **105**, 121–139. https://doi.org/10.1016/j.earscirev.2011.01.006.

**Gatto, F., Marocco, R., 1993.** *Morfometria e geometria idraulica dei canali della Laguna di Grado (Friuli-Venezia Giulia). Geografia Fisica e Dinamica Quaternaria* **16**, 107–120.

**Gebreegziabher, B.G., Qufa, C.A., 2017.** *Plant physiological stimulation by seeds salt priming in maize (Zea mays L.): Prospect for salt tolerance. African Journal of Biotechnology* **16**, 209–223. https://doi.org/10.5897/AJB2016.15819.

**Gharsallah, C., Fakhfakh, H., Grubb, D., Gorsane, F., 2016.** *Effect of salt stress on ion concentration, proline content, antioxidant enzyme activities and gene expression in tomato cultivars. AoB PLANTS* **8**, plw055. https://doi.org/10.1093/aobpla/plw055.

**Giblin, A.E., Howarth, R.W., 1984.** *Porewater evidence for a dynamic sedimentary iron cycle in salt marshes. Limnology and Oceanography* **29**, 47–53. https://doi.org/10.4319/lo.1984.29.1.0047.

**Gigante, D., Venanzoni, R., Zuccarello, V., 2011.** *Reed die-back in southern Europe? A case study from Central Italy. Comptes Rendus Biologies* **334**, 327–336. https://doi.org/10.1016/j.crvi.2011.02.004.

**Gigliotti, G., Giusquiani, P.L., Businelli, D., Macchioni, A., 1997.** *Composition changes of dissolved organic matter in a soil amended with municipal waste compost. Soil Science* **162**, 919–926. https://doi.org/10.1097/00010694-199712000-00007.

**Gilbert, B., Frenzel, P., 1998.** *Rice roots and CH4 oxidation: the activity of bacteria, their distribution and the microenvironment. Soil Biology and Biochemistry* **30**, 1903–1916. https://doi.org/10.1016/S0038-0717(98)00061-3.

**Gimeno, L., Stohl, A., Trigo, R.M., Dominguez, F., Yoshimura, K., Yu, L., Drumond, A., Durán-Quesada, A.M., Nieto, R., 2012.** *Oceanic and terrestrial sources of continental precipitation. Reviews of Geophysics* **50**, RG4003. https://doi.org/10.1029/2012RG000389.

**Gledhill, M., Buck, K.N., 2012.** *The organic complexation of iron in the marine environment: a review. Frontiers in Microbiology* **3**, 69. https://doi.org/10.3389/fmicb.2012.00069.

**Gondek, M., Weindorf, D.C., Thiel, C., Kleinheinz, G., 2020.** *Soluble salts in compost and their effects on soil and plants: A review. Compost Science & Utilization* **28**, 59–75. https://doi.org/10.1080/1065657X.2020.1772906.

**Grace, J. B., 2006.** *Structural equation modeling and natural systems.* Cambridge University Press.

**Greipsson, S., 1994.** *Effects of iron plaque on roots of rice on growth and metal concentration of seeds and plant tissues when cultivated in excess copper. Communications in Soil Science and Plant Analysis* **25**, 2761–2779. https://doi.org/10.1080/00103629409369223.

**Greipsson, S., Crowder, A.A., 1992.** *Amelioration of copper and nickel toxicity by iron plaque on roots of rice (Oryza sativa). Canadian Journal of Botany* **70**, 824–830. https://doi.org/10.1139/b92-105.

**Griggs, G., Reguero, B.G., 2021.** *Coastal adaptation to climate change and sea-level rise. Water* **13**, 2151. https://doi.org/10.3390/w13162151.

**Guo, L., Cutright, T.J., 2014.** *Effect of citric acid and rhizosphere bacteria on metal plaque formation and metal accumulation in reeds in synthetic acid mine drainage solution. Ecotoxicology and Environmental Safety* **104**, 72–78. https://doi.org/10.1016/j.ecoenv.2014.02.019.

**Gutteridge, J.M.C., 1991.** *Hydroxyl radical formation from the auto-reduction of a ferric citrate complex. Free Radical Biology and Medicine* **11**, 401–406. https://doi.org/10.1016/0891-5849(91)90157-X.

**Hansel, C.M., Fendorf, S., Sutton, S., Newville, M., 2001.** *Characterization of Fe plaque and associated metals on the roots of mine-waste impacted aquatic plants. Environmental Science & Technology* **35**, 3863–3868. https://doi.org/10.1021/es0105459.

**Hansel, C.M., Benner, S.G., Neiss, J., Dohnalkova, A., Kukkadapu, R.K., Fendorf, S., 2003.** *Secondary mineralization pathways induced by dissimilatory iron reduction of ferrihydrite under advective flow. Geochimica et Cosmochimica Acta* **67**, 2977–2992. https://doi.org/10.1016/S0016-7037(03)00276-X.

**Hardej, M., Ozimek, T., 2002.** *The effect of sewage sludge flooding on growth and morphometric parameters of Phragmites australis (Cav.) Trin. ex Steudel. Ecological Engineering* **18**, 343–350. https://doi.org/10.1016/S0925-8574(01)00095-7.

**Hartog, D., Kvet, C.J., Sukopp, H., 1989.** *Reed: a common species in decline. Aquatic Botany* **35**, 1–4.

**Hassani, A., Azapagic, A., Shokri, N., 2021.** *Global predictions of primary soil salinization under changing climate in the 21st century. Nature Communications* **12**, 6663. https://doi.org/10.1038/s41467-021-26907-3.

**Ha-Tran, D.M., Nguyen, T.T.M., Hung, S.-H., Huang, E., Huang, C.-C., 2021.** *Roles of plant growth-promoting rhizobacteria (PGPR) in stimulating salinity stress defence in plants: A review. International Journal of Molecular Sciences* **22**, 3154. https://doi.org/10.3390/ijms22063154.

**He, Z., Chen, J., Yuan, S., Chen, S., Hu, Y., Zheng, Y., Li, D., 2024.** *Iron plaque: A shield against soil contamination and key to sustainable agriculture. Plants* **13**, 1476. https://doi.org/10.3390/plants13111476.

**Held, I.M., Soden, B.J., 2006.** *Robust responses of the hydrological cycle to global warming. Journal of Climate* **19**, 5686–5699. https://doi.org/10.1175/JCLI3990.1.

**Hellings, S.E., Gallagher, J.L., 1992.** *The effects of salinity and flooding on Phragmites australis. Journal of Applied Ecology* **29**, 41–49. https://doi.org/10.2307/2404345.

**Herbert, E.R., Boon, P., Burgin, A.J., Neubauer, S.C., Franklin, R.B., Ardón, M., Hopfensperger, K.N., Lamers, L.P.M., Gell, P., 2015.** *A global perspective on wetland salinization: ecological consequences of a growing threat to freshwater wetlands. Ecosphere* **6**, art206. https://doi.org/10.1890/ES14-00534.1.

**Hoque, M.N., Hannan, A., Imran, S., Paul, N.C., Mondal, M.F., Sadhin, M.M.R., Bristi, J.M., Dola, F.S., Hanif, M.A., Ye, W., Brestic, M., Rhaman, M.S., 2023.** *Plant growth-promoting rhizobacteria-mediated adaptive responses of plants under salinity stress. Journal of Plant Growth Regulation* **42**, 1307–1326. https://doi.org/10.1007/s00344-022-10633-1.

**Hothorn, T., Bretz, F., Westfall, P., 2008.** *Simultaneous inference in general parametric models. Biometrical Journal* **50**, 346–363. https://doi.org/10.1002/bimj.200810425.

**Howard, R.J., Mendelssohn, I.A., 1999.** *Salinity as a constraint on growth of oligohaline marsh macrophytes. I. Species variation in stress tolerance. American Journal of Botany* **86**, 785–794. https://doi.org/10.2307/2656700

**Hu, Y., Li, J.-H., Zhu, Y.-G., Huang, Y.-Z., Hu, H.-Q., Christie, P., 2005.** *Sequestration of As by iron plaque on the roots of three rice (Oryza sativa L.) cultivars in a low-P soil with or without P fertilizer. Environmental Geochemistry and Health* **27**, 169–176. https://doi.org/10.1007/s10653-005-0132-5.

**Hu, K., Meselhe, E., Nyman, J.A., 2021.** *The effect of Phragmites australis dieback on channel sedimentation in the Mississippi River Delta: A conceptual modeling study. Water* **13**, 1407. https://doi.org/10.3390/w13101407.

**Hu, H., Bi, L., Wang, L., Zhan, F., Liang, X., Qin, L., Li, Y., 2024.** *The effects of different iron and phosphorus treatments on the formation and morphology of iron plaque in rice roots (Oryza sativa L). Frontiers in Plant Science* **14**, 1304505. https://doi.org/10.3389/fpls.2023.1304505.

**Huang, J., Li, Y., Fu, C., Chen, F., Fu, Q., Dai, A., Shinoda, M., Ma, Z., Guo, W., Li, Z., Zhang, L., Liu, Y., Yu, H., He, Y., Xie, Y., Guan, X., Ji, M., Lin, L., Wang, S., Yan, H., Wang, G., 2017.** *Dryland climate change: recent progress and challenges. Reviews of Geophysics* **55**, 719–778. https://doi.org/10.1002/2016RG000550.

**Hürlimann, H., 1951.** *Zur Lebensgeschichte des Schilfs an den Ufern der Schweizer Seen.* H. Huber.

**IPCC, 2023.** *Climate Change 2023: Synthesis Report. Contribution of Working Groups I, II and III to the Sixth Assessment Report of the Intergovernmental Panel on Climate Change.* Core Writing Team, Lee, H., Romero, J. (Eds.). IPCC, Geneva, Switzerland. https://doi.org/10.59327/IPCC/AR6-9789291691647.

**Interferences between root plaque formation and phosphorus availability for isoetids in sediments of oligotrophic lakes, n.d.** *[online]* Available at: http://ouci.dntb.gov.ua/en/works/lD8mQZzl/ (accessed 16 September 2025).

**Jensen, C.R., Luxmoore, R.J., van Gundy, S.D., 1969.** *Root tissue porosity measurements by pycnometer method. Plant and Soil* **31**, 211–215.

**Jia, X., Otte, M.L., Liu, Y., Qin, L., Tian, X., Lu, X., Jiang, M., Zou, Y., 2018.** *Performance of iron plaque of wetland plants for regulating iron, manganese, and phosphorus from agricultural drainage water. Water* **10**, 42. https://doi.org/10.3390/w10010042.

**Jones, D.L., 1998.** *Organic acids in the rhizosphere – a critical review. Plant and Soil* **205**, 25–44. https://doi.org/10.1023/A:1004356007312.

**Jones, D.L., Darah, P.R., Kochian, L.V., 1996.** *Critical evaluation of organic acid mediated iron dissolution in the rhizosphere and its potential role in root iron uptake. Plant and Soil* **180**, 57–66. https://doi.org/10.1007/BF00015411.

**Jordán, M.M., Navarro-Pedreño, J., García-Sánchez, E., Mateu, J., Juan, P., 2004.** *Spatial dynamics of soil salinity under arid and semi-arid conditions: geological and environmental implications. Environmental Geology* **45**, 448–456. https://doi.org/10.1007/s00254-003-0894-y.

**Jovanović, U.D., Marković, M.M., Cupać, S.B., Tomić, Z.P., 2013.** *Soil humic acid aggregation by dynamic light scattering and laser Doppler electrophoresis. Journal of Plant Nutrition and Soil Science* **176**, 674–679. https://doi.org/10.1002/jpln.201200346.

**Kalbitz, K., Solinger, S., Park, J.-H., Michalzik, B., Matzner, E., 2000.** *Controls on the dynamics of dissolved organic matter in soils: a review. Soil Science* **165**, 277.

**Karlsson, T., Persson, P., 2010.** *Coordination chemistry and hydrolysis of Fe(III) in a peat humic acid studied by X-ray absorption spectroscopy. Geochimica et Cosmochimica Acta* **74**, 30–40. https://doi.org/10.1016/j.gca.2009.09.023.

**Kaya, C., Akram, N.A., Ashraf, M., Sonmez, O., 2018.** *Exogenous application of humic acid mitigates salinity stress in maize (Zea mays L.) plants by improving some key physico-biochemical attributes. Cereal Research Communications* **46**, 67–78. https://doi.org/10.1556/0806.45.2017.064.

**Kerbab, S., Silini, A., Chenari Bouket, A., Cherif-Silini, H., Eshelli, M., Rabhi, N.E.H., Belbahri, L., 2021.** *Mitigation of NaCl stress in wheat by rhizosphere engineering using salt habitat adapted PGPR halotolerant bacteria. Applied Sciences* **11**, 1034. https://doi.org/10.3390/app11031034.

**Khan, N., Seshadri, B., Bolan, N., Saint, C.P., Kirkham, M.B., Chowdhury, S., Yamaguchi, N., Lee, D.Y., Li, G., Kunhikrishnan, A., Qi, F., Karunanithi, R., Qiu, R., Zhu, Y.-G., Syu, C.H., 2016.** *Root iron plaque on wetland plants as a dynamic pool of nutrients and contaminants.* In: Sparks, D.L. (Ed.), *Advances in Agronomy.* Academic Press, pp. 1–96. https://doi.org/10.1016/bs.agron.2016.04.002.

**Kiviat, E., 2013.** *Ecosystem services of Phragmites in North America with emphasis on habitat functions. AoB PLANTS* **5**, plt008. https://doi.org/10.1093/aobpla/plt008.

**Klötzli, F., 1971.** *Biogenous influence on aquatic macrophytes especially Phragmites communis. Hidrobiologia (București)* **12**, 107–111.

**Konnerup, D., Sorrell, B.K., Colmer, T.D., 2016.** *Evaluation of root porosity and radial oxygen loss of disomic addition lines of Hordeum marinum in wheat*. *Functional Plant Biology* **43**, 408–418. https://doi.org/10.1071/FP16272.

**Koppitz, H., 2004.** *Effects of flooding on the amino acid and carbohydrate patterns of Phragmites australis. Limnologica* **34**, 37–47. https://doi.org/10.1016/S0075-9511(04)80020-3.

**Kotula, L., Ranathunge, K., Schreiber, L., Steudle, E., 2009.** *Functional and chemical comparison of apoplastic barriers to radial oxygen loss in roots of rice (Oryza sativa L.) grown in aerated or deoxygenated solution. Journal of Experimental Botany* **60**, 2155–2167. https://doi.org/10.1093/jxb/erp089.

**LaFond-Hudson, S., Johnson, N.W., Pastor, J., Dewey, B., 2018.** *Iron sulfide formation on root surfaces controlled by the life cycle of wild rice (Zizania palustris). Biogeochemistry* **141**, 95–106. https://doi.org/10.1007/s10533-018-0491-5.

**Lakhdar, A., Rabhi, M., Ghnaya, T., Montemurro, F., Jedidi, N., Abdelly, C., 2009.** *Effectiveness of compost use in salt-affected soil. Journal of Hazardous Materials* **171**, 29–37. https://doi.org/10.1016/j.jhazmat.2009.05.132.

**Lamers, L.P.M., Govers, L.L., Janssen, I.C.J.M., Geurts, J.J.M., Van der Welle, M.E.W., Van Katwijk, M.M., Van der Heide, T., Roelofs, J.G.M., Smolders, A.J.P., 2013.** *Sulfide as a soil phytotoxin—a review. Frontiers in Plant Science* **4**, 268. https://doi.org/10.3389/fpls.2013.00268.

**Laufer, K., Byrne, J.M., Glombitza, C., Schmidt, C., Jørgensen, B.B., Kappler, A., 2016.** *Anaerobic microbial Fe(II) oxidation and Fe(III) reduction in coastal marine sediments controlled by organic carbon content. Environmental Microbiology* **18**, 3159–3174. https://doi.org/10.1111/1462-2920.13387.

**Lee, Y.P., Fujii, M., Terao, K., Kikuchi, T., Yoshimura, C., 2016.** *Effect of dissolved organic matter on Fe(II) oxidation in natural and engineered waters. Water Research* **103**, 160–169. https://doi.org/10.1016/j.watres.2016.07.033.

**Lefcheck, J.S., 2016.** *piecewiseSEM: Piecewise structural equation modelling in R for ecology, evolution, and systematics. Methods in Ecology and Evolution* **7**, 573–579. https://doi.org/10.1111/2041-210X.12512.

**Li, J., Wen, Y., Li, X., Li, Y., Yang, X., Lin, Z., Song, Z., Cooper, J.M., Zhao, B., 2018.** *Soil labile organic carbon fractions and soil organic carbon stocks as affected by long-term organic and mineral fertilization regimes in the North China Plain. Soil and Tillage Research* **175**, 281–290. https://doi.org/10.1016/j.still.2017.08.008.

**Li, J., Xie, S.-P., Cook, E.R., Chen, F., Shi, J., Zhang, D.D., Fang, K., Gou, X., Li, T., Peng, J., Shi, S., Zhao, Y., 2019.** *Deciphering human contributions to Yellow River flow reductions and downstream drying using centuries-long tree ring records. Geophysical Research Letters* **46**, 898–905. https://doi.org/10.1029/2018GL081090.

**Li, S., Liu, Z., Li, J., Liu, Z., Gu, X., Shi, L., 2022.** *Cow manure compost promotes maize growth and ameliorates soil quality in saline-alkali soil: Role of fertilizer addition rate and application depth. Sustainability* **14**, 10088. https://doi.org/10.3390/su141610088.

**Limmer, M.A., Evans, A.E., Seyfferth, A.L., 2021.** *A new method to capture the spatial and temporal heterogeneity of aquatic plant iron root plaque in situ. Environmental Science & Technology* **55**, 912–918. https://doi.org/10.1021/acs.est.0c02949.

**Lissner, J., Schierup, H.-H., 1997.** *Effects of salinity on the growth of Phragmites australis. Aquatic Botany* **55**, 247–260. https://doi.org/10.1016/S0304-3770(96)01085-6.

**Liu, X., Millero, F.J., 2002.** *The solubility of iron in seawater. Marine Chemistry* **77**, 43–54. https://doi.org/10.1016/S0304-4203(01)00074-3.

**Liu, W.-J., Zhu, Y.-G., Smith, F.A., 2005.** *Effects of iron and manganese plaques on arsenic uptake by rice seedlings (Oryza sativa L.) grown in solution culture supplied with*

*arsenate and arsenite. Plant and Soil* **277**, 127–138. https://doi.org/10.1007/s11104-005-6453-4.

**Liu, J., Leng, X., Wang, M., Zhu, Z., Dai, Q., 2011.** *Iron plaque formation on roots of different rice cultivars and the relation with lead uptake. Ecotoxicology and Environmental Safety* **74**, 1304–1309. https://doi.org/10.1016/j.ecoenv.2011.01.017.

**Liu, Z., Shang, H., Han, F., Zhang, M., Li, Q., Zhou, W., 2021a.** *Improvement of nitrogen and phosphorus availability by Pseudoalteromonas sp. during salt-washing in saline-alkali soil. Applied Soil Ecology* **168**, 104117. https://doi.org/10.1016/j.apsoil.2021.104117.

**Liu, Y., Luo, M., Chen, J., Ye, R., Tan, J., Zhai, Z., Yang, Y., Huang, J., 2021b.** *Root iron plaque abundance as an indicator of carbon decomposition rates in a tidal freshwater wetland in response to salinity and flooding. Soil Biology and Biochemistry* **162**, 108403. https://doi.org/10.1016/j.soilbio.2021.108403.

**Liu, N., Lou, X., Li, X., Shuai, Z., Liu, H., Jiang, Z., Wei, S., 2021c.** *Rhizosphere dissolved organic matter and iron plaque modified by organic amendments and its relations to cadmium bioavailability and accumulation in rice. Science of The Total Environment* **792**, 148216. https://doi.org/10.1016/j.scitotenv.2021.148216.

**Logozzo, L.A., Hosen, J.D., McArthur, J., Raymond, P.A., 2023.** *Distinct drivers of two size fractions of operationally dissolved iron in a temperate river. Limnology and Oceanography* **68**, 1185–1200. https://doi.org/10.1002/lno.12338.

**Lowe, L.E., 1975.** *Fractionation of acid-soluble components of soil organic matter using PVP (poly-vinyl-pyrrolidone). Canadian Journal of Soil Science* **55**, 109–126.

**Lüdecke, D., Ben-Shachar, M.S., Patil, I., Waggoner, P., Makowski, D., 2021.** *performance: An R package for assessment, comparison and testing of statistical models. Journal of Open Source Software* **6**, 3139. https://doi.org/10.21105/joss.03139.

**Mahdy, A.M., Fathi, N.O., 2012.** *Interactive effects between biofertilizer and antioxidant on salinity mitigation and nutrition and yield of okra plants (Abelmoschus esculentus L.). Journal of Soil Science and Agricultural Engineering* **3**, 189–205. https://doi.org/10.21608/jssae.2012.53845.

**Mahmood, F., Khan, I., Ashraf, U., Shahzad, T., Hussain, S., Shahid, M., Abid, M., Ullah, S., 2017.** *Effects of organic and inorganic manures on maize and their residual impact on soil physico-chemical properties. Journal of Soil Science and Plant Nutrition* **17**, 22–32. https://doi.org/10.4067/S0718-95162017005000002.

**Maisch, M., Lueder, U., Kappler, A., Schmidt, C., 2020.** *From plant to paddy—how rice root iron plaque can affect the paddy field iron cycling. Soil Systems* **4**, 28. https://doi.org/10.3390/soilsystems4020028.

**Maiwan, N., Tunçtürk, M., Tunçtürk, R., 2023.** *Effect of humic acid applications on physiological and biochemical properties of soybean (Glycine max L.) grown under salt stress conditions. YYU Journal of Agricultural Science* **33**, 1–9. https://doi.org/10.29133/yyutbd.1057288.

**Malik, A.I., Colmer, T.D., Lambers, H., & Schortemeyer, M., 2003.** *Aerenchyma formation and radial $O_2$ loss along adventitious roots of wheat with only the apical root portion exposed to $O_2$ deficiency*. *Plant, Cell & Environment* **26**, 1713–1722. https://doi.org/10.1046/j.1365-3040.2003.01089.x.

**Malik, Z., Malik, N., Noor, I., Kamran, M., Parveen, A., Ali, M., Sabir, F., Elansary, H.O., El-Abedin, T.K.Z., Mahmoud, E.A., Fahad, S., 2023.** *Combined effect of rice-straw biochar and humic acid on growth, antioxidative capacity, and ion uptake in maize (Zea mays L.) grown under saline soil conditions. Journal of Plant Growth Regulation* **42**, 3211–3228. https://doi.org/10.1007/s00344-022-10786-z.

**Mazhar, S., Pellegrini, E., Contin, M., Bravo, C., De Nobili, M., 2022.** *Impacts of salinization caused by sea level rise on the biological processes of coastal soils—A review. Frontiers in Environmental Science* **10**, 909415. https://doi.org/10.3389/fenvs.2022.909415.

**Meharg, A.A., Zhao, F.-J., 2012.** *Arsenic & Rice.* Springer Netherlands, Dordrecht. https://doi.org/10.1007/978-94-007-2947-6.

**Meharg, A.A., Williams, P.N., Adomako, E., Lawgali, Y.Y., Deacon, C., Villada, A., Cambell, R.C.J., Sun, G., Zhu, Y.-G., Feldmann, J., Raab, A., Zhao, F.-J., Islam, R., Hossain, S., Yanai, J., 2009.** *Geographical variation in total and inorganic arsenic content of polished (white) rice. Environmental Science & Technology* **43**, 1612–1617. https://doi.org/10.1021/es802612a.

**Mendelssohn, I.A., Kleiss, B.A., Wakeley, J.S., 1995.** *Factors controlling the formation of oxidized root channels: A review. Wetlands* **15**, 37–46. https://doi.org/10.1007/BF03160678.

**Meng, H., Yan, Z., Li, X., 2022.** *Effects of exogenous organic acids and flooding on root exudates, rhizosphere bacterial community structure, and iron plaque formation in Kandelia obovata seedlings. Science of The Total Environment* **830**, 154695. https://doi.org/10.1016/j.scitotenv.2022.154695.

**Meyerson, L.A., Saltonstall, K., Windham, L., Kiviat, E., Findlay, S., 2000.** *A comparison of Phragmites australis in freshwater and brackish marsh environments in North America. Wetlands Ecology and Management* **8**, 89–103. https://doi.org/10.1023/A:1008432200133.

**Miao, F., Zhang, X., Fu, Q., Hu, H., Islam, Md.S., Fang, L., Zhu, J., 2024.** *Sulfur enhances iron plaque formation and stress resistance to reduce the transfer of Cd and As in the soil-rice system. Science of The Total Environment* **927**, 171689. https://doi.org/10.1016/j.scitotenv.2024.171689.

**Millero, F.J., Sotolongo, S., Izaguirre, M., 1987.** *The oxidation kinetics of Fe(II) in seawater. Geochimica et Cosmochimica Acta* **51**, 793–801. https://doi.org/10.1016/0016-7037(87)90093-7.

**Mimmo, T., Del Buono, D., Terzano, R., Tomasi, N., Vigani, G., Crecchio, C., Pinton, R., Zocchi, G., Cesco, S., 2014.** *Rhizospheric organic compounds in the soil–microorganism–plant system: their role in iron availability. European Journal of Soil Science* **65**, 629–642. https://doi.org/10.1111/ejss.12158.

**Mimura, N., 2013.** *Sea-level rise caused by climate change and its implications for society. Proceedings of the Japan Academy, Series B* **89**, 281–301. https://doi.org/10.2183/pjab.89.281.

**Mitsch, W.J., Gosselink, J.G., 2015.** *Wetlands.* 5th Edition, John Wiley & Sons, Inc., Hoboken.

**Morgan, B., Lahav, O., 2007.** *The effect of pH on the kinetics of spontaneous Fe (II) oxidation by O2 in aqueous solution – basic principles and a simple heuristic description. Chemosphere* **68**, 2080–2084. https://doi.org/10.1016/j.chemosphere.2007.02.015.

**Morrissey, E.M., Gillespie, J.L., Morina, J.C., Franklin, R.B., 2014.** *Salinity affects microbial activity and soil organic matter content in tidal wetlands. Global Change Biology* **20**, 1351–1362. https://doi.org/10.1111/gcb.12431.

**Mucha, A.P., Almeida, C.M.R., Bordalo, A.A., Vasconcelos, M.T.S.D., 2010.** *LMWOA (low molecular weight organic acid) exudation by salt marsh plants: natural variation and response to Cu contamination. Estuarine, Coastal and Shelf Science* **88**, 63–70. https://doi.org/10.1016/j.ecss.2010.03.008.

**Munns, R., Tester, M., 2008.** *Mechanisms of salinity tolerance. Annual Review of Plant Biology* **59**, 651–681. https://doi.org/10.1146/annurev.arplant.59.032607.092911.

**Naorem, A., Jayaraman, S., Dang, Y.P., Dalal, R.C., Sinha, N.K., Rao, C.S., Patra, A.K., 2023.** *Soil constraints in an arid environment—challenges, prospects, and implications. Agronomy* **13**, 220. https://doi.org/10.3390/agronomy13010220.

**Nardi, S., Pizzeghello, D., Muscolo, A., Vianello, A., 2002.** *Physiological effects of humic substances on higher plants. Soil Biology and Biochemistry* **34**, 1527–1536. https://doi.org/10.1016/S0038-0717(02)00174-8.

**Neubauer, S.C., Toledo-Durán, G.E., Emerson, D., Megonigal, J.P., 2007.** *Returning to their roots: iron-oxidizing bacteria enhance short-term plaque formation in the wetland-plant rhizosphere. Geomicrobiology Journal* **24**, 65–73. https://doi.org/10.1080/01490450601134309.

**Nicholls, R.J., Cazenave, A., 2010.** *Sea-level rise and its impact on coastal zones. Science* **328**, 1517–1520. https://doi.org/10.1126/science.1185782.

**Oades, J.M., 1989.** *An introduction to organic matter in mineral soils.* In: Dixon, J.B., Weed, S.B. (Eds.), *Minerals in Soil Environments*, 2nd ed. Soil Science Society of America, Madison, WI, USA, pp. 89–160. https://doi.org/10.2136/sssabookser1.2ed.c3.

**Oki, T., Kanae, S., 2006.** *Global hydrological cycles and world water resources. Science* **313**, 1068–1072. https://doi.org/10.1126/science.1128845.

**Olivares, F.L., Aguiar, N.O., Rosa, R.C.C., Canellas, L.P., 2015.** *Substrate biofortification in combination with foliar sprays of plant growth promoting bacteria and humic substances boosts production of organic tomatoes. Scientia Horticulturae* **183**, 100–108. https://doi.org/10.1016/j.scienta.2014.11.012.

**Olk, D.C., Bloom, P.R., Perdue, E.M., McKnight, D.M., Chen, Y., Farenhorst, A., Senesi, N., Chin, Y.-P., Schmitt-Kopplin, P., Hertkorn, N., Harir, M., 2019.** *Environmental and agricultural relevance of humic fractions extracted by alkali from soils and natural waters. Journal of Environmental Quality* **48**, 217–232. https://doi.org/10.2134/jeq2019.02.0041.

**Oppenheimer, M., Glavovic, B.C., Hinkel, J., van de Wal, R., Magnan, A.K., Abd-Elgawad, A., Cai, R., Cifuentes-Jara, M., DeConto, R.M., Ghosh, T., Hay, J., Isla, F., Marzeion, B., Meyssignac, B., Sebesvari, Z., 2019.** *Sea level rise and implications for low-lying islands, coasts and communities.* In: Pörtner, H.-O., Roberts, D.C., Masson-Delmotte, V., Zhai, P., Tignor, M., Poloczanska, E., Mintenbeck, K., Alegría, A., Nicolai, M., Okem, A., Petzold, J., Rama, B., Weyer, N.M. (Eds.), *IPCC Special Report on the Ocean and Cryosphere in a Changing Climate.* Cambridge University Press, Cambridge, UK and New York, NY, USA, pp. 321–445. https://doi.org/10.1017/9781009157964.006.

**Ostendorp, W., 1989.** *'Die-back' of reeds in Europe — a critical review of literature. Aquatic Botany* **35**, 5–26. https://doi.org/10.1016/0304-3770(89)90063-6.

**Ouni, Y., Ghnaya, T., Montemurro, F., Abdelly, C., Lakhdar, A., 2014.** *The role of humic substances in mitigating the harmful effects of soil salinity and improve plant productivity. International Journal of Plant Production* **8**, 353–374. https://doi.org/10.22069/ijpp.2014.1614.

**Palutikof, J.P., Wu, S., IPCC (Eds.), 2008.** *Climate change and water.* IPCC Technical Paper VI. IPCC Secretariat, Geneva, Switzerland.

**Pardo, T., Martínez-Fernández, D., de la Fuente, C., Clemente, R., Komárek, M., Bernal, M.P., 2016.** *Maghemite nanoparticles and ferrous sulfate for the stimulation of iron plaque formation and arsenic immobilization in Phragmites australis. Environmental Pollution* **219**, 296–304. https://doi.org/10.1016/j.envpol.2016.10.014.

**Patrick, W.H. Jr., Delaune, R.D., 1977.** *Chemical and biological redox systems affecting nutrient availability in coastal wetlands. Geoscience and Man* **18**, 131–137.

**Pedersen, O., Sauter, M., Colmer, T.D., Nakazono, M., 2021.** *Regulation of root adaptive anatomical and morphological traits during low soil oxygen. New Phytologist* **229**, 42–49. https://doi.org/10.1111/nph.16375.

**Pellegrini, E., Contin, M., Vittori Antisari, L., Vianello, G., Ferronato, C., De Nobili, M., 2018.** *A new paper sensor method for field analysis of acid volatile sulfides in soils. Environmental Toxicology and Chemistry* **37**, 3025–3031. https://doi.org/10.1002/etc.4279.

**Pendergrass, A.G., Knutti, R., Lehner, F., Deser, C., Sanderson, B.M., 2017.** *Precipitation variability increases in a warmer climate. Scientific Reports* **7**, 17966. https://doi.org/10.1038/s41598-017-17966-y.

**Peralta Ogorek, L. L.; Pellegrini, E.; Pedersen, O., 2021.** *Novel functions of the root barrier to radial oxygen loss - radial diffusion resistance to $H_2$ and water vapour. New Phytologist*, **231** (4), 1365-1376.

**Peralta Ogorek, L.L., Takahashi, H., Nakazono, M., Pedersen, O., 2023.** *The barrier to radial oxygen loss protects roots against hydrogen sulphide intrusion and its toxic effect. New Phytologist* **238**, 1825–1837. https://doi.org/10.1111/nph.18883.

**Pertusatti, J., Prado, A.G.S., 2007.** *Buffer capacity of humic acid: thermodynamic approach. Journal of Colloid and Interface Science* **314**, 484–489. https://doi.org/10.1016/j.jcis.2007.06.006.

**Pettersson, C., Arsenie, I., Ephraim, J., Boren, H., Allard, B., 1989.** *Properties of fulvic acids from deep groundwaters. Science of The Total Environment* **81–82**, 287–296. https://doi.org/10.1016/0048-9697(89)90135-6.

**Pezeshki, S.R., 2001.** *Wetland plant responses to soil flooding. Environmental and Experimental Botany* **46**, 299–312. https://doi.org/10.1016/S0098-8472(01)00107-1.

**Pezeshki, S.R., DeLaune, R.D., 2012.** *Soil oxidation-reduction in wetlands and its impact on plant functioning. Biology* **1**, 196–221. https://doi.org/10.3390/biology1020196.

**Pham, A.N., Rose, A.L., Feitz, A.J., Waite, T.D., 2006.** *Kinetics of Fe(III) precipitation in aqueous solutions at pH 6.0–9.5 and 25 °C. Geochimica et Cosmochimica Acta* **70**, 640–650. https://doi.org/10.1016/j.gca.2005.10.018.

**Piccolo, A., 2001.** *The supramolecular structure of humic substances. Soil Science* **166**, 810. https://doi.org/10.1097/00010694-200111000-00007.

**Poldini, L., Vidali, M., Fabiani, M.L., 1999.** *La vegetazione del litorale sedimentario del Friuli-Venezia Giulia (NE Italia) con riferimenti alla regione alto-adriatica. Studia Geobotanica* **17**, 3–68.

**Povidisa, K., Delefosse, M., Holmer, M., 2009.** *The formation of iron plaques on roots and rhizomes of the seagrass Cymodocea serrulata (R. Brown) Ascherson with implications for sulphide intrusion. Aquatic Botany* **90**, 303–308. https://doi.org/10.1016/j.aquabot.2008.11.008.

**Qadir, M., Ghafoor, A., Murtaza, G., 2000.** *Amelioration strategies for saline soils: a review. Land Degradation & Development* **11**, 501–521. https://doi.org/10.1002/1099-145X(200011/12)11:6<501::AID-LDR405>3.0.CO;2-S.

**Qadir, M., Quillérou, E., Nangia, V., Murtaza, G., Singh, M., Thomas, R.J., Drechsel, P., Noble, A.D., 2014.** *Economics of salt-induced land degradation and restoration. Natural Resources Forum* **38**, 282–295. https://doi.org/10.1111/1477-8947.12054.

**R Core Team, 2025.** *R: A Language and Environment for Statistical Computing.* R Foundation for Statistical Computing, Vienna, Austria. Available at: https://www.R-project.org/

**Rai, A.K., Basak, N., Sundha, P., 2021.** *Chemistry of salt-affected soils.* In: Minhas, P.S., Yadav, R.K. (Eds.), *Managing Salt-Affected Soils for Sustainable Agriculture.* ICAR, New Delhi, India, pp. 128–148.

**Rath, K.M., Fierer, N., Murphy, D.V., Rousk, J., 2019.** *Linking bacterial community composition to soil salinity along environmental gradients. ISME Journal* **13**, 836–846. https://doi.org/10.1038/s41396-018-0313-8.

**Reddy, K.R., DeLaune, R.D., Inglett, P.W., 2022.** *Biogeochemistry of Wetlands: Science and Applications,* 2nd ed. CRC Press, Boca Raton. https://doi.org/10.1201/9780429155833.

**Rengasamy, P., 2006.** *World salinization with emphasis on Australia. Journal of Experimental Botany* **57**, 1017–1023. https://doi.org/10.1093/jxb/erj108.

**Rengasamy, P., 2018.** *Irrigation water quality and soil structural stability: A perspective with some new insights. Agronomy* **8**, 72. https://doi.org/10.3390/agronomy8050072.

**Rengasamy, P., Olsson, K.A., 1991.** *Sodicity and soil structure. Australian Journal of Soil Research* **29**(6), 935–952. https://doi.org/10.1071/SR9910935.

**Richards, L.A. (Ed.), 1954.** *Diagnosis and Improvement of Saline and Alkali Soils.* USDA Handbook No. 60. U.S. Government Printing Office, Washington, DC.

**Rickard, D., Morse, J.W., 2005.** *Acid volatile sulfide (AVS). Marine Chemistry* **97**, 141–197. https://doi.org/10.1016/j.marchem.2005.08.004.

**Rickard, D., Luther, G.W., 2007.** *Chemistry of iron sulfides. Chemical Reviews* **107**, 514–562. https://doi.org/10.1021/cr0503658.

**Ritchie, J.D., Perdue, E.M., 2003.** *Proton-binding study of standard and reference fulvic acids, humic acids, and natural organic matter. Geochimica et Cosmochimica Acta* **67**, 85–96. https://doi.org/10.1016/S0016-7037(02)01044-X.

**Rocha, A.C.S., Almeida, C.M.R., Basto, M.C.P., Vasconcelos, M.T.S.D., 2015.** *Influence of season and salinity on the exudation of aliphatic low molecular weight organic acids (ALMWOAs) by Phragmites australis and Halimione portulacoides roots. Journal of Sea Research* **95**, 180–187. https://doi.org/10.1016/j.seares.2014.07.001.

**Roden, E.E., Wetzel, R.G., 2002.** *Kinetics of microbial Fe(III) oxide reduction in freshwater wetland sediments. Limnology and Oceanography* **47**, 198–211. https://doi.org/10.4319/lo.2002.47.1.0198.

**Rohrbacher, F., St-Arnaud, M., 2016.** *Root exudation: the ecological driver of hydrocarbon rhizoremediation. Agronomy* **6**, 19. https://doi.org/10.3390/agronomy6010019.

**Rose, A.L., Waite, T.D., 2003.** *Effect of dissolved natural organic matter on the kinetics of ferrous iron oxygenation in seawater. Environmental Science & Technology* **37**, 4877–4886. https://doi.org/10.1021/es034152g.

**Sahab, S., Suhani, I., Srivastava, V., Chauhan, P.S., Singh, R.P., Prasad, V., 2021.** *Potential risk assessment of soil salinity to agroecosystem sustainability: current status and management strategies. Science of The Total Environment* **764**, 144164. https://doi.org/10.1016/j.scitotenv.2020.144164.

**Saidimoradi, D., Ghaderi, N., Javadi, T., 2019.** *Salinity stress mitigation by humic acid application in strawberry (Fragaria × ananassa Duch.). Scientia Horticulturae* **256**, 108594. https://doi.org/10.1016/j.scienta.2019.108594.

**Santana-Casiano, J.M., González-Dávila, M., Millero, F.J., 2005.** *Oxidation of nanomolar levels of Fe (II) with oxygen in natural waters. Environmental Science & Technology* **39**, 2073–2079. https://doi.org/10.1021/es049748y.

**Schindelin, J., Arganda-Carreras, I., Frise, E., Kaynig, V., Longair, M., Pietzsch, T., Preibisch, S., Rueden, C., Saalfeld, S., Schmid, B., Tinevez, J.-Y., White, D.J., Hartenstein, V., Eliceiri, K., Tomancak, P., Cardona, A., 2012.** *Fiji: an open-source platform for biological-image analysis. Nature Methods* **9**, 676–682. https://doi.org/10.1038/nmeth.2019.

**Schneider, T., Keiblinger, K.M., Schmid, E., Sterflinger-Gleixner, K., Ellersdorfer, G., Roschitzki, B., Richter, A., Eberl, L., Zechmeister-Boltenstern, S., Riedel, K., 2012.** *Who is who in litter decomposition? Metaproteomics reveals major microbial players and their biogeochemical functions. ISME Journal* **6**, 1749–1762. https://doi.org/10.1038/ismej.2012.11.

**Schröder, R., 1979.** *The decline of reed swamps in Lake Constance.* In: *Symposia Biologica Hungarica*, pp. 43–48.

**Sebastian, A., Prasad, M.N.V., 2016.** *Iron plaque decreases cadmium accumulation in Oryza sativa L. and serves as a source of iron. Plant Biology (Stuttgart)* **18**, 1008–1015. https://doi.org/10.1111/plb.12484.

**Seneviratne, S.I., Zhang, X., Adnan, M., Badi, W., Dereczynski, C., Luca, A.D., Ghosh, S., Iskandar, I., Kossin, J., Lewis, S., Otto, F., Pinto, I., Satoh, M., Vicente-Serrano, S.M., Wehner, M., Zhou, B., Allan, R., 2021.** *Weather and climate extreme events in a changing climate.* In: Masson-Delmotte, V.P., Zhai, A., Pirani, S.L., Connors, C. (Eds.), *Climate Change 2021: The Physical Science Basis*, IPCC Sixth Assessment Report. Cambridge University Press, Cambridge, UK, pp. 1513–1766. https://doi.org/10.1017/9781009157896.013.

**Seyfferth, A.L., Webb, S.M., Andrews, J.C., Fendorf, S., 2010.** *Arsenic localization, speciation, and co-occurrence with iron on rice (Oryza sativa L.) roots having variable Fe coatings. Environmental Science & Technology* **44**, 8108–8113. https://doi.org/10.1021/es101139z.

**Shaaban, M.M., El-Fouly, M.M., 2002.** *Nutrient contents and salt removal potential of some wild plants grown in salt-affected soils. Acta Horticulturae* **573**, 377–385. https://doi.org/10.17660/ActaHortic.2002.573.45.

**Shahid, S.A., Zaman, M., Heng, L., 2018a.** *Soil salinity: historical perspectives and a world overview of the problem.* In: Zaman, M., Shahid, S.A., Heng, L. (Eds.), *Guideline*

*for Salinity Assessment, Mitigation and Adaptation Using Nuclear and Related Techniques.* Springer, Cham, pp. 43–53. https://doi.org/10.1007/978-3-319-96190-3_2.

**Shahid, S.A., Zaman, M., Heng, L., 2018b.** *Salinity and sodicity adaptation and mitigation options.* In: Zaman, M., Shahid, S.A., Heng, L. (Eds.), *Guideline for Salinity Assessment, Mitigation and Adaptation Using Nuclear and Related Techniques.* Springer, Cham, Switzerland, pp. 55–89.

**Shipley, B., 2009.** *Confirmatory path analysis in a generalized multilevel context. Ecology*, **90**(2), 363-368. https://doi.org/10.1890/08-1034.1.

**Shrivastava, P., Kumar, R., 2015.** *Soil salinity: a serious environmental issue and plant growth promoting bacteria as one of the tools for its alleviation. Saudi Journal of Biological Sciences* **22**, 123–131. https://doi.org/10.1016/j.sjbs.2014.12.001.

**Shukry, W.M., Abu-Ria, M.E., Abo-Hamed, S.A., Anis, G.B., Ibraheem, F., 2023.** *The efficiency of humic acid for improving salinity tolerance in salt-sensitive rice (Oryza sativa): growth responses and physiological mechanisms. Gesunde Pflanzen* **75**, 2639–2653. https://doi.org/10.1007/s10343-023-00885-6.

**Six, J., Elliott, E.T., Paustian, K., 2000.** *Soil macroaggregate turnover and microaggregate formation: a mechanism for C sequestration under no-tillage agriculture. Soil Biology and Biochemistry* **32**, 2099–2103. https://doi.org/10.1016/S0038-0717(00)00179-6.

**Six, J., Conant, R.T., Paul, E.A., Paustian, K., 2002.** *Stabilization mechanisms of soil organic matter: implications for C-saturation of soils. Plant and Soil* **241**, 155–176. https://doi.org/10.1023/A:1016125726789.

**Smajgl, A., Toan, T.Q., Nhan, D.K., Ward, J., Trương, N.H., Tri, V.P.D., Vu, P.T., 2015.** *Responding to rising sea levels in the Mekong Delta. Nature Climate Change* **5**, 167–174. https://doi.org/10.1038/nclimate2469.

**St-Cyr, L., Crowder, A.A., 1988.** *Iron oxide deposits on the roots of Phragmites australis related to the iron bound to carbonates in the soil. Journal of Plant Nutrition* **11**, 1253–1261. https://doi.org/10.1080/01904168809363883.

**St-Cyr, L., Crowder, A.A., 1989.** *Factors affecting iron plaque on the roots of Phragmites australis (Cav.) Trin. ex Steudel. Plant and Soil* **116**, 85–93. https://doi.org/10.1007/BF02327260.

**Stevenson, F.J., 1982.** *Humus Chemistry: Genesis, Composition, Reactions,* 2nd ed. John Wiley & Sons, New York, NY, USA.

**Stevenson, F.J., 1994.** *Humus Chemistry: Genesis, Composition, Reactions.* John Wiley & Sons.

**Sukopp, H., Markstein, B., 1989.** *Changes of the reed beds along the Berlin Havel, 1962–1987. Aquatic Botany* **35**, 27–39. https://doi.org/10.1016/0304-3770(89)90064-8.

**Tan, K.H., 2014.** *Humic Matter in Soil and the Environment: Principles and Controversies,* 2nd ed. CRC Press, Boca Raton, FL. https://doi.org/10.1201/b17037.

**Taylor, G.J., Crowder, A.A., 1983.** *Use of the DCB technique for extraction of hydrous iron oxides from roots of wetland plants. American Journal of Botany* **70**, 1254–1257. https://doi.org/10.1002/j.1537-2197.1983.tb12474.x.

**Taylor, G.J., Crowder, A.A., Rodden, R., 1984.** *Formation and morphology of an iron plaque on the roots of Typha latifolia L. grown in solution culture. American Journal of Botany* **71**, 666–675. https://doi.org/10.1002/j.1537-2197.1984.tb14173.x.

**Tejada, M., Garcia, C., Gonzalez, J.L., Hernandez, M.T., 2006.** *Use of organic amendment as a strategy for saline soil remediation: influence on the physical, chemical and biological properties of soil. Soil Biology and Biochemistry* **38**, 1413–1421. https://doi.org/10.1016/j.soilbio.2005.10.017.

**Teodorescu, M., Lungu, A., Stanescu, P.O., Neamţu, C., 2009.** *Preparation and properties of novel slow-release NPK agrochemical formulations based on poly(acrylic acid) hydrogels and liquid fertilizers. Industrial & Engineering Chemistry Research* **48**, 6527–6534. https://doi.org/10.1021/ie900254b.

**Tipping, E., 1986.** *Humic substances in soil, sediment and water: geochemistry, isolation and characterization,* edited by G.R. Aiken, D.M. McKnight, R.L. Wershaw and P. MacCarthy. Wiley, Chichester, 692 pp. *Geological Journal* **21**, 213–214. https://doi.org/10.1002/gj.3350210213.

**Trenberth, K.E., Dai, A., van der Schrier, G., Jones, P.D., Barichivich, J., Briffa, K.R., Sheffield, J., 2014.** *Global warming and changes in drought. Nature Climate Change* **4**, 17–22. https://doi.org/10.1038/nclimate2067.

**Tülp, H.C., Fenner, K., Schwarzenbach, R.P., Goss, K.-U., 2009.** *Sorption of polar organic compounds to mineral surfaces. Environmental Science & Technology* **43**, 9189–9195. https://doi.org/10.1021/es902272j.

**Valkama, E., Lyytinen, S., Koricheva, J., 2008.** *The impact of reed management on wildlife: A meta-analytical review of European studies. Biological Conservation* **141**, 364–374. https://doi.org/10.1016/j.biocon.2007.11.006.

**Van Der Ent, R.J., Savenije, H.H.G., Schaefli, B., Steele-Dunne, S.C., 2010.** *Origin and fate of atmospheric moisture over continents. Water Resources Research* **46**, W09525. https://doi.org/10.1029/2010WR009127.

**van der Putten, W.H., 1997.** *Die-back of Phragmites australis in European wetlands: an overview of the European Research Programme on Reed Die-back and Progression (1993–1994). Aquatic Botany* **59**, 263–275. https://doi.org/10.1016/S0304-3770(97)00060-0.

**Van Der Welle, M.E.W., Smolders, A.J.P., Op Den Camp, H.J.M., Roelofs, J.G.M., Lamers, L.P.M., 2007.** *Biogeochemical interactions between iron and sulphate in freshwater wetlands and their implications for interspecific competition between aquatic macrophytes. Freshwater Biology* **52**, 434–447. https://doi.org/10.1111/j.1365-2427.2006.01683.x.

**Vasquez, E.A., Glenn, E.P., Brown, J.J., Guntenspergen, G.R., Nelson, S.G., 2005.** *Salt tolerance underlies the cryptic invasion of North American salt marshes by an introduced haplotype of the common reed Phragmites australis (Poaceae). Marine Ecology Progress Series* **298**, 1–8. https://doi.org/10.3354/meps298001.

**Villalobos, F.J., Fereres, E. (Eds.), 2024.** *Principles of Agronomy for Sustainable Agriculture,* 2nd ed. Springer, Cham, Switzerland. ISBN 978-3-031-69149-2.

**Vitti, A., Coviello, L., Nuzzaci, M., Vinci, G., Deligiannakis, Y., Giannakopoulos, E., Ronga, D., Piccolo, A., Scopa, A., Drosos, M., 2024.** *Biostimulation of humic acids on Lepidium sativum L. regulated by their content of stable phenolic O· radicals. Chemical and Biological Technologies in Agriculture* **11**, 92. https://doi.org/10.1186/s40538-024-00613-w.

**Von Lützow, M., Kögel-Knabner, I., Ekschmitt, K., Flessa, H., Guggenberger, G., Matzner, E., Marschner, B., 2007.** *SOM fractionation methods: relevance to functional pools and to stabilization mechanisms. Soil Biology and Biochemistry* **39**, 2183–2207. https://doi.org/10.1016/j.soilbio.2007.03.007.

**Wang, L., Sun, X., Li, S., Zhang, T., Zhang, W., Zhai, P., 2014.** *Application of organic amendments to a coastal saline soil in North China: Effects on soil physical and chemical properties and tree growth. PLoS ONE* **9**, e89185. https://doi.org/10.1371/journal.pone.0089185.

**Warren, R.S., Fell, P.E., Grimsby, J.L., Buck, E.L., Rilling, G.C., Fertik, R.A., 2001.** *Rates, patterns, and impacts of Phragmites australis expansion and effects of experimental Phragmites control on vegetation, macroinvertebrates, and fish within tidelands of the lower Connecticut River. Estuaries* **24**, 90–107. https://doi.org/10.2307/1352816.

**Weaver, A.R., Kissel, D.E., Chen, F., West, L.T., Adkins, W., Rickman, D., Luvall, J.C., 2004.** *Mapping soil pH buffering capacity of selected fields in the coastal plain. Soil Science Society of America Journal* **68**, 662–668. https://doi.org/10.2136/sssaj2004.6620.

**Weiss, J.V., Emerson, D., Megonigal, J.P., 2004.** *Geochemical control of microbial Fe(III) reduction potential in wetlands: comparison of the rhizosphere to non-rhizosphere soil. FEMS Microbiology Ecology* **48**, 89–100. https://doi.org/10.1016/j.femsec.2003.12.014.

**Wetzel, P.R., van der Valk, A.G., 1998.** *Effects of nutrient and soil moisture on competition between Carex stricta, Phalaris arundinacea, and Typha latifolia. Plant Ecology* **138**, 179–190. https://doi.org/10.1023/A:1009751703827.

**White, E., Kaplan, D., 2017.** *Restore or retreat? Saltwater intrusion and water management in coastal wetlands. Ecosystem Health and Sustainability* **3**, e01258. https://doi.org/10.1002/ehs2.1258.

**Wilske, B., Bai, M., Lindenstruth, B., Bach, M., Rezaie, Z., Frede, H.G., Breuer, L., 2014.** *Biodegradability of a polyacrylate superabsorbent in agricultural soil. Environmental Science and Pollution Research* **21**, 9453–9460. https://doi.org/10.1007/s11356-013-2103-1.

**Wilson, M.A., 1981.** *Application of nuclear magnetic resonance spectroscopy to the study of the structure of soil organic matter. Journal of Soil Science* **32**, 167–186. https://doi.org/10.1111/j.1365-2389.1981.tb01698.x.

**Wong, V.N.L., Dalal, R.C., Greene, R.S.B., 2009.** *Carbon dynamics of sodic and saline soils following gypsum and organic material additions: a laboratory incubation. Applied Soil Ecology* **41**, 29–40. https://doi.org/10.1016/j.apsoil.2008.08.006.

**Wong, V.N.L., Greene, R.S.B., Dalal, R.C., Murphy, B.W., 2010.** *Soil carbon dynamics in saline and sodic soils: a review. Soil Use and Management* **26**, 2–11. https://doi.org/10.1111/j.1475-2743.2009.00251.x.

**Woodruff, J.D., Irish, J.L., Camargo, S.J., 2013.** *Coastal flooding by tropical cyclones and sea-level rise. Nature* **504**, 44–52. https://doi.org/10.1038/nature12855.

**Wright, R.J., Hossner, L.R., 1984.** *Cultivar differences in iron coatings formed on rice roots. Cereal Research Communications* **12**(3–4), 265–266.

**Wu, Z., Meng, R., Feng, W., Li, Z., Lu, X., Chen, Y., Deng, X., Chen, T., Xue, Z., Wang, X., 2024.** *Soil-improving effect of Sesbania–Sorghum rotation in a heavily saline–alkaline coastal region. Agronomy* **14**, 2139. https://doi.org/10.3390/agronomy14092139.

**Xie, J., Fan, Q., Liang, T., Liang, H., Wang, H., Gui, Z., Wu, J., Gao, S., Cao, W. 2024.** *Green manuring reduces cadmium accumulation in rice: Roles of iron plaque and dissolved organic matter. Environ Res.* **251**(Pt 2):118719. https://doi.org/10.1016/j.envres.2024.118719.

**Xiong, L., Zhu, J.-K., 2002.** *Molecular and genetic aspects of plant responses to osmotic stress. Plant, Cell & Environment* **25**, 131–139. https://doi.org/10.1046/j.1365-3040.2002.00782.x

**Yang, F., Tang, C., Antonietti, M., 2021.** *Natural and artificial humic substances to manage minerals, ions, water, and soil microorganisms. Chemical Society Reviews* **50**, 6221–6239. https://doi.org/10.1039/D0CS01363C.

**Yang, J., Liu, X., Fei, C., Lu, H., Ma, Y., Ma, Z., Ye, W., 2023.** *Chemical-microbial effects of acetic acid, oxalic acid and citric acid on arsenic transformation and migration in the rhizosphere of paddy soil. Ecotoxicology and Environmental Safety* **259**, 115046. https://doi.org/10.1016/j.ecoenv.2023.115046.

**Yu, H. Y., Xu, Y., Wang, Q., Hu, M., Zhang, X., Liu, T. 2024.** *Controlling factors of iron plaque formation and its adsorption of cadmium and arsenic throughout the entire life cycle of rice plants. Science of the Total Environment*, **953**, 176106. https://doi.org/10.1016/j.scitotenv.2024.176106.

**Yuan, Y., Ding, C., Wu, H., Tian, X., Luo, M., Chang, W., Qin, L., Yang, L., Zou, Y., Dong, K., Zhu, X., Jiang, M., Otte, M.L., 2022.** *Dissimilatory iron reduction contributes to anaerobic mineralization of sediment in a shallow transboundary lake. Fundamental Research* **3**, 844–851. https://doi.org/10.1016/j.fmre.2022.12.002.

**Zhang, X., Zhang, F., Mao, D., 1999.** *Effect of iron plaque outside roots on nutrient uptake by rice (Oryza sativa L.): phosphorus uptake. Plant and Soil* **209**, 187–192. https://doi.org/10.1023/A:1004505431879.

**Zhang, Q., Chen, H., Xu, C., Zhu, H., Zhu, Q., 2019.** *Heavy metal uptake in rice is regulated by pH-dependent iron plaque formation and the expression of the metal transporter genes. Environmental and Experimental Botany* **162**, 392–398. https://doi.org/10.1016/j.envexpbot.2019.03.004.

**Zhang, Q., Yan, Z., Li, X., 2020.** *Ferrous iron facilitates the formation of iron plaque and enhances the tolerance of Spartina alterniflora to artificial sewage stress. Marine Pollution Bulletin* **157**, 111379. https://doi.org/10.1016/j.marpolbul.2020.111379.

**Zhang, Q., Yan, Z., Li, X., 2021.** *Iron plaque formation and rhizosphere iron bacteria in Spartina alterniflora and Phragmites australis on the redoxcline of tidal flat in the Yangtze River Estuary. Geoderma* **392**, 115000. https://doi.org/10.1016/j.geoderma.2021.115000.

**Zhang, Z., Jiang, W., Peng, K., Wu, Z., Ling, Z., Li, Z., 2023.** *Assessment of the impact of wetland changes on carbon storage in coastal urban agglomerations from 1990 to 2035 in support of SDG15.1. Science of The Total Environment* **877**, 162824. https://doi.org/10.1016/j.scitotenv.2023.162824.

**Zhong, S., Wu, Y., Xu, J., 2009.** *Phosphorus utilization and microbial community in response to lead/iron addition to a waterlogged soil. Journal of Environmental Sciences* **21**, 1415–1423. https://doi.org/10.1016/S1001-0742(08)62434-1.

**Zörb, C., Geilfus, C.-M., Dietz, K.-J., 2019.** *Salinity and crop yield. Plant Biology* **21**, 31–38. https://doi.org/10.1111/plb.12884.

# *Appendix*

## Chapter 1

**Figure S1**. Sampling sites along the Cormor – Stella rivers delta system inside the Grado and Marano Lagoon (north-eastern Adriatic Sea) and GPS coordinates.


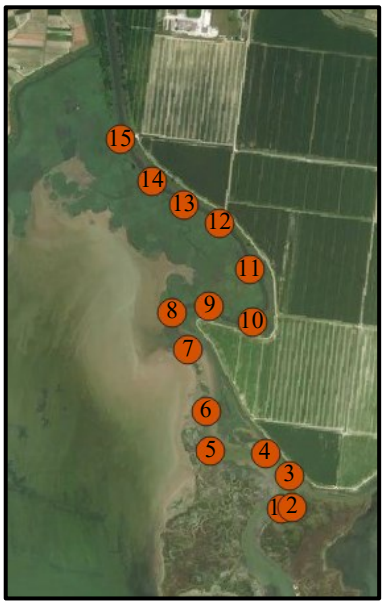


**Stella river**

| Sampling site | Geographical coordinates (EPSG: 32633) |
|---|---|
| 1 | 354037.7N, 5065962.7E |
| 2 | 354066.6N, 5066193.7E |
| 3 | 353999.2N, 5066328.4E |
| 4 | 353960.7N, 5066487.2E |
| 5 | 353802.0N, 5066564.1E |
| 6 | 353667.3N, 5066371.7E |
| 7 | 353465.2N, 5066405.4E |
| 8 | 353340.1N, 5066294.7E |
| 9 | 353215.0N, 5066241.8E |
| 10 | 353065.9N, 5066328.4E |
| 11 | 353191.0N, 5066496.8E |
| 12 | 353176.5N, 5066751.8E |
| 13 | 353041.8N, 5066665.2E |
| 14 | 352705.0N, 5066544.9E |
| 15 | 352276.8N, 5066405.4E |

**Cormor river**

| Sampling site | Geographical coordinates (EPSG: 32633) |
|---|---|
| 1 | 355466.6N, 5067973.8E |
| 2 | 355524.3N, 5067993.0E |
| 3 | 355514.7N, 5068127.7E |
| 4 | 355404.1N, 5068248.0E |
| 5 | 355153.9N, 5068248.0E |
| 6 | 355125.0N, 5068435.7E |
| 7 | 355043.2N, 5068729.1E |
| 8 | 354966.3N, 5068907.2E |
| 9 | 355139.5N, 5068936.0E |
| 10 | 355341.5N, 5068863.9E |
| 11 | 355322.3N, 5069109.2E |
| 12 | 355197.2N, 5069325.7E |
| 13 | 355019.2N, 5069407.5E |
| 14 | 354870.0N, 5069513.4E |
| 15 | 354720.9N, 5069725.0E |

| Progressive number | SEM model | AICc |
|---|---|---|
| 1 | 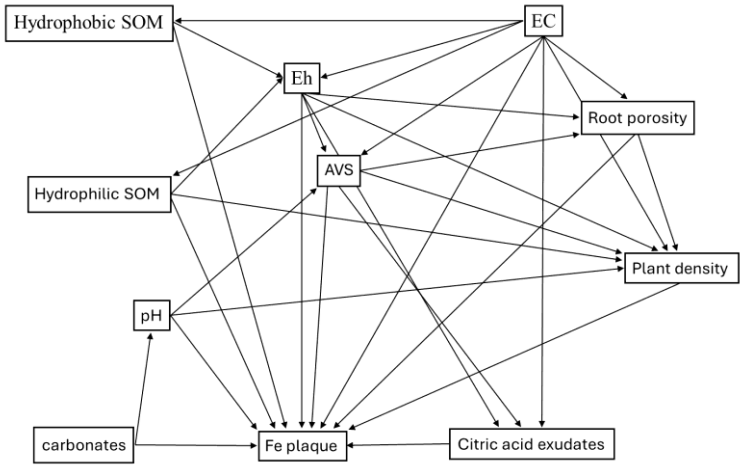 | 1824.1 |
| 2 | 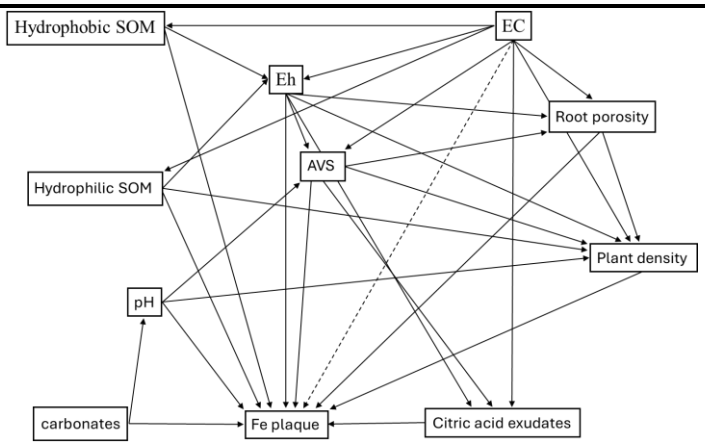 | 1831.6 |
| 3 | 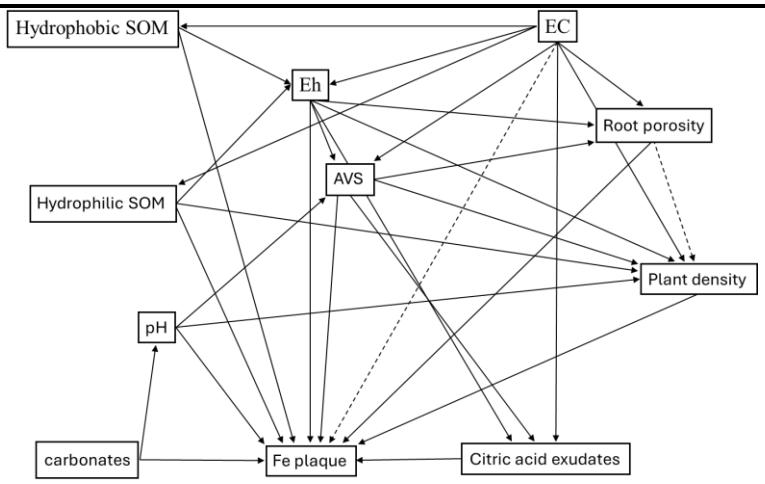 | 1829.4 |

| | | |
|---|---|---|
| **4** | 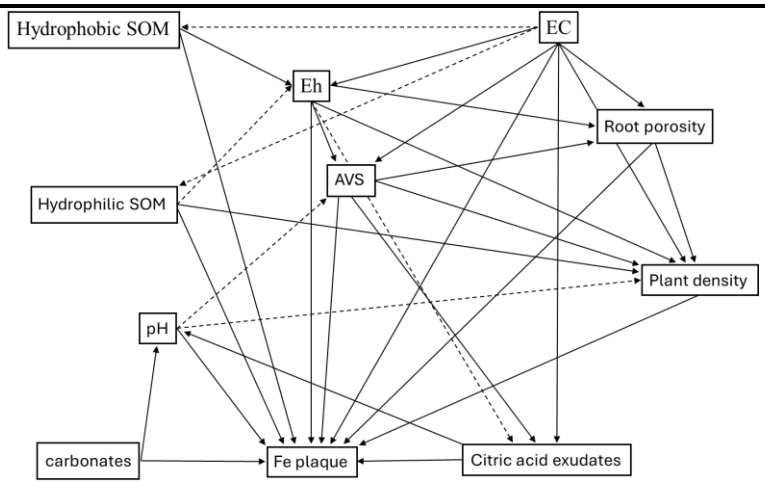 | **1621.3** |
| 5 | 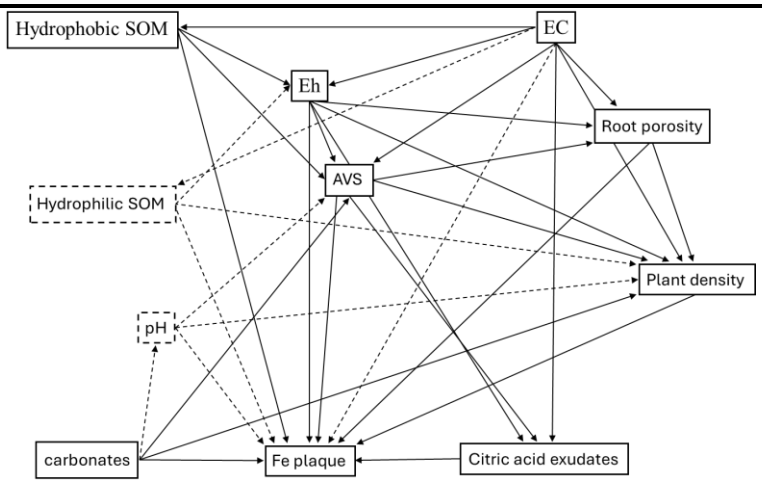 | 1696.6 |
| 6 | 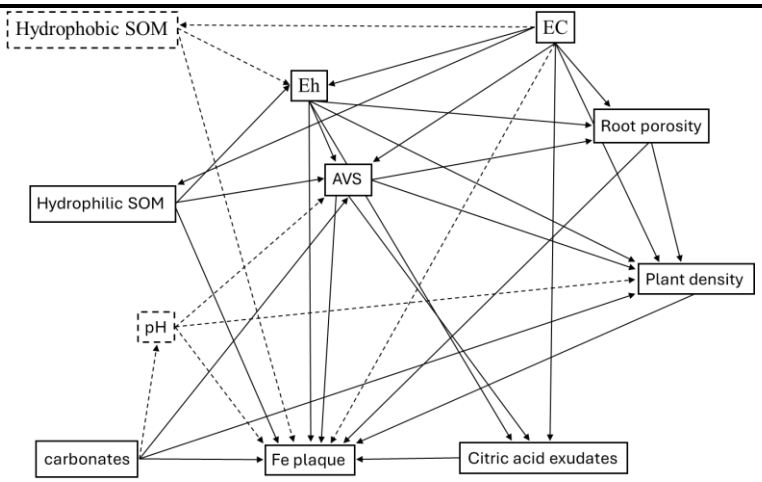 | 1692.7 |

| | | |
|---|---|---|
| 7 | 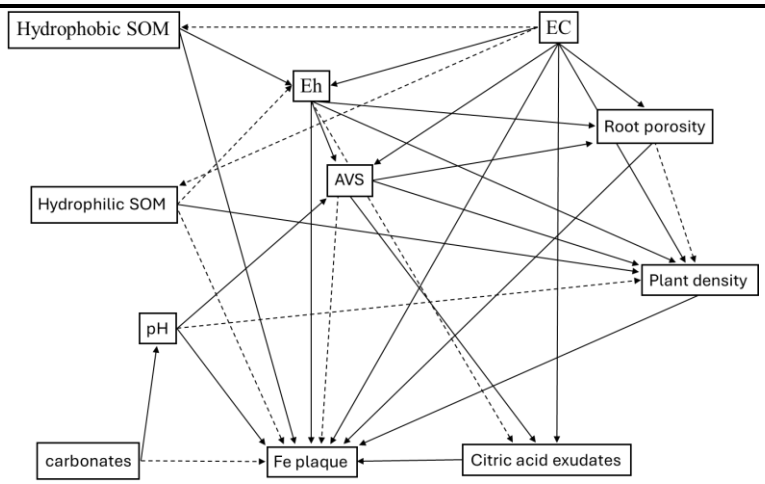 | 1658.8 |
| 8 | 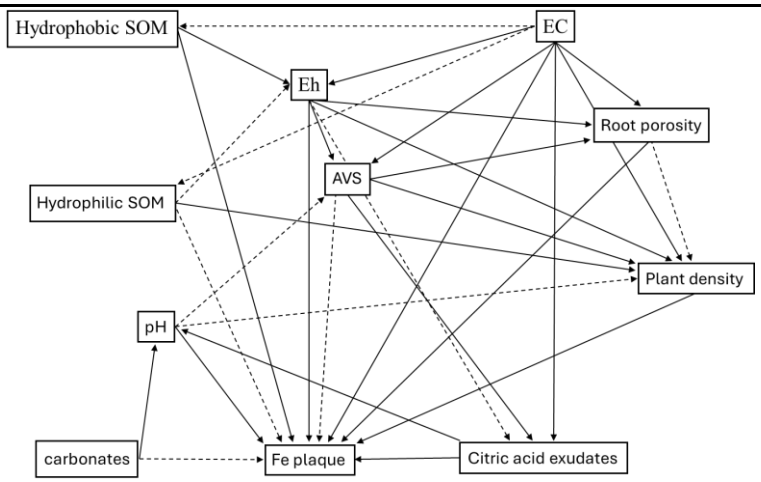 | 1651.9 |

**Figure S2.** Model selection based on lowest Akaike Information Criterion corrected for small sample size (AICc). The first model shows the highest number of interactions between the tested variables. Dashed arrows refer to relationships removed during the model selection. The final model selected is highlighted in bold (corresponding to the progressive number 7).

| Cormor river | | | | | | | | | | | |
|---|---|---|---|---|---|---|---|---|---|---|---|
| **Sample point** | **Carbonate content** | **Soil conductivity (EC)** | **Soil pH** | **Soil redox potential** | **Acid Volatile Sulphides (AVS)** | **Hydrophobic OM** | **Hydrophilic OM** | **Plant stand density** | **Root leakage** | **Porosity** | **Root Fe plaque** |
| | **g Kg $^{-1}$** | **dS m $^{-1}$** | **-** | **mV** | **µmol g $^{-1}$ dry soil** | **mg g $^{-1}$ dry root** | **mg g $^{-1}$ dry root** | **plants m $^{-2}$** | **mg mg $^{-1}$ dry root** | **%** | **µg Fe g $^{-1}$ dry root** |
| 1 | 155.7 | 8.06 | 7.38 | -242 | 29.84 | 1.57 | 2.43 | 156 | 0.017 | 44.96 | 26890.81 |
| 2 | 104.32 | 15.33 | 6.89 | -386 | 51.39 | 4.76 | 1.797 | 88 | 0.007 | 55.25 | 8312.93 |
| 3 | 187.32 | 5.61 | 7.88 | -241 | 0.85 | 4.12 | 2.57 | 140 | 0.006 | 36.33 | 9175.75 |
| 4 | 294.93 | 18.03 | 6.89 | -377 | 11.27 | 4.75 | 2.22 | 140 | 0.008 | 43.54 | 6034.53 |
| 5 | 139.54 | 10.59 | 7.07 | -388 | 8.59 | 8.09 | 3.45 | 172 | 0.008 | 45.29 | 4050.16 |
| 6 | 222.86 | 4.52 | 7.6 | -396 | 56.79 | 4.21 | 2.25 | 316 | 0.006 | 47.16 | 5765.49 |
| 7 | 169.09 | 1.06 | 7.75 | -60 | 1.92 | 3.18 | 1.64 | 204 | 0.007 | 38.47 | 1680.88 |
| 8 | 229.58 | 1.55 | 7.55 | -154 | 8.92 | 8.01 | 3.04 | 268 | 0.01 | 47.82 | 3304.23 |
| 9 | 191.94 | 8.45 | 7.24 | -233 | 24.64 | 7.26 | 3.1 | 176 | 0.004 | 42.49 | 3818.24 |
| 10 | 233.55 | 1.05 | 7.56 | -117 | 1.17 | 7.96 | 2.42 | 136 | 0.01 | 43.21 | 1435.96 |
| 11 | 62.88 | 0.97 | 7.75 | 42 | 3.89 | 4.46 | 1.84 | 228 | 0.005 | 50.36 | 3938.76 |
| 12 | 307.63 | 0.35 | 7.82 | -6 | 0.46 | 3.67 | 1.71 | 120 | 0.005 | 25.09 | 1616.60 |
| 13 | 301.19 | 0.12 | 8.14 | 83 | 7.71 | 4.27 | 1.93 | 84 | 0.007 | 38.36 | 696.22 |
| 14 | 288.33 | 0.65 | 7.7 | -130 | 8.51 | 4.75 | 2.74 | 80 | 0.011 | 39.93 | 1723.65 |
| 15 | 308.76 | 8.71 | 8.19 | -45 | 13.85 | 3.75 | 2.33 | 108 | 0.015 | 43.7 | 1650.12 |

**Table S2.** Summary of the individual values for each environmental, plant and soil variables studied at the 15 sampling points along the Cormor river estuarine system.

| Stella river | | | | | | | | | | | |
|---|---|---|---|---|---|---|---|---|---|---|---|
| **Sample station** | **Carbonate content** | **Soil conductivity (EC)** | **Soil pH** | **Soil redox potential** | **Acid Volatile Sulphides (AVS)** | **Hydrophobic OM** | **Hydrophilic OM** | **Plant stand density** | **Root leakage** | **Porosity** | **Root Fe plaque** |
| | **g $Kg^{-1}$** | **dS $m^{-1}$** | **-** | **mV** | **µmol $g^{-1}$ dry soil** | **mg $g^{-1}$ dry root** | **mg $g^{-1}$ dry root** | **plants $m^{-2}$** | **mg $mg^{-1}$ dry root** | **%** | **µg Fe $g^{-1}$ dry root** |
| 1 | 82.82 | 20.00 | 7.02 | -467 | 21.20 | 7.01 | 3.21 | 68 | 0.005 | 44.54 | 2475.06 |
| 2 | 17.30 | 8.34 | 5.68 | -461 | 10.76 | 3.39 | 1.50 | 112 | 0.004 | 39.64 | 1276.04 |
| 3 | 24.28 | 10.45 | 7.00 | -254 | 238.39 | 1.47 | 3.23 | 320 | 0.005 | 29.92 | 2317.74 |
| 4 | 0 | 17.29 | 5.79 | -368 | 22.87 | 4.37 | 2.13 | 196 | 0.005 | 34.02 | 3294.29 |
| 5 | 42.55 | 3.82 | 7.52 | -171 | 0.82 | 7.71 | 2.76 | 140 | 0.005 | 33.54 | 2629.57 |
| 6 | 47.91 | 0.56 | 6.75 | -376 | 13.03 | 9.99 | 4.38 | 236 | 0.005 | 32.86 | 6391.70 |
| 7 | 57.36 | 3.30 | 7.45 | -174 | 5.87 | 7.04 | 2.30 | 196 | 0.006 | 38.30 | 9390.35 |
| 8 | 0 | 7.34 | 5.51 | -414 | 9.00 | 3.85 | 1.91 | 180 | 0.006 | 32.39 | 2424.73 |
| 9 | 9.84 | 11.53 | 7.01 | -295 | 12.68 | 2.78 | 3.01 | 112 | 0.006 | 38.99 | 5135.88 |
| 10 | 112.84 | 5.27 | 7.41 | -357 | 25.76 | 14.55 | 4.70 | 204 | 0.004 | 20.37 | 6311.13 |
| 11 | 58.62 | 1.47 | 7.38 | -295 | 2.75 | 5.24 | 2.48 | 88 | 0.004 | 41.52 | 4249.56 |
| 12 | 9.94 | 2.56 | 7.45 | 191 | 0.71 | 9.86 | 3.70 | 100 | 0.004 | 32.86 | 524.20 |
| 13 | 38.02 | 1.28 | 7.53 | 93 | 0.33 | 9.52 | 5.57 | 120 | 0.006 | 48.68 | 1514.95 |
| 14 | 64.31 | 1.48 | 7.55 | -92 | 1.69 | 9.83 | 3.76 | 80 | 0.006 | 40.35 | 1228.77 |
| 15 | 56.69 | 0.94 | 7.77 | -12 | 0 | 7.36 | 2.76 | 84 | 0.006 | 18.41 | 882.88 |

**Table S3.** Summary of the individual values for each environmental, plant and soil variables studied at the 15 sampling points along the Stella river estuarine system

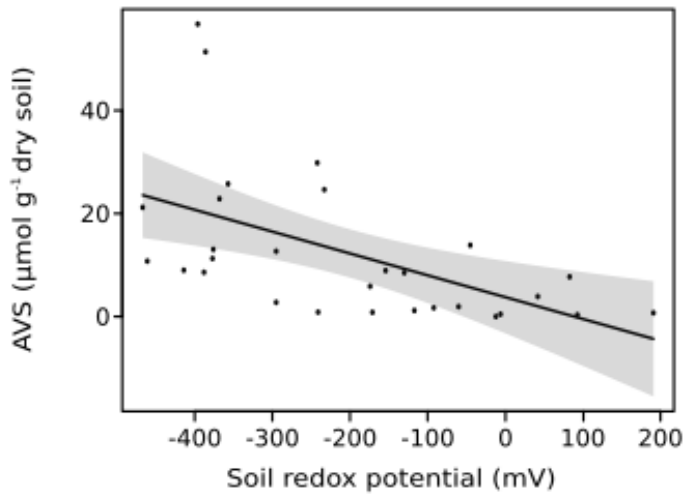


**Figure S4.** Effect plots of the acid volatile sulphides (AVS) model calculated with the linear mixed-effects model included in the piecewise structural equation modelling analysis. The solid black line represents a smoothed regression fit. Confidence intervals (95%) are shown as the shaded areas.

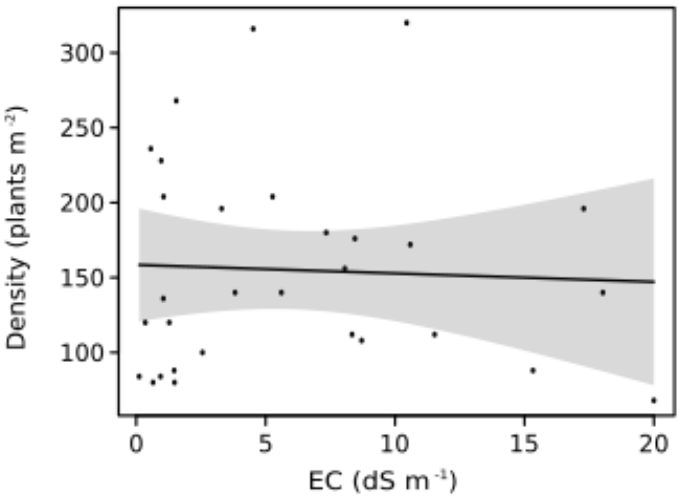


**Figure S5.** Effect plots of the plant stand density model calculated with the linear mixed-effects model included in the piecewise structural equation modelling analysis. The solid black line represents a smoothed regression fit. Confidence intervals (95%) are shown as the shaded areas.

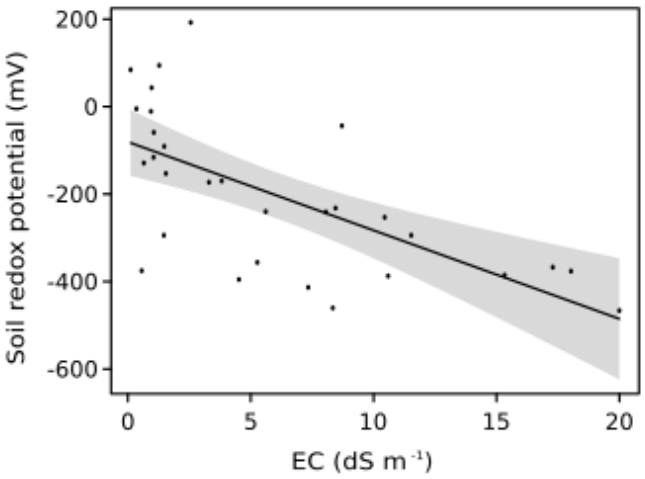


**Figure S6.** Effect plots of the soil Eh model calculated with the linear mixed-effects model included in the piecewise structural equation modelling analysis. The solid black line represents a smoothed regression fit. Confidence intervals (95%) are shown as the shaded areas.

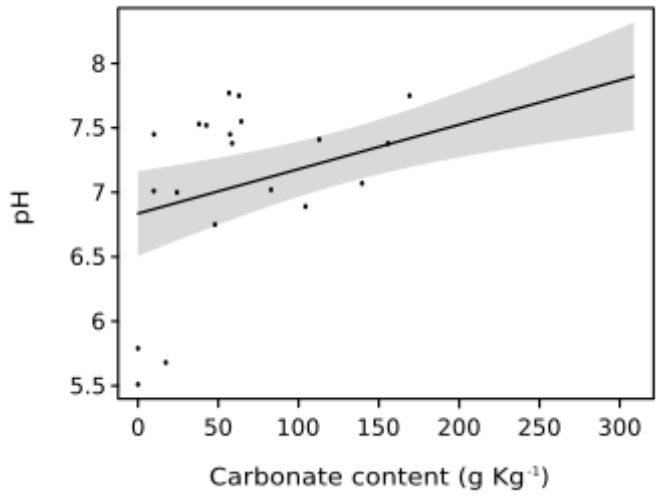


**Figure S7.** Effect plots of the pH model calculated with the linear mixed-effects model included in the piecewise structural equation modelling analysis. The solid black line represents a smoothed regression fit. Confidence intervals (95%) are shown as the shaded areas.

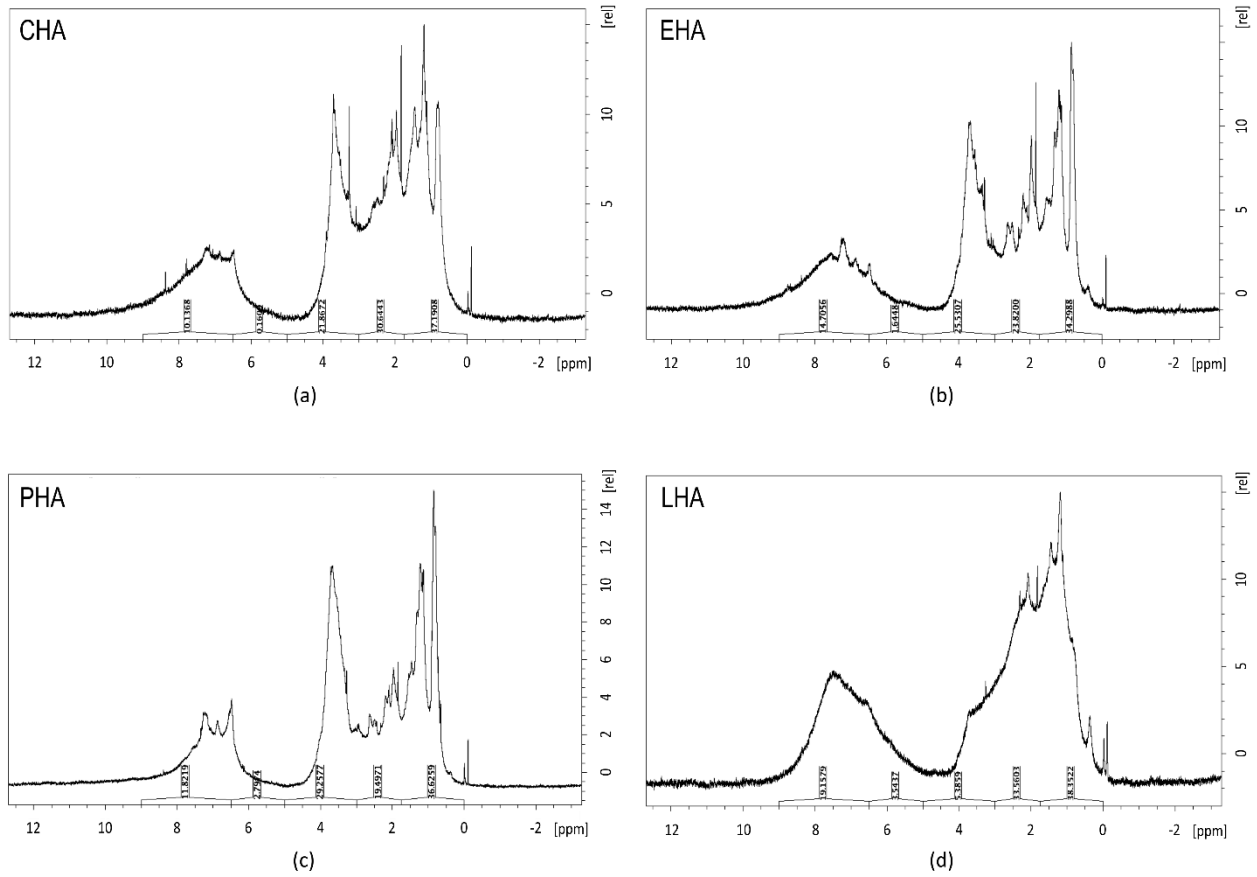


**Figure S1.** Comparative 1H-NMR spectra of HA of different origin (compost CHA, soil EHA, peat PHA and Leonardite LHA).

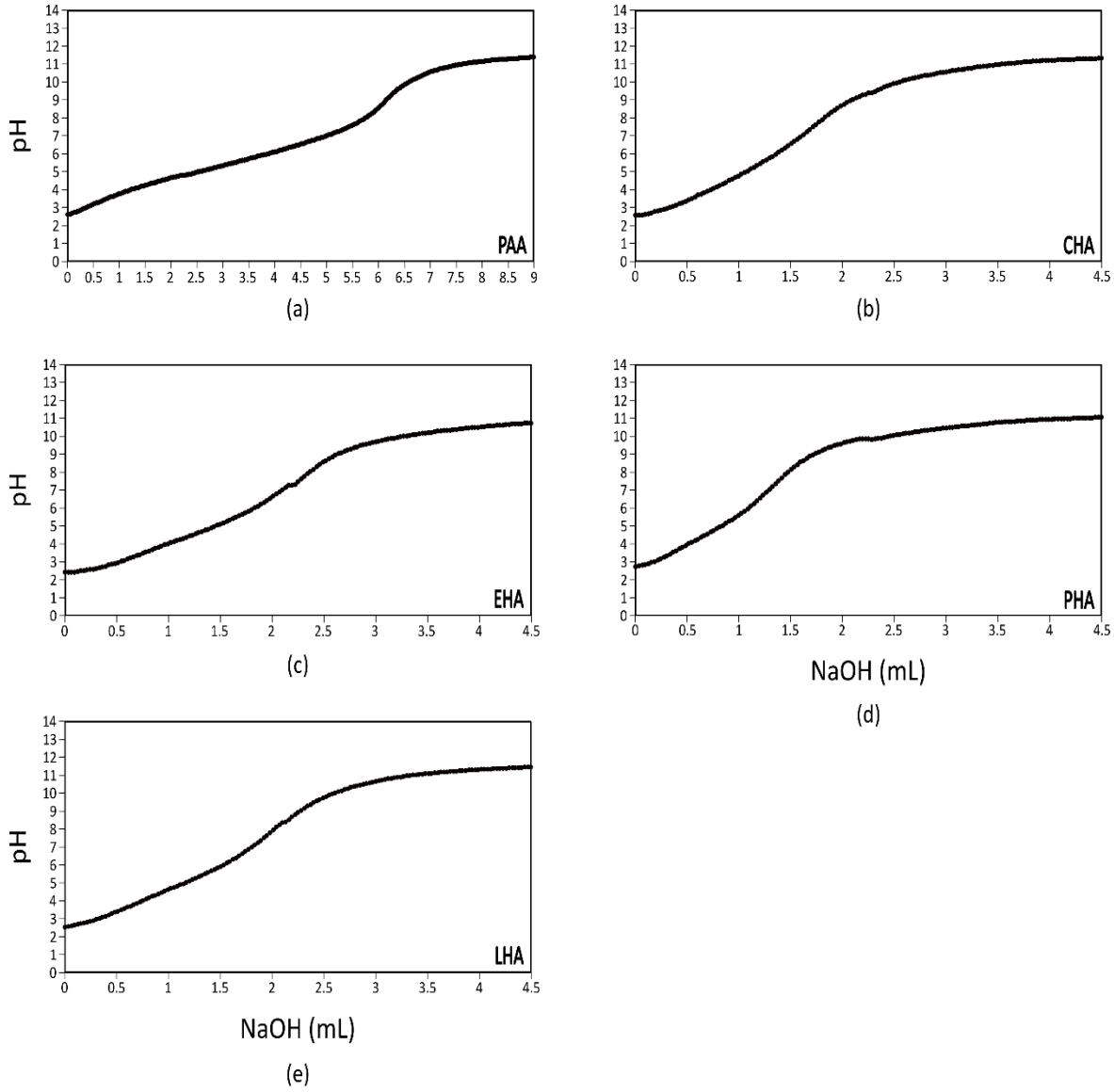


**Figure S2.** Acid – base titration curves of PAA (polyacrylic acid) and HA of different origin (compost CHA, soil EHA, peat PHA and Leonardite LHA).

**Table S3.** Summaries of the ANOVA analysis regarding Germination rate of *Zea mays* seeds under different salt types and concentrations. Salt levels and increasing concentrations of HA were used as predictive variables, while the percentage of germination was used as the response variable. The analysis was conducted separately for each of the two salts and for each of the three days of image collection.

**24 h after germination**

| | **Df** | **Sum Sq** | **Mean Sq** | **F value** | **Pr(>F)** |
|---|---|---|---|---|---|
| | | | NaCl | | |
| Humic acids | 1 | 128.0 | 128.04 | 0.9741 | 0.3335 |
| level | 2 | 5720.3 | 2860.13 | 21.7599 | 4.068e-06 *** |
| Humic acids:level | 2 | 395.0 | 197.49 | 1.5025 | 0.2428 |
| Residuals | 24 | 3154.6 | 131.44 | | |
| | | | $Na_2CO_3$ | | |
| Humic acids | 1 | 71.2 | 71.2 | 0.2258 | 0.6389 |
| level | 2 | 21206.7 | 10603.3 | 33.6399 | 1.092e-07 *** |
| Humic acids:level | 2 | 924.0 | 462.0 | 1.4657 | 0.2509 |
| Residuals | 24 | 7564.8 | 315.2 | | |

**48 h after germination**

| | Df | Sum Sq | Mean Sq | F value | Pr(>F) |
|---|---|---|---|---|---|
| | | | NaCl | | |
| Humic acids | 1 | 263.3 | 263.3 | 1.1697 | 0.2902 |
| level | 2 | 16721.7 | 8360.8 | 37.1439 | 4.493e-08 *** |
| Humic acids:level | 2 | 137.0 | 68.5 | 0.3043 | 0.7405 |
| Residuals | 24 | 5402.2 | 225.1 | | |
| | | | $Na_2CO_3$ | | |
| Humic acids | 1 | 12 | 11.8 | 0.1071 | 0.7463 |
| level | 2 | 38783 | 19391.7 | 175.8919 | 4.606e-15 *** |
| Humic acids:level | 2 | 157 | 78.6 | 0.7127 | 0.5004 |
| Residuals | 24 | 2646 | 110.2 | | |

**72 h after germination**

| | Df | Sum Sq | Mean Sq | F value | Pr(>F) |
|---|---|---|---|---|---|
| | | | NaCl | | |
| Humic acids | 1 | 58.0 | 58.0 | 0.560 | 0.4615 |
| level | 2 | 7208.6 | 3604.3 | 34.793 | 8.091e-08 *** |
| Humic acids:level | 2 | 307.9 | 153.9 | 1.486 | 0.2464 |
| Residuals | 24 | 2486.2 | 103.6 | | |
| | | | $Na_2CO_3$ | | |
| Humic acids | 1 | 117 | 116.7 | 1.7590 | 0.1972 |
| level | 2 | 46759 | 23379.6 | 352.4743 | <2e-16 *** |
| Humic acids:level | 2 | 100 | 49.8 | 0.7501 | 0.4831 |
| Residuals | 24 | 1592 | 66.3 | | |

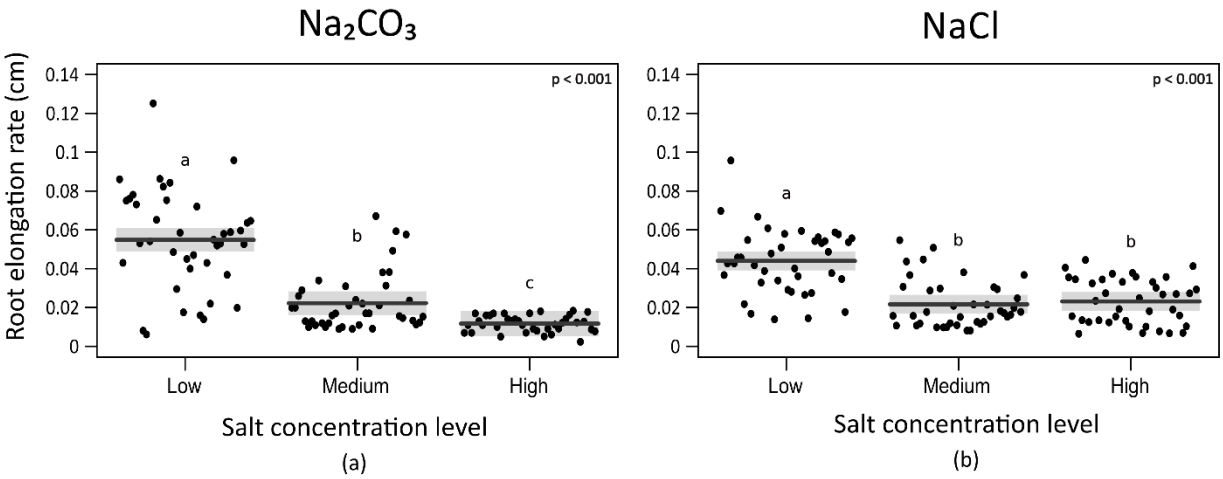


**Figure S4.** Root elongation rates of *Zea mays* seeds under different salt types and concentrations. Root length was measured after 12 hours since the emergence of the first root. "Low", "Medium", "High" correspond to the three concentration levels of the salts used in the test. Dots represent the percentage of seeds germinated at increasing concentrations of CHA. Different letters refer to statistically significant differences based on Tukey's post hoc test ($p < 0.001$).

**Table S5.** Summary of the ANOVA analysis regarding root elongation rate of *Zea mays* seeds under different salt types and concentrations. Salt levels and increasing concentrations of HAs were used as predictive variables, while the percentage of germination was used as the response variable. The analysis was conducted separately for each of the two salts.

| | **Df** | **Sum Sq** | **Mean Sq** | **F value** | **Pr(>F)** |
|---|---|---|---|---|---|
| | | | NaCl | | |
| Humic acids | 1 | 0.0000042 | 0.0000042 | 0.0213 | 0.8841 |
| level | 2 | 0.0114946 | 0.0057473 | 29.3884 | 5.092e-11 *** |
| Humic acids:level | 2 | 0.0007869 | 0.0003935 | 2.0120 | 0.1384 |
| Residuals | 114 | 0.0222943 | 0.0001956 | 10.5 | |
| | | | $Na_2CO_3$ | | |
| Humic acids | 1 | 0.000530 | 0.0005305 | 1.6732 | 0.1985 |
| level | 2 | 0.035467 | 0.0177337 | 55.9347 | <2e-16 *** |
| Humic acids:level | 2 | 0.000525 | 0.0002623 | 0.8273 | 0.4399 |
| Residuals | 111 | 0.035192 | 0.0003170 | | |

**S6.** Example of calculations of quantity of compost required to reduce salinity in one hectare of land, based on $SAP_{HA\ eff}$.

We will consider, for instance, a silty-loam soil with a pH of 8.5, a water content of 25% and a bulk density of 1.3 g $cm^{-3}$ (Bai et al., 2017) and that this soil has an EC, measured in a 1:4 extract of 4 dS $m^{-1}$. Let us also suppose that our aim is to reduce salinity from EC 4 to EC 2 dS $m^{-1}$.

Knowing that the $SAP_{HA\ eff}$ of CHA is approximately 25 mg of $Na_2CO_3$ per gram of HA when the pH increases from 7.0 to 8.5, we can calculate the amount of this compost that should be applied in the field to obtain the desired decrease in EC.

Total salts to be removed per liter of solution:

Salinity of solutions (mg $L^{-1}$) = EC • 640

Salinity at $EC_4$ = 2560 mg $L^{-1}$

Salinity at $EC_2$ = 1280 mg $L^{-1}$

Total salts to be removed: 2560 - 1280 = 1280 mg $L^{-1}$ i.e. 1.28 g $L^{-1}$

Volume of one hectare slice of soil to 5 cm depth: 10.000 $m^2$ • 0.05 m = 500 $m^3$

Weight of same volume assuming a bulk density of 1.3 t $m^{-3}$: 500 • 1.3 = 650 t

Volume of water in same volume, assuming a moisture content of 25%: 650 • 0.25 = 162.500 L

Total salts to be removed from such volume: 162500 • 1.28 / 1000 = 208 kg

Considering CHA can remove about 25 mg $Na_2CO_3$ per gram, to remove 208 kg salts we will need: 208 / 25 = 8.32 t HA from compost

If compost have an average content of about 40% of HS, the quantity of dry compost required is: 8.32 / 0.4 = 20.8 t

Since mean moisture content of fresh compost is about 50%, 20.08 / 0.50 = 42 t fresh compost needs to be applied to achieve the desired EC reduction.

Application of this quantity is not uncommon when using compost as amendment for arable and fruit trees crops.